DELFT UNIVERSITY OF TECHNOLOGY

Faculty of Civil Engineering – Track of Environmental Engineering

Department of Water Management – Sector of Sanitary Engineering

MSc Thesis

Cation competition in ammonia recovery from reject water through electrodialysis and bipolar membranes

---

Author:

Papadopoulou Maria Anna

February, 2024

Committee: Dr. Ir. Henri Spanjers
Prof. Dr. Ir. Jules van Lier
Dr. Ir. David Vermaas

Daily supervisor: Iosif Kaniadakis

DELFT UNIVERSITY OF TECHNOLOGY

Faculty of Civil Engineering – Track of Environmental Engineering

Department of Water Management – Sector of Sanitary Engineering

MSc Thesis

Cation competition in ammonia recovery from reject water through electrodialysis and bipolar membranes

Papadopoulou Maria Anna

Student Number: 5611547

February 2024, Delft, The Netherlands

Supervisors: Dr. Ir. Henri Spanjers
Prof. Dr. Ir. Jules van Lier
Dr. Ir. David Vermaas

Daily supervisor: Iosif Kaniadakis

Acknowledgements

This MSc thesis represents the final step to this challenging and fascinating two-year journey that tested me and my limits, contributed to my skills' development and broadened my overall horizons. TU Delft taught me a lot of valuable lessons, gave me experiences that I would have never imagined and gave me friends that each of them individually contributed to the person I am today. Three years ago, I would never have expected that the day of graduating from such a prestigious and well-known university would come and I will start my future professional life with this significant final step.

Regarding that, I would like to express my sincere gratitude to all the people that, with their own piece, contributed to this thesis. First, I would like to thank my supervisors, Henri Spanjers, Jules van Lier and David Vermaas for their constructive feedback, insightful suggestions and scholarly guidance they offered me in the entire educational period. Their offered knowledge enriched my research and unlocked several educational pathways that I could not think of alone.

However, one of the biggest contributors for the conduction of this thesis is the PhD candidate, Iosif Kaniadakis, who was next to me every time I needed instant solutions and further explanation, for giving me the opportunity to get involved in such an interesting and challenging topic and for supporting me until the end of this journey. This thesis would not have been successfully defended without him. In addition, I would like to extend my heartfelt thanks to the Water-Lab technicians for the constant advice and supervision in my laboratory work and to the electrodialysis team for their valuable feedback they offered me during the bi-weekly meetings.

Last but not least, I would like to express my deepest gratitude for the fundamental stones in my life, my family and my friends who support me from the very first day with their unconditional love, who offered me encouragement until the last day and believed in me more than anyone. Thank you for being a very special part of my life and for this unique experience.

Maria Anna Papadopoulou

February 2024

Abstract

Nutrient recovery has lately been a concerning topic regarding the environmental friendliness of it and the high availability of technologies. Ammonia is one of the main compounds in reject water that could be recovered and utilized further in the agricultural sector. Several methods have been found, including conventional electrodialysis, in which anion and cation exchange membranes are being used and, with the application of electrical current, there is production of clean and desalinated water, creating at the same time a concentrated solution. As a further evolution of electrodialysis, bipolar membranes could be added in the configuration, leading to acid and base production. However, ammonium is not the only cation included in reject water, but also Na^+, K^+, Mg^{2+} and Ca^{2+} are present and affect the overall performance electrodialysis. Thus, the competition between the cations needs to be investigated further regarding the operational parameters of each configuration.

This study investigated the cation competition in electrodialysis and bipolar membrane configuration regarding the ammonia removal efficiency and the overall energy consumption. The research questions were focused on the effect of enriched solutions with cations on ED and BPC to the efficiency parameters, to the impact of cation composition in the feed solution when NH_4^+, Na^+, K^+, Mg^{2+} and Ca^{2+} are included in an ED and finally, the effect of municipal reject water cation molar ratios in a combined ED and BPC configuration. The experiments included batch mode systems, with several mass and molar ratios of NH_4^+ applied, the above-mentioned parameters were measured. More specifically, BPC and ED configurations were tested with mass ratios of other cations in an enriched NH_4^+ solution, while molar ratios were tested in case of an ED configuration with NH_4^+, Na^+, K^+, Mg^{2+} and Ca^{2+} be present in the feed solution. Finally, the two configurations were tested in a sequence batch, with ED to be the pretreatment step and BPC the final stage. The phenomena that were also investigated were proton production from bipolar membranes and EC pattern on the diluate solution in this case.

In ED removal efficiency was presented as a linear curve on time while in BPC the same value took a logarithmic trend, which is attributed to proton production and finally competition. During BPC operation, there was constant production of H^+ through water dissociation that led to the acidic environment in the diluate solution but also to stabilization of EC when H^+ presence was dominant. In addition, in molar ratio experiments with the application of ED, removal efficiency was higher for more challenging reject waters compositions such as molar ratios between 0.30 and 0.60. Considering 75% removal efficiency as an effective case, percent demineralization was also calculated. For removal efficiency below the effective case, percent demineralization presented a minimum for molar ratio of 0.60, while for higher removal efficiency the overall trend was slightly different, having a more exponential shape. Finally, energy consumption in molar ratio experiments, for removal efficiency of 75% presented a gradual decreasing linear trend with the increase of molar ratio.

Based on the results occurred in batch experiments, a sequence batch of ED to concentrate the feed solution was established, by applying the more challenging molar ratios of 0.30, 0.45 and 0.60 and the concentrate was then fed to a BPC to explore the proton effect in a concentrated solution. The percent demineralization and removal efficiency remained stable during the experimental phase while transport number had a notable increase with the increase of molar ratio, remaining approximately the same in every individual batch. Moreover, energy consumption had an important increase with the decrease of molar ratio due to the high membrane resistance and the observed scaling effect.

Abbreviations

NH_4^+ - Ammonium

NH_4OH- Ammonium hydroxide

NO_2^- - Nitrite

NO_3^- - Nitrate

N_2 – Dinitrogen gas

N_2O – Nitrous oxide

WWTP – Wastewater Treatment Plant

ED – Electrodialysis

TAN – Total Ammoniacal Nitrogen

Mg^{2+} - Magnesium

PO_4^{3-} - Phosphate

Ca^{2+} - Calcium

CO_3^{2-} - Carbonate

SO_4^{2-} - Sulphate

RO – Reverse Osmosis

AEM – Anion Exchange Membrane

CEM – Cation Exchange Membrane

CEEM – Cation Exchange End Membrane

BPC – Bipolar/Cation Exchange Membrane

BPMED – Bipolar Membrane Electrodialysis

BPSED – Bipolar Membrane Selective Electrodialysis

SBE – Sequence Batch Experiments

ERS – Electrode Rinse Solution

NH_3 – Ammonia

OH^- - Hydroxide

H^+ - Proton

NH_4Cl – Ammonium Chloride

NaCl – Sodium Chloride

IEX – Ion Exchange

SED – Selective Electrodialysis

KCl – Potassium Chloride

$Mg(OH)_2$ – Magnesium Hydroxide

$CaCO_3$ – Calcium Carbonate

NF – Nanofiltration

EC – Electrical Conductivity

Na^+ - Sodium

K^+ - Potassium

NH_4HCO_3 – Ammonium Bicarbonate

Na_2SO_4 – Sodium Sulphate

K_2HPO_4 – Potassium phosphate dibasic

KH_2PO_4 – Potassium phosphate monobasic

$MgCl_2$ – Magnesium Chloride

$CaCl_2$ – Calcium Chloride

IC – Ion Chromatography

HCO_3^- - Bicarbonate

PD – Percent Demineralization

H_2 - Hydrogen

Table of Contents

1 Introduction

1.1 Nitrogen cycle

Nitrogen is one of the most abundant elements in both the human body and environment, presented in both organic and inorganic forms. In nature the inorganic compounds of nitrogen are controlled through the nitrogen cycle (Figure 1.1).

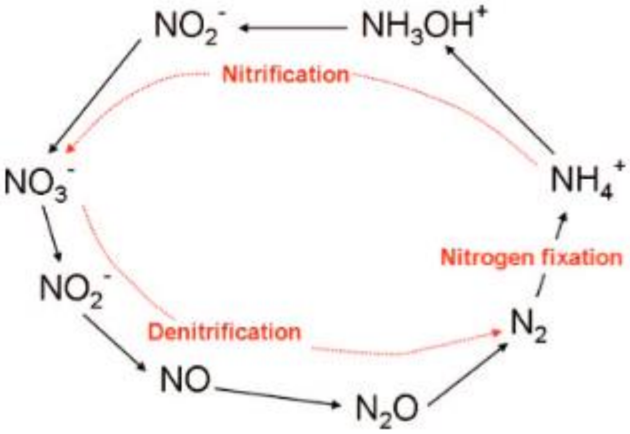

Figure 1.1. Simplified scheme of nitrogen cycle (Rosca et al., 2009)

More specifically, starting from ammonium (NH_4^+), it is turning into NH_3OH^+ (ammonium hydroxide) and through nitrification process, NH_3OH^+ turns into nitrite (NO_2^-) and finally nitrate (NO_3^-). Then, denitrification takes place where nitrogen takes its final form, from NO_3^- to dinitrogen gas (N_2), with intermediate product nitrous oxide (N_2O). Finally, nitrogen fixation is the process where atmospheric nitrogen N_2 is converted into a form that can be used from plants, which is NH_3. The same processes are followed also in a wastewater treatment plant (WWTP), most of the times, to remove ammonium, starting from nitrification, and ending to denitrification where NH_4^+ is fully converted to N_2 when optimal conditions are present. Alternatively, partial nitrification and anammox could be used (deammonification) to fully remove NH_3, without the addition of organic source that denitrification requires.

1.2 Importance of NH_3

NH_3 is an easily found compound, existing in the environment in both gaseous and molecular form (Sutton et al., 2008). It is used in a variety of sectors such as agriculture, as nitrogen fertilizer. However, the emissions are increasing, causing environmental problems, extending in water and soil, such as eutrophication, acidification of soil or formation of fine particulate matter in the atmosphere respectively (Sutton et al., 2008). Despite that, nitrogen is considered a very valuable energy source. By hydrogen or carbon-neutral hydrogen derivates, such as NH_3, carbon storage of energy could be applied, since NH_3 is a sustainable fuel for mobile and remote applications (Valera-Medina et al., 2018). Some worth highlighted advantages of NH_3 over hydrogen (H_2) are its lower cost per unit of stored energy, the easier and widespread production of it and its better commercial viability (Valera-Medina et al., 2018). In addition, NH_3 production is safer compared to other sources of energy such as H_2. Hence, in case of escaping to atmosphere it dissipates rapidly, it could be detected easily through smell in leakage situations, for concentrations as low as 5 ppm, and finally it has a narrow flammability range (Zamfirescu and Dincer, 2009).

1.3 Nitrogen in reject water

Reject water is produced after anaerobic digestion takes place and contains more than 30% of the NH_4^+ (Kim et al., 2020). Feeding a treatment process with reject water, increases the cost for additional nitrification/denitrification and determines the final quality of the WWTPs effluent (lower efficiency of denitrification and nitrification, lower carbon/nitrogen ratio) (Kim et al., 2020). In addition, it increases the oxygen requirement costs of the WWTP, leading to higher operational costs of the plant. Therefore, the need to recover NH_3 from reject water becomes a necessity, by using the least energy consuming method and achieving the highest potential efficiency. To recover ammoniacal nitrogen from residual waters as fertilizer, technologies such as struvite precipitation and air stripping in combination with acid scrubbing are used (Mehta et al., 2015). However, the addition of chemicals makes that technology less desired. Finally, electrodialysis (ED) has been demonstrated as an efficient method to recover Total Ammoniacal Nitrogen (TAN), where chemicals are not needed for the process (van Linden et al., 2020).

1.4 Nitrogen as fertilizer

The current global situation has brought a supply chain crisis and a disruption in bioeconomy. The prices of fertilizers' production have been increased due to natural gas availability (Chojnacka et al., 2023). Thus, nitrogen fertilizers by chemical synthesis are expected to become even more expensive in the next years. As an alternative, nitrogen could be recovered from reject water, which is already discharged in water bodies, leading to a double profit, both sustainable nitrogen recovery and treatment of reject water.

Currently NH_3 synthesis is the main nitrogen source that could be used as a fertilizer because it is a component of proteins, nucleic acids and chlorophyll. In Europe, the main products used as nitrogen fertilizers are NO_3^--based, such as ammonium nitrate (NH_4NO_3), calcium ammonium nitrate (CAN), urea ($CO(NH_2)_2$) and urea ammonium nitrate (UAN) (Fertilizers Europe, 2023).

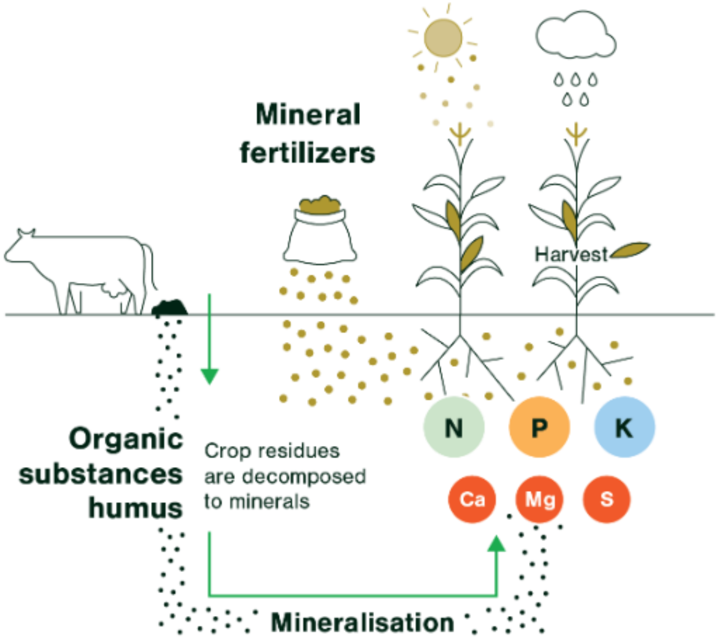

Figure 1.2. Mineral fertilizers application (Fertilizers Europe, 2023)

Due to war in Ukraine, it is expected that the global economy will be negatively affected since the prize of nitrogen fertilizer increases 6 times while resource problems come up, with Russia and Belarus as the main producers of potassium salt. The first one is also the principal manufacturer of metal catalysts which are necessary for NH_3 synthesis. Therefore, it is undeniable that the need to find alternatives has arisen, with wastewater to be the main target (Chojnacka et al., 2023).

1.5 Recovery methods of NH_3 from wastewater

Wastewater is a rich source of NH_4^+, which can be recovered with different methods. Some of them are struvite precipitation or NH_3 stripping coupled with adsorption and membrane concentration (Ye et al., 2018). The first is the most common method, where NH_4^+ and PO_4^{3-} are recovered simultaneously at alkaline pH. The pH in this case plays an important role in the final species of PO_4^{3-} and NH_4^+. In addition, Tansel et al. (2018) indicated that struvite precipitation is also affected by temperature and ionic interactions. The stoichiometric equation that describes struvite precipitation is shown below:

$$\mathrm{Mg^{2+} + PO_4^{3-} + NH_4^+ + 6H_2O \rightarrow MgNH_4PO_4 \cdot 6H_2O} \downarrow$$

In addition, NH_4^+ recovery through NH_4^+ stripping-adsorption process can be achieved at high reaction temperature and/or pH. In this case, NH_4^+ can be converted to volatile NH_3. The reaction is described as below:

$$\mathrm{NH_3 + H_2O \leftrightarrow NH_4^+ + OH^-}$$

By shifting the equilibrium towards the gaseous phase, followed by NH_3 stripping then it could be recovered (Ye et al., 2018). Stripped NH_3 can be adsorbed by acid solutions to form NH_4^+ salts. Alternatively, it could be recovered as an NH_3-rich solution.

Moreover, membrane technology can enrich NH_4^+ and separate it from foreign substances such as heavy metals and pathogens. More specifically, NH_4^+ could be recovered through forward osmosis, reverse osmosis, membrane distillation and ED. In the first case, natural osmotic pressure is used to force movement of water molecules from the feed solution to draw side. Thus, NH_4^+ is being concentrated in the feed.

On the other hand, in reverse osmosis, more energy is consumed and application of hydraulic pressure, so that the water molecules are driven from low concentration solution to high concentration of solute. Compared to forward osmosis, an advantage is that in the first NH_4^+ is gradually diluted, which decreases the osmotic pressure gradient and it affects the NH_4^+ concentration in the feed.

Furthermore, in membrane distillation the feed solution is heated, which results in a temperature gradient between feed and permeate. NH_4^+ ions are converted to volatile form and driven to transfer across the membrane distillation membrane (i.e. microporous hydrophobic membrane). Therefore, NH_4^+ ions could be condensed on the permeate with lower temperatures (Ye et al., 2018).

Finally, in ED cation-exchange and anion-exchange membranes are used. An electrical current is applied to the stack to drive NH_4^+ ions through the cation exchange membrane towards the cathode side. NH_4^+ is then accumulated in the concentrate chamber. However, in case of ED there is higher energy consumption, compared to other methods.

1.6 Problem definition

1.6.1 Complex composition of reject water

Reject water is the product from anaerobic digestion and it is highly related to the initial wastewater and its composition. It could present some differences in its composition based on the initial source, such as in food-based wastewater or chemical-based wastewater. However, the content of heavy metals in industrial wastewater limits the application of any by-product as a fertilizer, whereas the reject water produced by municipal wastewater or food waste is more suitable.

Municipal wastewater is often treated with anaerobic digestion in the sludge line since it offers waste reduction, energy recovery and carbon emissions reduction (Breunig et al., 2019). One of the by-products, which is not further used, is reject water, and has high salinity content which hinders the application of it in agriculture. More specifically, Wang et al. (2022), investigated ED in mature and fresh digestate collected from two different full-scale biogas plants in Shanghai, fed with catering food waste and operated in mesophilic conditions. K^+, NH_4^+ and Cl^- were found to be the components with higher migration priority and ED achieved a 90% removal of salts and N and P recovery between 35 to 70%. However, the membrane fouling appeared to be a challenging aspect in a full-scale operation regarding the costs.

1.6.2 Scaling in ED

Scaling is one of the main problems in ED due to the presence of cations, such as Mg^{2+}, Ca^{2+}, CO_3^{2-} and SO_4^{2-} or other multivalent ions in the solution. It can appear on both surface sides of ion-exchange membranes facing concentrate and diluate compartments. The precipitation of salts leads to an increase in the applied voltage in the system due to the membranes' resistance, having as a result the rise of energy consumption (Andreeva et al., 2018). Scaling in ED can occur due to the deviation of solubility equilibrium. When the solution region where the product of ion concentrations exceeds the solubility product near the membrane/solution interface, then scaling can occur in the membrane surface.

Usually, in reject water, ions such as Ca^{2+}, Mg^{2+}, CO_3^{2-} are present, rendering membranes to be more prone to scaling formation. Some studies have been conducted related to scaling formation during the operation of an ED system. For example, Asraf-Snir et al. (2016) investigated the gypsum scaling of an anion exchange membrane in ED. A comparison of two different anion exchange membrane was made, one homogeneous and one heterogeneous. In the later one, the scaling was mainly internal while in the other the precipitation occurred mainly on the membrane's surface. Stack resistance also followed the same pattern as the scaling, indicating that it is highly connected with it.

In addition, Zhang et al. (2011) studied the feasibility of ED on a RO concentrate to reduce the volume of salts and to improve the overall water recovery. In those experiments, a factor named Critical Scaling Concentration (CSC) was introduced to predict the scaling potential. Finally, the overall recovery of the system, including a RO that produced the feed of the ED unit, reached 95%.

Finally, Dufton et al. (2018) investigated how the different ED configurations affect the acid whey deacidification and membrane scaling. In this case, a conventional electrodialysis set-up was operated and a set-up including the addition of bipolar membranes. In both cases, scaling was observed since amorphous calcium phosphate was identified in the anion exchange membrane and calcite and brucite in the cation exchange membranes. This phenomenon was connected to the migration of divalent ions and water splitting phenomenon by the bipolar membranes.

1.7 Research plan

1.7.1 Research objective

The main objective of the research is to analyze the effect of composition on overall efficiency in ED and BPC, targeting on NH_4^+ recovery. By testing several compositions, regarding mass and molar ratios of cations, the potential cationic competition was investigated based on the energy consumption and removal efficiency of NH_4^+. For that scope two different configurations were operated, where synthetic water was used in ED and BPC. Standard IEXs and bipolar membranes were used in all batch and sequence batch experiments. As additional experiments, real reject water from Horstermeer was tested in a BPC, ED and BPSED configurations, and finally the combination of ED and BPC in sequence was operated to investigate the application of operational limitations in a more realistic scenario.

1.7.2 Knowledge gaps and problem statement

The gradual increase in NH_3 demand, given that NH_4^+ is one of the main compounds for fertilizers and thus it plays an important role in food security, has led to the need to investigate different methods to achieve the highest production with the lowest cost. In addition, wastewater treatment residues, such as reject water, containing high concentrations of NH_4^+, are further recirculated to the WWTP, leading to increased energy consumption and higher operational costs. In that case, taking advantage of the high concentration of NH_4^+ in reject water, we can aim to improve NH_4^+ recovery than NH_4^+ production (Wu and Modin, 2013). Moreover, ED is a promising method, since most ammoniacal nitrogen methods investigated are energy consuming biochemical processes (van Linden et al., 2020). BPMED (van Linden et al., 2020) and conventional ED (van Linden et al., 2019) were investigated as configurations, with the first giving removal efficiency of 85-91% and energy consumption of 19 MJ/kg-N removed while in the second case the removal efficiency reached was 90% with energy consumption of 5.4 MJ/kg-N removed. ED was used to concentrate the NH_4^+ while the BPMED had as a main goal to produce concentrated NH_3 resulting in a basic product in one of its compartments.

An important factor for the performance of the system is also the initial composition of the feed. Domestic wastewater is composed of various cations that can affect the ionic competition, such as Na^+, K^+, Mg^{2+} and Ca^{2+} with NH_4^+. Yang et al. (2023) investigated the mixed cation transport including all the abovementioned cations in an ED system, aiming for nutrient recovery and desalt of wastewater. The results of this research were promising with higher current densities leading to higher NH_4^+ concentration efficiency, but with leakage of NH_4^+ in the electrode solution.

ED and RO have also been investigated for ammoniacal nitrogen recovery from swine manure with interesting results in concentrating NH_4^+ (Mondor et al., 2008). However, in the given literature the importance of feed water composition has not yet been highlighted in either conventional ED or ED with bipolar membranes. Therefore, the knowledge gaps that contribute in the formation of the main research questions are the following:

- Built-up composition including NH_4^+ as the main component and Na^+, K^+, Mg^{2+} and Ca^{2+} as additional cations in ED and bipolar membrane system in collaboration with cation membrane. The competition of cations has been roughly investigated, with the efficiency parameters to be underlined less. Both systems require further research to understand their potential advantages and disadvantages.
- Feed composition when NH_4^+, Na^+, K^+, Mg^{2+} and Ca^{2+} are present has not been analyzed for different molar ratios in ED system, since in real case scenarios it could be differentiated, regarding the variety of reject water and its source.
- The combination of ED as a pre-treatment method with bipolar membrane with cation exchange membrane as the final treatment method needs to be investigated for concentrating NH_3 under basic conditions, since it also consists a more realistic scenario.

Thus, the research questions were formed as follows:

RQ1: What is the effect of enriched NH_4^+ solutions with Na^+, K^+, Mg^{2+} and Ca^{2+} in ED and BPC efficiency parameters?

RQ1.1: What is the impact of non-cationic competition (when only NH_4^+ is included in the feed) in an ED and a BPC configuration individually in removal efficiency of NH_4^+ and energy consumption?

RQ1.2: What is the impact of cationic competition (when Na^+, K^+, Mg^{2+} and Ca^{2+} are added gradually in the feed) with mass ratios for monovalent cations 1 and divalent cations 0.5 in ED and BPC?

RQ1.3: What is the effect of proton (H^+) production from BPC operation for the efficiency parameters of removal efficiency and energy consumption?

Hypothesis: It is expected that the addition of cations will promote the competition in the ED and BPC. Transport number of NH_4^+ will decrease since less of the applied current will be available for NH_4^+, while removal efficiency will also be lower. As for the energy consumption, it is expected to be higher when divalent cations are added to the feed solution due to higher scaling potential and resistance in both configurations. In addition, proton production from bipolar membranes will lead to additional competition with NH_4^+. Energy consumption will also be higher, due to the bipolar membrane nature that develops high resistance. Removal efficiency is expected to be lower compared to ED, due to the acidic conditions in the feed solution after some time in combination with the already existing proton competition.

RQ2: What is the impact of cationic composition in the feed solution when NH_4^+, Na^+, K^+, Mg^{2+} and Ca^{2+} are included in an ED configuration?

RQ2.1: What is the effect of cationic molar ratio in removal efficiency in an ED system (with molar ratios of 0.30, 0.45, 0.60, 0.75, 0.90)?

RQ2.2: What is the effect of cationic molar ratio in energy consumption in an ED system (with molar ratios of 0.30, 0.45, 0.60, 0.75, 0.90)?

Hypothesis: The smaller the molar ratio the more condensed the feed solution will be. Thus, it is expected to have higher energy consumption due to the higher resistance of the configuration. As for removal efficiency, due to the EC difference removal efficiency is expected to be lower for lower molar ratios.

RQ3: What is the effect of the application of municipal reject water cationic molar ratios in a SBE system with combined ED, as pre-treatment, and BPC?

RQ3.1: What are the operational conditions that could be beneficially applied in controlling a SBE configuration regarding removal efficiency, energy consumption and percent demineralization?

RQ3.2: What is the transport effect and the energy consumption in the SBE?

Hypothesis: In sequence batch experiments scaling potential is expected to be higher due to the longer operational time. Current efficiency will be approximately stable, since the applied current will be the same and the initial feed solution of each batch will be the same. Energy consumption will be higher in the lower molar ratios, due to higher resistance of configuration. Finally, removal efficiency will be approximately the same in any case since it is the control factor for this series of experiments.

2 Theoretical Background

In this chapter, the already existing knowledge concerning the research topic will be described.

2.1 Electrodialysis

One commonly applied desalination technique is ED, which is an electrochemical process, in which an electric potential difference is used to separate ionic species through charged ion exchange membranes (Nakayama et al., 2017). A conventional ED unit consists of two electrodes and alternately placed anion exchange membranes (AEM) and cation exchange membranes (CEM). Between them, a spacer gasket is placed, which also determines the flow to the different flow channels. A feed stream is the input of the ED while two streams are produced, the diluate, which is the "clean" product, and the concentrate, where all the ions were transferred. In order for this separation to take place, a current is applied and the ions are moved towards the oppositely charged electrodes and are blocked by the equally charged membranes.

This membrane method is not only based on the size of ions needed to be removed, like any other case, but there is ionic selectivity, depending on the ionic charge, the operational conditions and the membrane characteristics (thickness, ion affinity, fixed charged density) (Ozkul et al., 2023). In addition, as mentioned before, an electric current is applied, which is a fundamental difference with all the conventional membrane methods used. Ions migrate through feed water and ion-exchange membranes, while the conductance of the feed water increases the resistance against ion migration reduces, leading to lower energy consumption (Galama et al., 2014).

Finally, as for the configuration of a conventional ED system, CEM and AEM are placed alternately under the applied electric field, while at the electrode interfaces, an electrode rinse solution (ERS), with high salinity, is recirculated to interconnect current transfer between the electrode and the ED cells. An end exchange membrane, either cation or anion, is used to separate ERS from the ED electrolyte feed waters. More details about the ED configuration are provided in Figure 2.1.

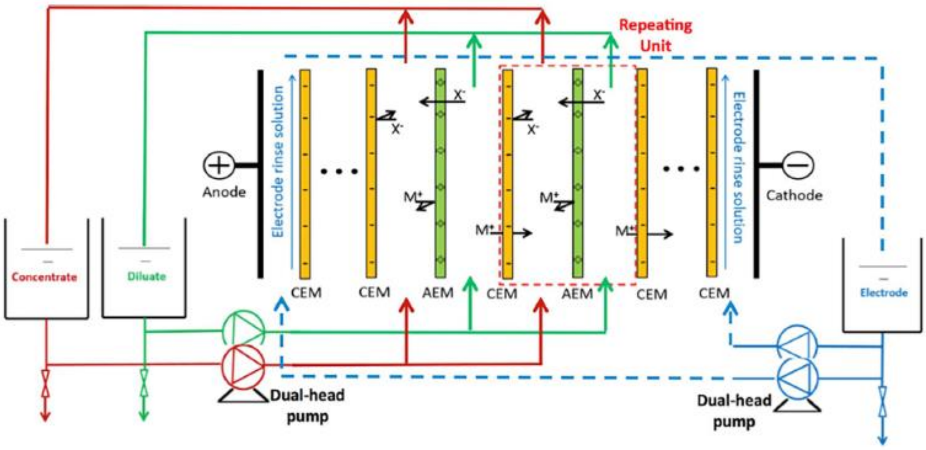

Figure 2.1 Detailed scheme of the ED system, where M^+ refers to positively charged ions and X^- to the negatively charged ions, which pass through the CEM and AEM, respectively, leading to charge cell balance (Modified) (Al-Amshawee et al., 2020)

ED has been tested as a method to help resolve the excess of nutrient problem by swine producers, but also as an alternative to chemical nitrogen fertilizer production (Mondor et al., 2008). The maximum total NH_3 concentration achievable by ED was limited by water transport from the manure to the concentrate compartment and NH_3 volatilization from the open concentrate compartment. In this case also, RO was included for NH_3 recovery and the results were promising, but the minimization of NH_3 volatilization or trap volatilized NH_3 should be investigated. Furthermore, the need to recover valuable nutrients for further utilization in the agricultural field was the main goal of Ippersiel et al. (2012), which investigated ED to transfer the manure NH_3

in the diluate solution. Then, air stripping was applied to the concentrate solution to isolate NH_3 in an acidic solution, without pH modification. However, the pH was not favorable for NH_3 recovery since it ranged in a neutral value.

2.2 Electrodialysis with Bipolar Membranes

An advanced system of ED is the application of bipolar membranes where acids and bases are produced from salts. In this case, bipolar membranes are installed in alternating series in an ED stack, including CEM and AEM. Therefore, three separate flow streams are produced, a flow feed stream solution, an acid flow stream and a base flow stream. A typical scheme of the system is indicated in Figure 2.2.

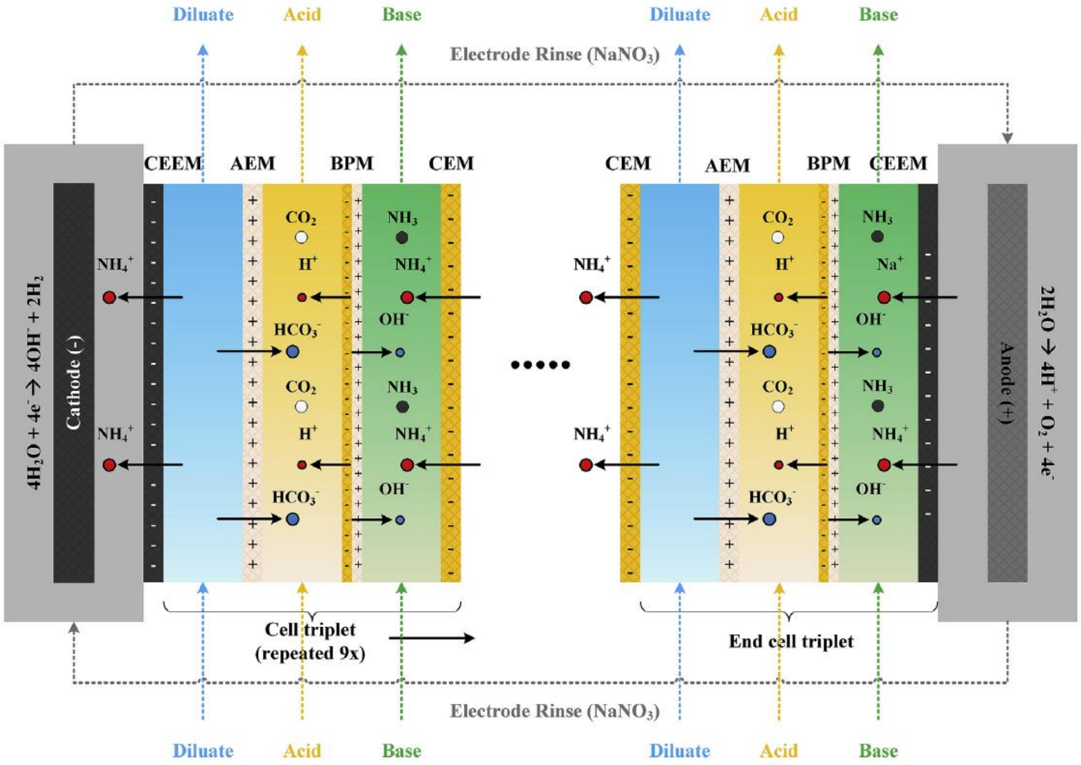

Figure 2.2-Membrane and cell (flow) sequence in the BPMED membrane stack and the intended ion transport (electro-migration and water dissociation) as a result of the applied current. H^+ and HCO_3^- are combined and react to CO_2 in the acid cell, OH^- and NH_4^+ are combined and react to NH_3 in the base. NH_4^+ is transported to the electrode rinse at the cathode while Na^+ and NH_4^+ are transported to the base at the anode, resulting in the accumulation of the latter in the electrode rinse and the wash-out of the cations to the base (van Linden et al., 2020).

Applying ED with bipolar membranes could sometimes be more economically feasible compared to conventional ED. In case of NH_3 removal, BPMED can be used to avoid the chemical addition and change the pH by using only electrical energy (van Linden et al., 2020). Ions are removed from the feed stream and cations concentrate in the base stream with hydroxide ions (OH^-), while in the acid stream anions concentrate, combined with protons (H^+). OH^- and H^+ are produced through water dissociation in case of electric current application when there is bipolar membrane in the configuration.

A lot of research has been conducted in case of BPMED for NH_3 recovery. Van Linden et al. (2019) investigated the NH_4^+ removal from water and the simultaneous NH_3 production without using any chemicals. The removal efficiency of TAN ranged between 85 to 91% and the energy consumption was stable at 19 MJ/kg-N removed. In another study, the applicability of BPMED was investigated and resulted that NH_3, NaOH and HCl could be produced by NH_4Cl and NaCl mixed solution (Öner et al., 2021). However, an important disadvantage was the energy consumption and NH_3 loss. Finally, NH_3 recovery was also investigated by Li et al. (2021), using as a feed stream urine, where the recovery reached approximately 90%, in combination with a membrane contactor after the BPMED system. At a current density of 20 mA/cm^2 the energy consumed for 67.5% NH_3 recovery in a 7 hour batch mode was 92.8 MJ/kgN for a bench-scale system with one membrane stack, whereas for a large scale system with multiple membrane stacks it could be minimized to 25.8 MJ/kg-N removed.

BPMED has been used for NH_3 recovery and tested mostly for synthetic wastewater. Based on Li et al. (2021), BPMED process can be an effective alternative for NH_3 removal and recovery from source-separated urine. The main configuration consisted of a bipolar membrane and a membrane contactor, where there is production of an acid stream, from water dissociation. NH_4^+ was recovered, as an NH_4^+ salt, that can be used as fertilizer. In this experiment, the continuous BPMED-membrane contactor process can achieve 90% NH_3 recovery with energy consumption 12.5 MJ/kg-N removed. In addition, NH_3 recovery was investigated by van Linden et al. (2020), proving that BPMED could be used to simultaneously remove NH_4^+ and produce concentrated NH_3. The TAN removal efficiency for BPMED ranged between 85 to 91%, while the energy consumption remained stable at 19 MJ/kg-N removed. Furthermore, research was conducted by Guo et al. (2023) for NH_3 recovery from low NH_4^+ strength. Compared to the other cases, this system included an IEX step before BPMED, to remove NH_4^+ and then enriched in the acidic product, produced by BPMED, and eventually purified and recovered in membrane contactor, without the addition of acid and base. The overall removal efficiency was 97% and recovery efficiency started from 9% to 74%, with energy consumption 8.12 to 11.9 kWh/kg-N removed. Finally, Saabas and Lee (2022), examined the most suitable experimental configuration and the most appropriate operational conditions. The highest NH_3 recovery, with the lowest energy consumption was presented for the split-AEM configuration, compared to split-CEM configuration and separate base loop. In this case, the configuration used the X^-/OH^- substitution and the sulfate (SO_4^{2-}) ions in the base migrated to the acid compartment and were replaced with OH^- from the BPM. The increasing of base-acid volume ratio had the largest impact on NH_3 recovery, while the system recovered up to 68% of the theoretically recoverable NH_3. The conclusion of this study was that the NH_3 recovery could be further increased by increasing the base-acid volume ratio, by using a higher initial pH or by using a 3-compartment BMPED.

2.3 Selective electrodialysis

The need to separate specific ions from any solution, based on the porous size or based on the compound's charge, created the necessity to develop a new method, called Selective Electrodialysis (SED). In this case, ED is equipped with selective cation or anion exchange membranes and employ the fractionation of valuable nutrient compounds (Ye et al., 2019). In that process, there is either an anionic or cationic membrane, based on the ions that needed to be fractionated and the production of two streams, a diluate and a concentrate. Monovalent and divalent ions are separated as well, while the later ones are retained on the membrane (Reig et al., 2016). More specifically, when a current is applied, cations migrate towards the cathode and anions towards the anode. Thus, the monovalent cations (NH_4^+, Na^+, K^+) migrate through CEM which have negative fixed groups and are retained by the AEM which have positive exchange groups. The divalent cations (Mg^{2+}, Ca^{2+}) are blocked by the monovalent selective CEM and moved to the desalting compartment. This migration leads to an increase of the monovalent ion concentration in the concentrate compartments and a decrease in the diluate compartments (Chen et al., 2018).

The implementation of SED was researched in case of NH_4^+ recovery, in combination with phosphorus separating recovery, from Kedwell at al. (2021), where the nutrients were extracted from digester supernatant and a 4-compartment SED was used to extract NH_4^+ and phosphate in two separate compartments. The NH_4^+ recovery was 18 times higher than the one of phosphate, with average recovery of 72±1% and 90±10%

respectively after 3 hours of operation. Another study (Ye et al., 2019) evaluated the application of selective anion and cation exchange membranes into a membrane stack for nutrient recovery. The results revealed that nutrient recovery was achieved by fractionating PO_4^{3-} and SO_4^{2-} into the anionic product stream, the divalent cations were extracted into the cationic stream and the monovalent cations, such as NH_4^+, K^+ were concentrated into the brine stream. Finally, the permeation sequence for the cations was $NH_4^+ \sim K^+ > Ca^{2+} > Mg^{2+} \sim Na^+$.

SED has been investigated in nutrient recovery, to separate PO_4^{3-} and SO_4^{2-} into an anionic product stream and a cationic (Ye et al., 2019). In the anionic, the divalent cations (Mg^{2+} and Ca^{2+}) were extracted, while in the cationic the monovalent cations (Na^+ and NH_4^+) were concentrated. In that case, both monovalent selective cationic membrane and monovalent selective anionic membranes were used, a constant voltage was applied (6,8 and 10 V each time), while the pH of the system was retained constant at 10.0. Three different streams were produced, a brine composed NH_4^+ and K^+, a cationic with Mg^{2+} and Ca^{2+} and finally an anionic with PO_4^{3-} and SO_4^{2-}. In addition, monovalent selective anionic membrane was used in the fractionation of Cl^- and SO_4^{2-} from wastewater (Reig et al., 2016). For that research, two different streams were produced, a NaCl-rich stream and Na_2SO_4-rich stream, and the system was followed by BPMED to produce HCl and H_2SO_4.

Another research investigated the cation selectivity of concentrate RO brines through ED. In this case, the selectivity of Mg^{2+} to Na^+ and Ca^{2+} and Na^+ were evaluated (Reig et al., 2015). Since, the ionic radius of Ca^{2+} is somewhat larger than that of Na^+, even though the charge is doubled in an electrical field with higher voltage, it seems to more attract toward the cathode than Na^+ and thus the selectivity is higher. Finally, Cohen et al. (2018), tested groundwater upgrading by removing the monovalent SED. The optimal removal ratio of Na^+, Ca^{2+} and Mg^{2+} ranged between 40-70%, with the lowest mean removal ratio to be the one of Mg^{2+}.

2.4 Key performance parameters

2.4.1 Current density

During ED the ions transferred through the membranes are carrying current which is flowing through the membrane, applied in its surface area. This value is called current density. More specifically, the total summation of ionic charges passing through a solution is the current density, integrated over the whole cross-sectional area and it can be estimated by Faraday's equation (Luo et al., 2018):

$$i = \frac{I}{A} = F \sum_{i}^{n} |z_i| \, J_i \qquad (2.1)$$

Where i is the current density (A/m^2), I is the current (A) and A is the effective membrane surface area (m^2) for ion transport through ED.

2.4.2 Transport efficiency

Current efficiency is an important parameter that measures the number of ions transported from the feed solution during a specific time interval and the total amount of charge passed through the membrane (Sadrzadeh and Mohammadi, 2009). Membrane's performance could be described by current efficiency or transport efficiency for a specific process in different operating conditions. Current efficiency or else transport number could be estimated for every ion included in the system through formula (2.2).

$$n_{NH_4^+} = \frac{z \cdot F \cdot \Delta M_{NH_4^+}}{N \cdot \sum_{t=0}^{t} I_t \cdot \Delta t} \qquad (2.2)$$

Where n_{NH4+} is the current efficiency (%), z is the ion valence, F is the Faraday constant (s-A /mol), ΔM is the mass of transported species (mol), N is the number of pair cells, Δt is the time interval and I_t is the current during that time interval (A).

2.4.3 Energy consumption

To remove NH_4^+ from a solution through ED high levels of energy are needed. Energy is described as the energy consumed per kg of N removed from the feed. It is an important parameter in comparing the different applied techniques and investigating the most efficient energetically. Energy consumption is described as follows:

$$\mathrm{E}_{\mathrm{NH}_4^+} = \frac{\sum_i^n \mathrm{Current} \cdot \Delta t \ \cdot \mathrm{Voltage} \cdot 3.6}{\Delta \mathrm{M}} \qquad (2.3)$$

Where Current (A) is the current applied in the cell, Δt (sec) is the time step, Voltage (V) is the voltage applied, ΔM (kg of N) is the mass difference of the feed stream from the starting point till the end point.

2.4.4 Removal efficiency

In ED the total mass of the target ion that has been transported from the feed compared to the initial value is being estimated as the removal efficiency of this ionic species. This could be calculated through equation (2.4):

$$\mathrm{R.E_i} = \left(1 - \frac{\mathrm{M_i^{dil,end}}}{\mathrm{M_i^{dil,start}}}\right) \cdot 100\% \qquad (2.4)$$

Where RE_i is the removal efficiency of each specific ion (%), $M_i^{dil,end}$ is the final mass of the ion (mol) and $M_i^{dil,start}$ is the initial mass of the ion (mol) in the diluate.

2.4.5 Water transport

During ED, membranes selectively remove ions or charged molecules, to produce clean water. However, even though they have fixed charge, they let counterions to pass through them, such as water molecules. Membranes cannot be considered as ideally selective barriers, because of that phenomenon, as result the decrease of performance in ED (Tedesco et al, 2017).

Water transport is an important parameter for ion exchange membranes which gives an insight into the membrane structure and ion transport mechanism. This knowledge helps to understand the mechanism of “proton leakage” through anion-exchange membranes, their selectivity and the electrokinetic phenomena. Larchet et al. (2004) proposed two methods to estimate the water transport number: the one consists in the calculation from the counter-ion apparent transport number, membrane electric conductivity and diffusion permeability, while the second demands only the apparent transport number knowledge and the counter-ion transport number which is being supposed to be equal with 1. In this research, for simplicity the water transport number will be estimated through equation (2.5).

$$\mathrm{t_w} = \frac{\mathrm{V_{initial}}\,\rho_\mathrm{w} - \mathrm{V_{final}}\,\rho_\mathrm{w}}{\mathrm{V_{initial}}\,\rho_\mathrm{w}}\ 100\% \qquad (2.5)$$

2.4.6 Proton and hydroxide production from bipolar membranes

During a current application in a BPM, water dissociation occurs where H^+ and OH^- are produced and transferred to the acidic and to the basic compartment, respectively. The first one who studied water splitting in BPM was Frilette (1956), by using a multi-chamber cell. In this case the electric current passed and the individual chambers were drained. When low current densities were applied, the initial voltage rose rapidly. At higher current densities, polarization of the membrane appeared faster, having at the same time an increase in Coulomb efficiency for H^+ ion transfer, because of water dissociation (Tanaka, 2007).

A BPM consists of three parts, a cation selective region, an anion selective region and the interface between them. When a direct current is passed across the membrane with the cation selective side toward cathode, electrical conduction is achieved by the transport of H^+ and OH^- ions which are obtained by water dissociation. Efficient operation could be done when the membrane has good water permeability to provide water from the external solution to the interface and when the interface between anion and cation regions allows transport of H^+ and OH^- (Mani, 1991).

Water splitting is electrodialytic in nature, because the process merely involves changing the concentration of ions that are already present in solution. More specifically, the free energy change in going from the interior of the membrane to the outside is given by (Mani, 1991):

$$-\Delta G = nFE = RT\ln[(\alpha^{i}_{H+}\alpha^{i}_{OH-})/(\alpha^{o}_{H+}\alpha^{o}_{OH-})] \quad (2.6)$$

Where α corresponds to the activities of H^+ and OH^- ions, superscripts i and o refer to the interface and the outer surfaces of the membrane respectively, F is the Faraday constant, E is the reversible electromotive force (V), R is the gas constant, n represents the number of equivalents/mole of reactant and T is the absolute temperature.

In addition, in the operation of BPM there are ohmic resistances associated with ion transport in the acid, salt and base and through the cation, anion and BP membranes. The energy requirement in that case could be given by formulas (2.7) and (2.8).

$$E_{cell} = I_d(\Sigma R_m + \Sigma R_{sol}) + E_0 = I_d R_T + E_0 \quad (2.7)$$

$$P = 10AI_d E_{cell} = 10A\left(I_d^2 R_T + I_d E_0\right) \quad (2.8)$$

Where A is the effective membrane area (m^2), I_d is the current density (A/cm^2), R_m and R_{sol} are the individual resistances of the membranes and solutions (Ω-cm^2), E_{cell} is the unit cell potential (V) and P is the power requirement (kW).

2.4.7 Percent demineralization

Another parameter to evaluate the performance of an ED process is the Percent Demineralization (%) which is expressed as the ratio of EC difference between the initial and final EC in feed solution with the initial EC (Al-Amshawee et al., 2020). Analytically:

$$PD\,(\%) = 1 - \frac{EC_{final}}{EC_{initial}} \quad (2.9)$$

Where EC_{final} is the EC at the end of operational cycle in the feed solution and $EC_{initial}$ is the EC at the beginning of the process of the feed (mS/cm^2).

2.5 Electrochemical processes

2.5.1 Electrochemical potential

In ED an electrochemical potential should be applied to create flux between the different compartments. This means that electrochemical potential difference between diluate, where the concentration of ions is high, and concentrate, could create the flux. For this phenomenon, the Nerst-Planck equation can be used where most of the transport properties are unknown or where the complex interactions and phenomena are being investigated with simpler equations. The concentrated-solution approach could be described with the following equation (2.10).

$$d_i = c_i \nabla \mu_i = \sum_{j \neq i} K_{i,j}(v_j - v_i) \qquad (2.10)$$

Where d_i is the driving force per unit volume acting on species I and can be replaced by an electrochemical potential (μ) gradient of species.

2.5.2 Ion migration in ED

In ED ion migration from diluate to the concentrate is one of the most important parameters and it could be described by the Nerst-Planck equation. More specifically, the equation below (2.11) describes the ion transport in an electrolyte solution.

$$J_j = -D_j \frac{dc_j}{dx} + \frac{D_j z_j e E c_j}{kT} \qquad (2.11)$$

Where D_j is the diffusion coefficient for the ion z_j, is its charge, c_j the concentratrion of the ion in the supported liquid membrane, x the distance from the supported liquid membrane and acceptor interface, k the Boltzmann's constant, e the elementary charge and T is the absolute temperature. The first term describes the diffusion of the ionic substance in the supported liquid membrane and the second term describes the electromigration (Gjelstad et al., 2007).

2.5.3 Back diffusion

One of the main applications of ED is concentrating different salt effluents. However, one of the main problems that could arise is the back diffusion of ions. In a conventional ED the AEM and CEM are placed in an alternating pattern between the two electrodes. IEX membranes face on the one side a concentrated solution and on the other side a diluted solution. This concentration gradient leads to back diffusion of ions from concentrate to diluate (Rottiers et al., 2014). Therefore, a large diffusion constant before prevents a large concentration gradient across the membrane. In addition, for ED configurations with applied current densities above 50 A/m^2 energy losses, due to water transport and back diffusion together, could occur and can be less than 20% of the total losses (Galama et al., 2014). The main energy loss in the system is membrane stack resistance.

From previous research (Öner et al., 2021), in a BPMED system for mixed salt-water treatment, back diffusion from acid and base compartments, was enhanced by low salt concentration, which increases the transfer resistance in the salt compartment. Especially in batch BPMED, back diffusion of ions increases due to decrease of ions concentrations with time. However, increasing the applied current to increase electrical potential back diffusion could be prevented. Water dissociation and ion migration accelerate with the increase of applied potential and current, the processing time decreases, which prevents the co-ion and back diffusion between the adjacent compartments, and NH_3 loss (Öner et al., 2021).

2.5.4 Osmotic and electro-osmotic transport

It is important to note that during ion transport there is always water transport through the membrane, determining the overall efficiency of the system. Supposedly, the current applied targets the charged species but the ion transfer is always associated with water transfer that results from kinetic coupling with ion fluxes under current. This phenomenon is called electro-osmosis (Strathmann, 2004). The amount of water that each ion can carry is related to its corresponding hydration number. When both salt and water flux are known in a system, it is possible to determine the salt hydration number (Han et al., 2015).

In addition, in ED there is osmotic flux, due to chemical potential gradient across the membrane. However, when an electric current is applied in ED the water flux related to osmosis could be neglected compared to electro-osmosis (Borges et al., 2008). Therefore, the salt hydration number could be defined as the number of mol of water per mol of salt, knowing the simultaneous transfer of salt and the associated water as shown below (2.12).

$$n_h^S = \frac{\frac{j_w}{V_m^w}}{j_S} \quad (2.12)$$

Where V_m^w is the molar volume of water (m^3/mol), j_s the salt transfer and j_w is the water transfer. In general, the estimation of hydration number is a complex procedure and needs a lot to be considered.

The electro-osmotic water transport is being estimated by the following equation (2.13).

$$\theta_{H_2O,e\text{-}o} = \frac{(n^i_{NH4,d} - n^f_{NH4,d})(T_w^{NH4} + T_w^{HCO3}) \times MW_{H2O}}{v_{i,d} \times \rho_{H2O}} \times 100\% \qquad (2.13)$$

Where $\theta_{H2O,e\text{-}o}$ is the electro-osmotic water transport, $n^i_{NH4,d}$ and $n^f_{NH4,d}$ is the concentration of NH_4^+ in the diluate initially and finally respectively (mol/L), T_w^{NH4} is the hydration number of NH_4^+ and T_w^{HCO3} is the hydration number of HCO_3^-, $v_{i,d}$ is the initial volume of the feed (L) and ρ_{H2O} is the density of water (kg/m^3). Also, osmotic transport is being calculated as follows from (2.14).

$$\theta_{H_2O,o} = \theta_{H_2O,t} - \theta_{H_2O,e\text{-}o} \quad (2.14)$$

2.6 Scaling in ED

The presence of Mg^{2+}, Ca^{2+}, SO_4^{2-}, CO_3^{2-} and other multivalent ions in solutions treated by ED could lead to scale formation, which takes place from both sides of the membranes facing diluate and alkaline compartments (Andreeva et al., 2018). This phenomenon causes an increase in the electrical and hydraulic resistance of the membrane stack, leading to higher energy consumption and reducing the possibility of long-term operation. More specifically, scaling relates with the deviation from solubility equilibrium, deposition of particles on membrane is mainly due to the presence of the abovementioned compounds. Water splitting at the depleted interface of a CEM produces OH^- ions, which increase the pH of the near surface solution, leading to formation of precipitates such as $Mg(OH)_2$ and $CaCO_3$ in the diluate compartment (Andreeva et al., 2018).

In addition, the membrane characteristics can play an important role in scaling formation. Based on Hoek et al. (2003), colloidal deposition can be enhanced on rough RO and NF membrane surfaces. Thus, rough membrane surfaces are more prone to scaling formation compared to smoother. Finally, the homogeneity of a membrane could affect the scaling formation on its surface. A study was conducted by Asraf-Snir et al. (2016), to evaluate the gypsum scaling of an anion exchange membrane in ED. The results indicated that scaling directly affects the properties of the membrane and thus the overall stack resistance and the extent of water splitting. However, the more heterogeneous the membrane is, the higher the scaling effect will be. In the case of homogeneous membrane, scaling formation was limited on the membrane surface, whereas a heterogeneous membrane presented precipitates also internally. Therefore, the overall stack resistance is highly dependent on the membrane type and structure (Asraf-Snir et al., 2016).

3 Materials and Methods

In this chapter the analytical methods used during the experimental period are described and the equipment required, including the set-up established in the Waterlab. The monitored parameters and necessary formulas for their calculation are also reported in this chapter, while in the Methods section the experiments conducted are described in detail.

3.1 Materials

The basic technology used in the experiments was an ED cell, with 3 inputs and 3 outputs, given by Redstack BV. Based on the membranes used and the phase of the procedure the experiments are divided into different phases which will are described in Chapter 3.4.

The main operational phases, and thus the different configurations established were:

- A Bipolar-Cation Exchange configuration with 5 pairs of membranes (5 cells stack), 2 CEEMs, 5 BPMs, 5 CEMs, 10 flow-spacers and 2 electrode spacers.
- An ED configuration with 5 pairs of membranes (5 cells stack), 2 CEEMs, 5 AEMs, 5 CEMs, 10 flow-spacers and 2 electrode spacers.

The flow spacers used had thickness of 500 μm. All membranes placed in the stack had an effective surface membrane area of 0.10×0.10 m.

3.2 Analytic material and equipment

The analytical equipment used for the conduction of the experiment was:

- Membrane stack: A membrane stack from REDSTACK BV was used where the outer part consisted of the electrode cells (anode and cathode), the spacers and the membranes. In case of BPC, bipolar and cation membranes were placed, for ED there were anion and cation membranes.
- Electrical conductivity (EC), pH and temperature meter: during the experimental period conductivity and pH of diluate and concentrate/base were measured through one ‘WTW IDS digital conductivity cells Tetra Con®925’ and one ‘WTW universal IDS pH-electrodes Sen-Tix®-940’, connected with 3 probes each. The data reported was stored and transferred to a laptop for further analysis. The recording time was set to 5 seconds per measurement.
- Power supply: For this experiment a power supply ‘TEMNA 72-2535’ was used, set on constant current of 0.5 A and variable voltage of below 30 V. The measurements were recorded every second, while the data was collected automatic via the log in of the laptop with the power supply.
- Magnetic stirrers: inside every bottle a magnet was placed to ensure completely mixed conditions and to avoid any salt precipitation in the bottom. During the entire duration of the experiment, the rpm of the stirrer was constant.
- Sample analysis IC: the bulk of samples taken from each experiment were analyzed via ion chromatography (IC). Consisted of a Metrohm 919 autosampler, IC 818 anion system and 883 IC cation system the concentrations of ions in the samples were estimated. In this study, only the concentrations of cations, such as NH_4^+, Na^+, K^+, Mg^{2+} and Ca^{2+} were estimated. The dilutions differed since they were dependent on the initial concentrations of each salt at the beginning of the experiment. The system is connected to the computer with the MagicIC Net software, where it links the peak detection of standards to that of samples.
- Sample analysis photometry: In case of simple experiments where diluate contained only NH_4^+ the samples were analyzed by a ‘Macgerey-Nagel Spectophotometer NANOCOLOR’. For this purpose,

HACH kits for ammonium LCK 303, with range 2.0-47.0 mg/L NH_4-N, were used and the measurement was done in 694 nm. For more complex composition of the solution IC analysis was conducted.

- Watson Marlow 520s peristaltic pump: To supply the membrane cell, a peristaltic pump was used for the concentrate/ base (depending on the experiment) to recirculate the solution in the entire set-up. A calibration was done approximately every two weeks to accomplish the highest accuracy in the chosen flow. Thus, the rpm of the pump was approximately stable during the entire experimental phase.
- Masterflex peristaltic pump: For the feed supply in the membrane cell a second peristaltic pump was used. The solution was also recirculated as in the case of concentrate/base. A calibration was conducted in this pump to reassure that the resistance does not affect the chosen flow.

3.3 Experimental setup scheme

The experimental set-up was established in Waterlab where the analytical equipment described below (Figure 3.1) was used.

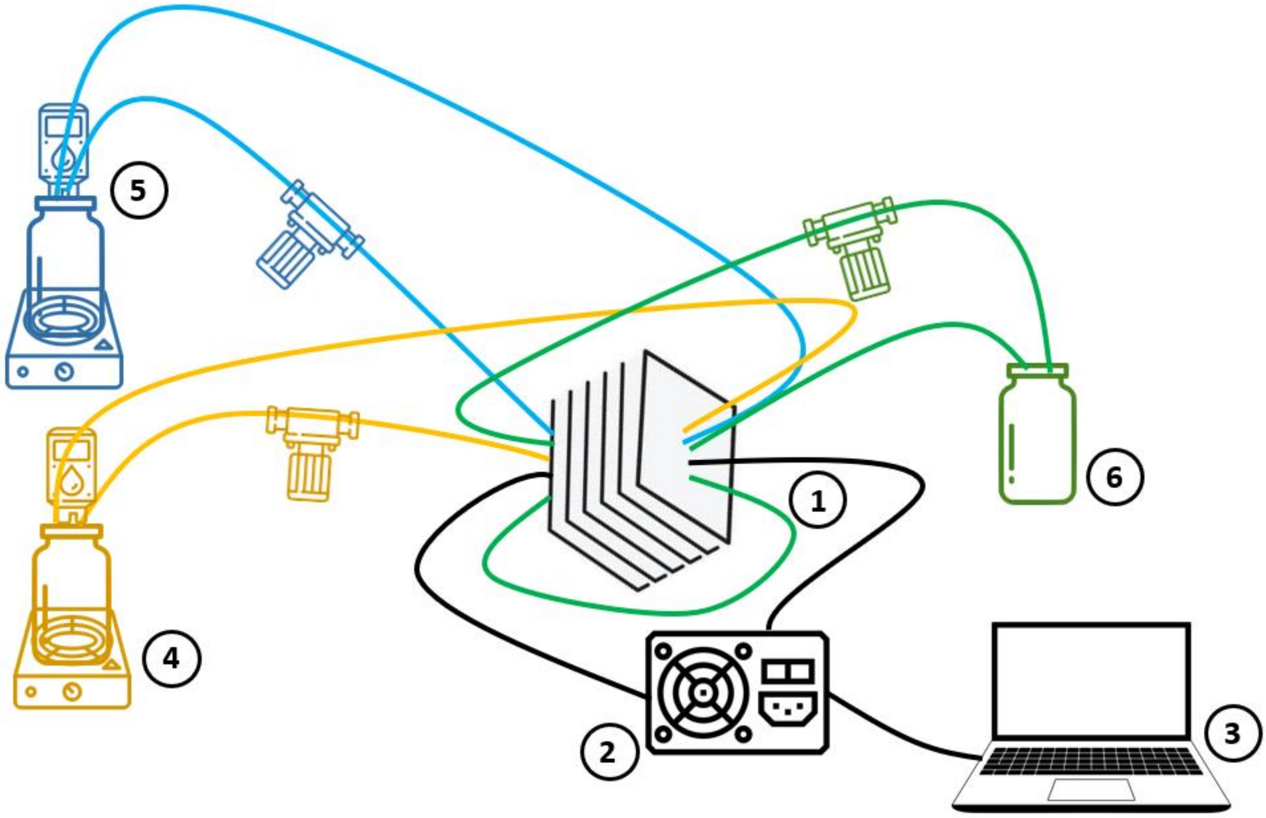

Figure 3.1. Experimental set-up established in Waterlab. The following equipment was used: (1) Membrane stack which included the membranes needed for each experimental phase, (2) Power supply with constant current and maximum applied voltage 30V, (3) Laptop to record the data from power supply, (4) Feed or diluate with initially synthetic water contained the specified cations, (5) Concentrate or base compartment (depending on the experiment conducted in each case). In case the stack was used for electrodialysis the compartment was the concentrate, while when it was operated as a BPC it was the base, (6) Electrode rinse solution.

All the batch experiments were independent of each other and they were conducted with the same equipment. The flow for both diluate and concentrate/base was set at a constant value of 19 L/h and there was a recirculation of each through a peristaltic pump. As for the volume of each compartment, it was set to 1 L and for the ERS the value varied between 0.3 to 0.4 L as initial volume. Finally, the current applied in the stack was constant and equal to 0.5 A, while the maximum voltage was 30 V.

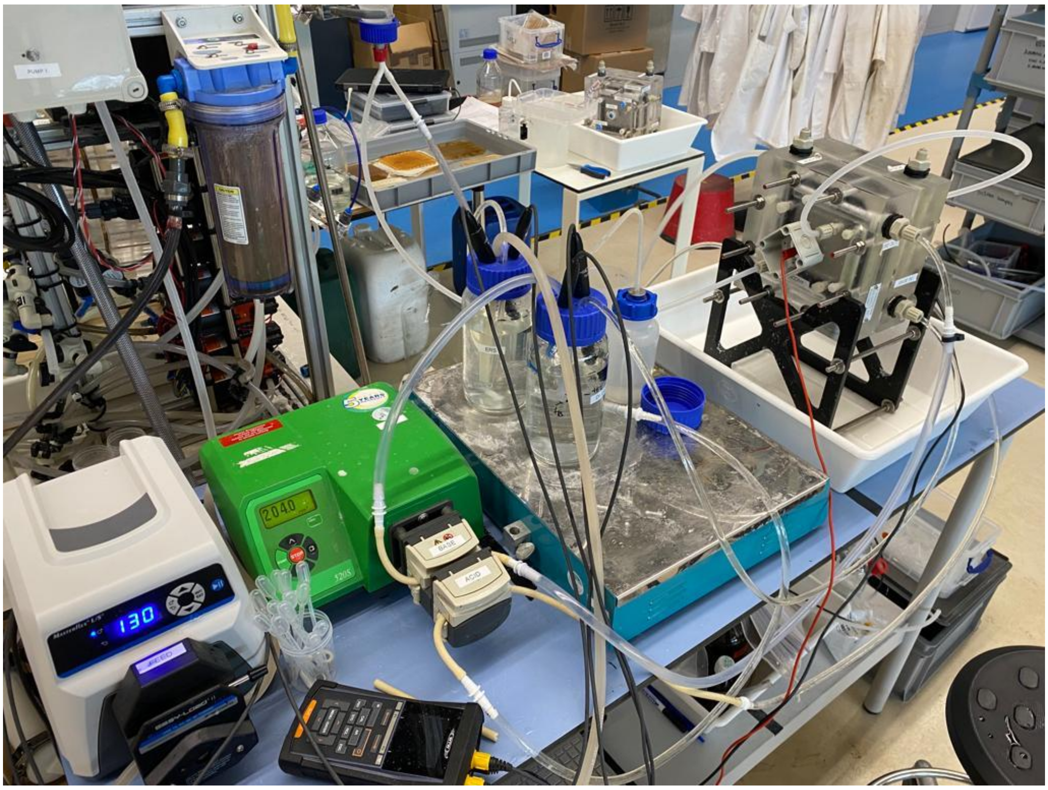

Figure 3.2. Experimental set-up in WaterLab. On the left side the feed, electrode rinse and concentrate pumps are presented. On the middle the feed and concentrate solution are stirred with a magnetic stirrer and on the right side the stack with the membranes is being placed.

3.4 Methodology

3.4.1 Experimental plan

The batch experiments that were conducted had the same operational conditions, as far as possible. Also, the chemicals used for stock solutions to add the corresponding salts were the following:

- For NH_4^+, NH_4HCO_3 was used.
- For Na^+, Na_2SO_4 was used.
- For K^+, three different chemicals were used depending on the experiments. In the experiments where mass ratio was used, K^+ was added as K_2HPO_4, while in the molar ratio experiments K^+ was added as KH_2PO_4. Finally, for the sequence batch experiments K^+ was added in the form of KCl. The latter one was considered as the optimal solution because the presence of PO_4^{3-} leads to scaling formation easier than Cl.
- For Mg^{2+}, $MgCl_2$ was used.
- For Ca^{2+}, $CaCl_2$ was used.

3.4.2 Bipolar-Cation configuration and experiments

Firstly, a BPC system was operated with different cationic mass ratios. Feed solution was synthetic water, and the stock solutions were prepared independently of the experiments. In Table 3.1 the exact tested ratios are presented including the concentration of each cation in the feed solution.

Table 3.1. Concentrations of cations in feed solutions for the mass ratio experiments

Experimental code	**Mass ratio**	**NH_4^+ (g/L)**	**Na^+ (g/L)**	**K^+ (g/L)**	**Mg^{2+} (g/L)**	**Ca^{2+} (g/L)**
NH_4	1	1.500				
NH_4 + Na	1:1	0.750	0.750			
NH_4 + Na + K	1:1:1	0.500	0.500	0.500		
NH_4 + Na + K + Mg	2:2:2:1	0.375	0.375	0.375	0.188	
NH_4 + Na + K + Mg + Ca	2:2:2:1:1	0.300	0.300	0.300	0.150	0.150

For electrode rinse solution (ERS) a solution of Na_2SO_4 was used with concentration of 20 g/L. This solution was reused for some experiments and thus the concentrations of cations were measured each time for every batch to be taken into account for the final mass balance.

3.4.3 Electrodialysis configuration and experiments

The same experiments were conducted also for an ED set-up to estimate the difference in energy consumption and NH_4^+ transport number. BPMs were replaced with AEMs and the applied mass ratios were the same as indicated in Table 3.1.

In addition, in the next phase of experiments, different molar ratios were tested, keeping the amount of added NH_4^+ the same in every batch to evaluate the transport number of NH_4^+ in different compositions. The molar ratio is defined in the equation (3.1).

$$\text{Molar ratio n} = \frac{n_{NH_4^+}}{n_{cations}} \qquad (3.1)$$

Where n_{NH4+} is the amount of NH_4^+ added (moles) and $n_{cations}$ is the summation of all cations in the feed (moles). The cations added in the feed solution are kept the same in all experiments. However, their concentration differed based on the experiment.

More specifically, the amount of NH_4^+ added was equal to 0.4 g while the amount of the rest is presented in the Appendix. The ratio of other cations added was determined based on a reference of real reject water from Horstermeer in Waterlab, which was between 0.60 and 0.64 respectively. However, a wider range was chosen in order to cover a wider area in our study. Molar ratio could be between 0 and 1, but since the molar ratio of 1 was already investigated in the previous experimental plan it was further neglected. Moreover, lower than 0.30 molar ratios were neglected due to practicality issues. Feed water for molar ratio below 0.30, by keeping the amount of NH_4^+ the same, was highly condensed and not entirely diluted in demi-water, leading to fouling of canals and tubes of the configuration. The chosen molar ratios for this experimental phase are presented in Table 3.2.

Table 3.2. Molar ratios applied for molar ratio experiments.

	Molar ratio
n_{NH4} / $n_{cations}$	0.30
	0.45
	0.60
	0.75
	0.90

3.4.4 Selection of molar ratio range

In order to estimate the effect of the amount of specific cations in the feed solution, a range of molar ratios was tested. The range was chosen based on already tested molar ratios in conventional ED, but also on the existing reject water in WaterLab that was used for the project Circulaire-N. As mentioned in Chapter 3.4.3, the range was between 0.30 and 0.90, with the amount of NH_4HCO_3 being the same for any ratio and variation of the supplementary salts. Main goal of this question was to investigate whether the removal efficiency and energy consumption depend on the amount of available NH_4^+ on the feed and independent from ion competition with Na^+, K^+, Mg^{2+} and Ca^{2+}.

Reject water of interest was collected from the WWTP in Horestermeer, which treat municipal wastewater, and was used also in the experiments with real reject water, as shown in Appendix. In case of Horestermeer, the cationic molar ratio was between 0.64 to 0.66 (based on the three tested configurations). The ratio between NH_4^+ and each individual cation was also an important point of interest to be investigated, to resemble as much as possible the real reject water composition. In case of a later sample from the same WWTP, the cationic molar ratio was 0.59, while both cases presented approximately the same ratio of NH_4^+ to any individual cation.

In addition, based on Wang et al. (2022) research two different types of digestate were tested, a mature digestate (MD), where it was the effluent of an anaerobic reactor with hydraulic retention time (HRT) of 28 days, and a fresh digestate (FD), which only experienced a day of pre-hydrolysis. Both digestates were collected from two different full-scale biogas plants in Shanghai, fed with catering food waste and operated in continuous stirred tank reactors, under mesophilic conditions. For the two different digestates, there were two corresponding cationic molar ratios. In case of MD the molar ratio was 0.59, with the difference that the form of N in digestate was NH_3, while for FD it was approximately two times lower and equal to 0.36. Another research (Wang et al., 2023) investigated the recovery of P from digestate through electrochemical leaching and precipitation, where the cationic molar ratio was 0.94, without the presence of Na^+ and K^+. Therefore, the selected range of cationic molar ratios was between 0.30 and 0.90, while the step was chosen to cover as many cases as possible in the given experimental time period.

3.4.5 Reject water

Additional experiments were conducted to test real reject water in three types of configurations. Tested reject water was collected from Horstermeer. More specifically, for the first type of experiment a conventional ED was operated. Then, a BPC was used, by replacing the AEMs with BPMs. Finally, this experimental phase closed with the operation of a combination of BPM and mono-selective cation exchange membrane. The results of those experiments are presented in the Appendix.

3.4.6 Sequence batch experiments with application of ED and BPC

As a final step SBE were conducted with synthetic water, with molar ratios of 0.30, 0.45 and 0.6. Initially, 1 L of feed water was treated with conventional ED until the EC reached the corresponding set-point that removal efficiency of NH_4^+ was 75%. In this case the feed bottle was changed by a new solution and the procedure was repeated until the EC of concentrate reached 20 mS/cm. In addition, the initial EC of the concentrate was 1 mS/cm in order to abet the ion migration from the feed solution and avoid the voltage peaks due to high salinity difference. Then, the concentrate of EC equal to 20 mS/cm was treated with a BPC system until the diluate reached acidic pH and EC started to increase, after reaching its corresponding minimum.

3.5 Sampling and Data analysis

During the experimental period samples from both diluate and concentrate/base were taken to measure the concentration of cations in them. For that purpose, Eppendorf vials of 1.5 mL and Pasteur pipettes were used and the samples were stored in the fridge in 4°C until the IC analysis was taken place, in the same or next day. Samples were taken every 5 minutes from the starting point of the experiment until the end. In addition, both final and initial samples were taken with the same procedure. However, for the IC analysis the samples that were measured had a time step of approximately 15 minutes, to reduce the overall cost of the experiment and maintain the accuracy of the method.

For samples preparation the corresponding dilution range was estimated based on the expected concentration of cation. The IC measurement range for an IC cation 883 is between 0 to 15 mS/cm and thus the range of dilution factors was between 0-100, depending on the conducted experiment and sample. In the IC measurement, nitric acid with concentration 0.1% was used to acidify the samples and avoid precipitates formation.

To answer the research questions, the parameters that were measured were:

- pH and EC for diluate and concentrate or base, depending on the configuration, with time step of 5 seconds
- applied voltage and current with time step of 1 second.
- the concentration of cations (NH_4^+, Na^+, K^+, Mg^{2+} and Ca^{2+}) in both compartments.
- the volume of each compartment for the time of sampling.

Based on those parameters the calculations conducted were referred to:

- removal efficiency of the system for NH_4^+.
- energy consumption per kg N removed.
- proton production, in case bipolar membrane operation.
- percent demineralization of the diluate.
- water transport.
- osmotic and electro-osmotic water transport.
- transport efficiency of NH_4^+ and for the rest cations present.

4 Results

In this chapter the results from the experiments are presented and to finally help in answering the main research questions.

4.1 Batch experiments

4.1.1 Mass ratio in BPC

During the operation of BP with CEM the operational parameters and conditions were recorded. Basic parameters include pH, EC, voltage, current, volume of each compartment and concentration of cations through sampling.

As mentioned above, in BPC operation, due to water dissociation there was H^+ and OH^- production in the acidic and basic compartment respectively. In this research, the focus was mainly in the acidic compartment which was the feed/diluate solution as a 2-chamber system. Thus, the results from diluate compartment are presented in this section.

Firstly, the pH recorded is presented in Figure 4.1 and the H^+ production in diluate with regards to EC in Figure 4.2. The values of H^+ are presented as a concentration on time, taking into consideration that the volume of diluate was approximately constant to 1L during the experimental period, with a variance of less than 3%.

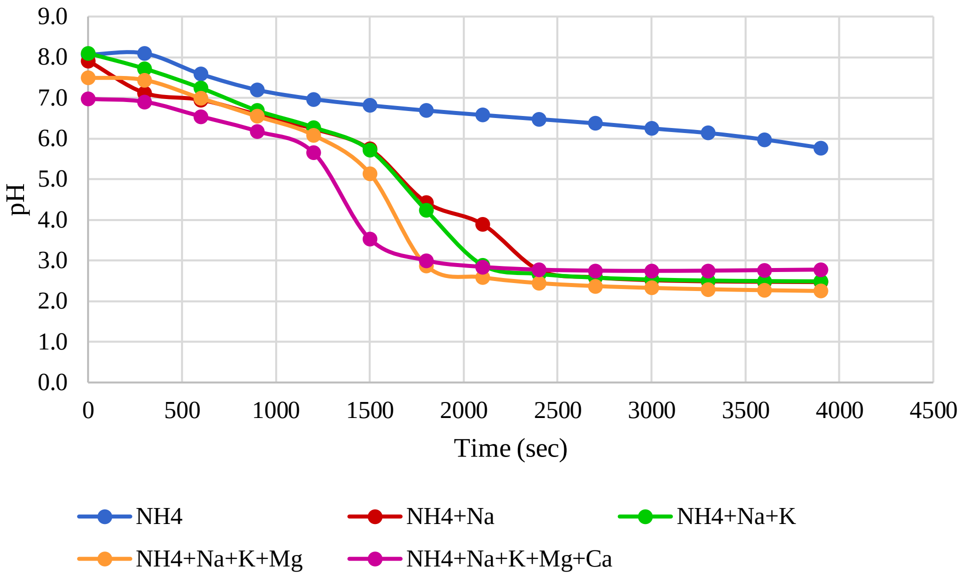

Figure 4.1. pH in diluate during BPC operation for the five different cases on time

In case of non-competition the pH showed a mild drop, from 8.1 to 5.8, to a slightly acidic environment. H^+ production in this case was low with higher concentration of 16×10^{-4} mg/L at the end of the experiment. The small H^+ production could also be attributed to the buffer capacity of HCO_3^- added, with NH_4^+ being in the form of NH_4HCO_3.

For the building-up compositions, the experiments started from the addition of Na_2SO_4. The pH indicated a small reduction until 1500 seconds of operation where the drop was steeper. Starting from 7.9 it reached the pH of 2.6, where it stabilized in 2400 seconds. Proton production was evident after 2000 seconds of operation where it had a major increase until it reached 3.4 mg/L of H^+ in diluate. Moreover, the addition of K^+ led to similar results with the initial pH being 8.1 and the final 2.5. A steep drop was also presented between 1500 and 2000 seconds of operation. The final H^+ concentration in the diluate compartment was 3.3 mg/L. In the next experiment, the additional cation was Mg^{2+}, that was added in form of $MgCl_2$. The pH curve presented a similar trend as before, with 7.5 starting and 2.3 final value. H^+ concentration had an evident increase, compared to the previous case with the final value to be 5.6 mg/L, while the turning point for this phenomenon appeared at 1500 seconds. Finally, the more complex composition with Ca^{2+} led to initial pH of 7.0 and final at 2.8, while the minimum value was observed in 3000 seconds of operation, indicating that probably the experiment did not reach an equilibrium in the operational time. In this case the proton concentration in the feed solution was 1.8 mg/L which was the maximum.

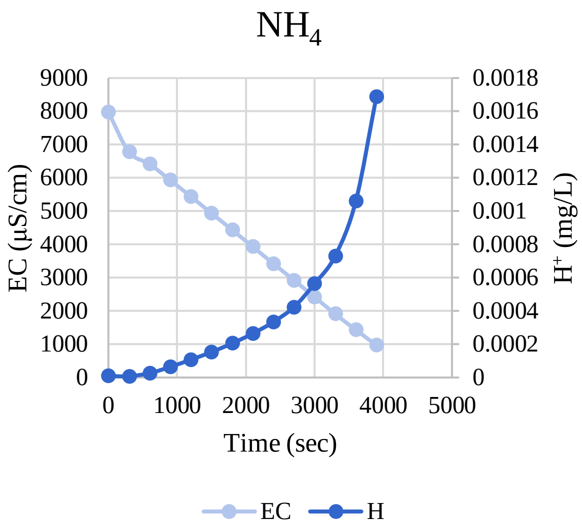

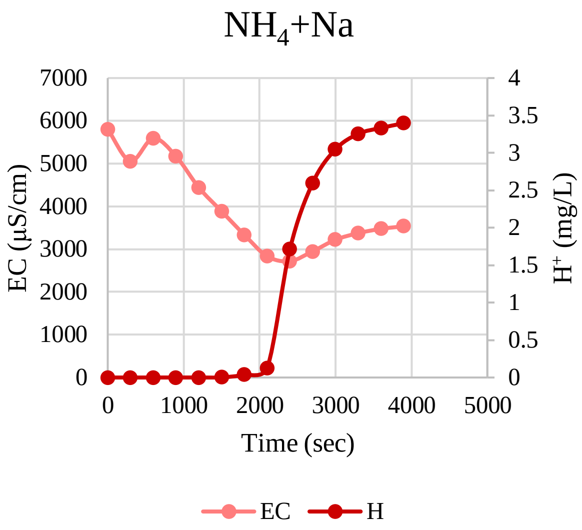

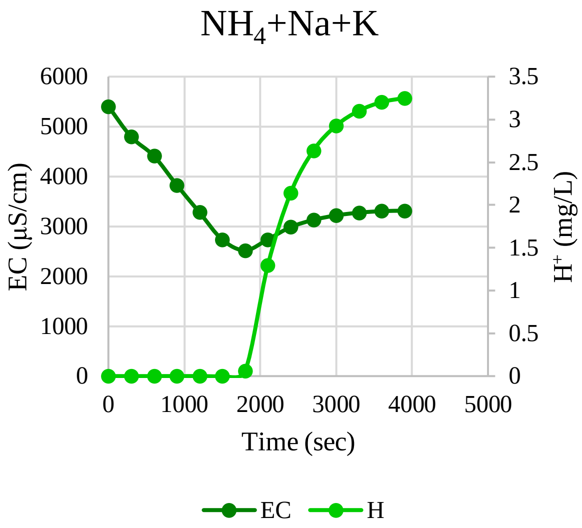

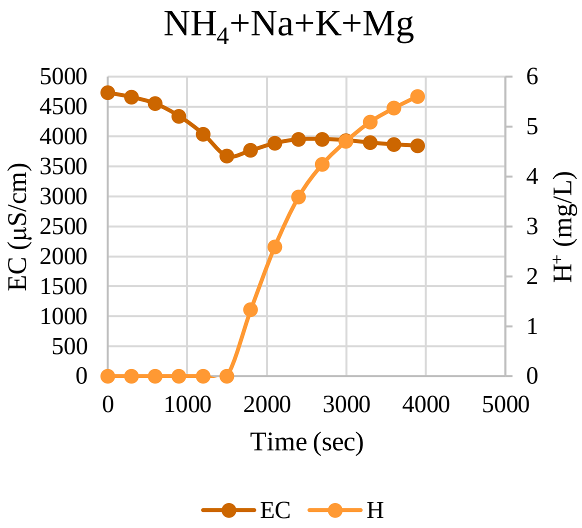

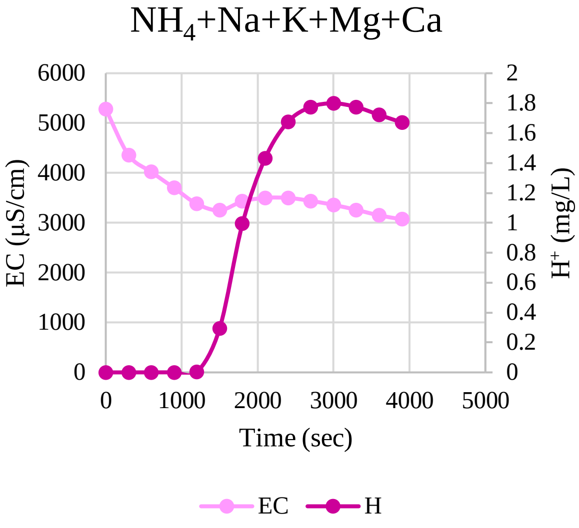

Figure 4.2. EC in diluate for the five cases with the corresponding proton production.

EC was highly related to the concentration of dissolved ions in the solution, indicating that high EC led to higher salinity. For the conducted batch experiments, EC was measured during the entire period and presented in Figure 4.2. Proton production in the diluate is also depicted in order to estimate the effect of proton leakage in each case.

When NH_4^+ was the only ion in the solution the initial EC was 7975 µS/cm and the drop was stable until it reached 971 µS/cm when the experiment ended, whereas in all other cases the EC reached a minimum point or stabilized in the final phase of operation. Proton production presented a stable exponential increase. Moreover, in the second batch with NH_4^+ and Na^+, EC started from 5800 µS/cm, reached a minimum of 2720 µS/cm in 2400 seconds of operation, and increased to 3535 µS/cm at the end. The turning point of the curve appeared at the same time also for the proton production, while stabilization of EC was observed with similar pattern for H^+ as shown in Figure 4.2b. The same pattern was observed also in the other feed solutions, such as when K^+ was added where a minimum EC value was observed at 2520 µS/cm at 1800 seconds of operation of BPC while the final value increased to 3315 µS/cm and reached an equilibrium after 3000 seconds of operation. Proton production on the other side had a steep increase in 1800 seconds of operation. For the solution that contained NH_4^+, Na^+, K^+ and Mg^{2+} the initial EC was lower compared to the other cases and equal to 4735 µS/cm, dropped to the minimum of 3675 µS/cm on 1500 seconds, where then it increased up to 3850 µS/cm. In addition, proton production followed a similar trend as in the previous experiments with an abrupt increase in 1500 seconds until it reached the maximum value of 5.6 mg/L. Finally, for the last batch the initial EC was 5280 µS/cm, the turning point was at 3250 µS/cm at 1500 seconds and at the end it did not show a stabilization and dropped to 3070 µS/cm at the end of operational period. The same phenomenon occurred also in proton production where the steep increase in concentration was at 1500 seconds whereas after 3000 seconds of operation it decreased gradually from 1.8 mg/L to 1.7 mg/L.

Considering the correlation of proton production from BPC and EC in the diluate compartment the conductivity ratio was also estimated as the ratio of EC in time t over the initial EC, in order to approximate the ratio when the proton production was taking place, based on the cations included in the feed solution.

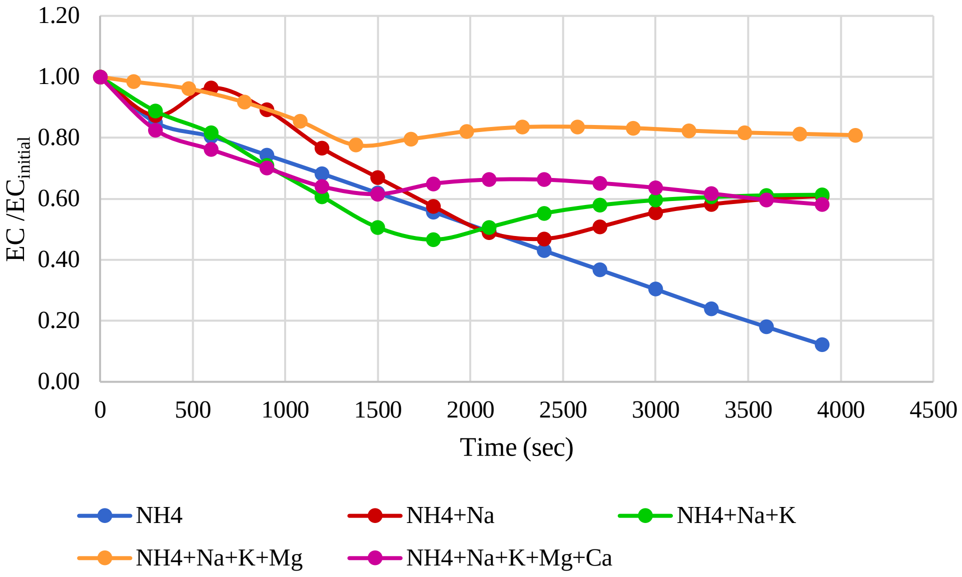

Figure 4.3. EC/EC$_{initial}$ in diluate compartment in the five different cases on time for BPC

The ratio of EC on time with the initial value of EC was calculated as shown in Figure 4.3. When the feed solution had only NH_4HCO_3, EC presented a stable decrease, starting from ratio of 1 and reaching 0.12 at the end, on 3900 seconds. When Na^+ was added, in the first minutes of operation, the ratio presented an instant drop and increased from 0.87 to 0.96, while in 600 seconds it fell gradually, reaching a minimum point on 2400 seconds with 0.47. In the 3rd experiment, the addition of K^+ led to the same trend, with an instant fall of ratio until 1800 seconds of operation and it reached 0.47. Later it increased to 0.61 after 3000 seconds. Then, in case of Mg^{2+} addition in the feed solution, the drop of the EC, compared to the initial EC value, was less noteworthy since the ratio had a minimum of 0.78 at 1380 seconds and stabilized approximately at 1580 seconds to 0.82. Finally, last case, where Ca^{2+} was added, the same trend occurred, with a minimum ratio of 0.62 at 1500 seconds and again increased to 0.65. At the end of operation it reduced to 0.58 indicating a non-equilibration of ratio until that time.

Another important parameter that was estimated was transport number of cations in each experiment and the results are presented in Figure 4.4.

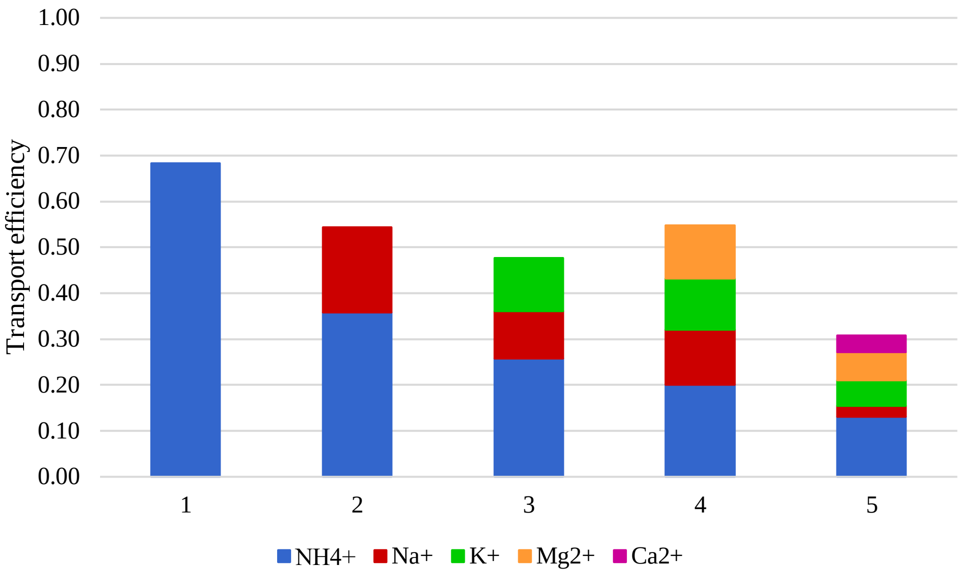

Figure 4.4. Transport number of cations in BPC with application of mass ratios. Experiment 1: NH_4, Experiment 2: NH_4:Na=1:1, Experiment 3: NH_4:Na:K=1:1:1, Experiment 4: NH_4:Na:K:Mg=1:1:1:0.5, Experiment 5: NH_4:Na:K:Mg:Ca=1:1:1:0.5:0.5.

NH_4^+ transport efficiency presented a gradual decrease when more cations were added. Initially, the value for NH_4^+ was 0.68 and when Na^+ was added it fell to half at 0.36. The additional of K^+ led to further decrease to 0.26. Divalent cations had also the same effect of decreasing the transport number of NH_4^+, to 0.20 and 0.13 for Mg^{2+} and Mg^{2+}+Ca^{2+} respectively. As for the other cations, they presented a reduction in their current efficiency, which could be attributed to the addition of salts and reduction of the corresponding salt in the feed solution, as referred in Chapter 3. Thus, the results could not be absolutely comparable due to the difference in added masses.

In addition, one important parameter that indicated the overall performance of the system was removal efficiency of NH_4^+, based on the mass removed from the feed solution. The results are shown below in Figure 4.5.

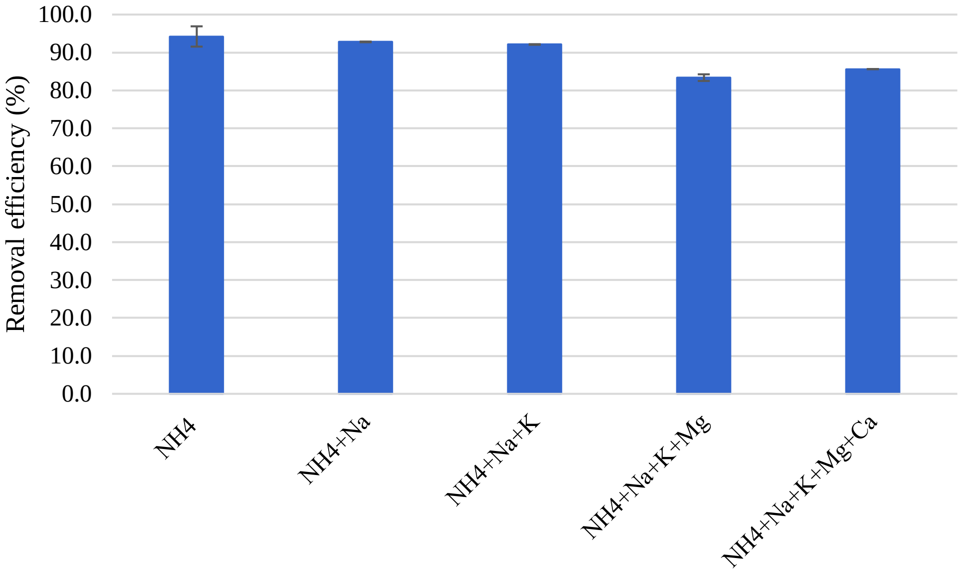

Figure 4.5. Removal efficiency of NH_4^+ in BPC in the five batch experiments. The removal efficiency in this case was calculated based on the initial and final NH_4^+ mass.

In total, when NH_4^+ did not have any competitions removal efficiency was approximately in the same range as in the case of the presence of the other cations. More specifically, in the first experiment removal efficiency was 94.2±2.7% while in the 2nd and 3rd experiment it was 92.8±0.1% and 92.1±0.1% respectively. With the presence of divalent cations led to slightly lower removal efficiency with the case of just Mg^{2+} presence it was 83.4±0.9% and with the case of both cations it was 85.6%.

Removal efficiency was also estimated based on operational time, regarding the required removal efficiency. The results are presented in Figure 4.6.

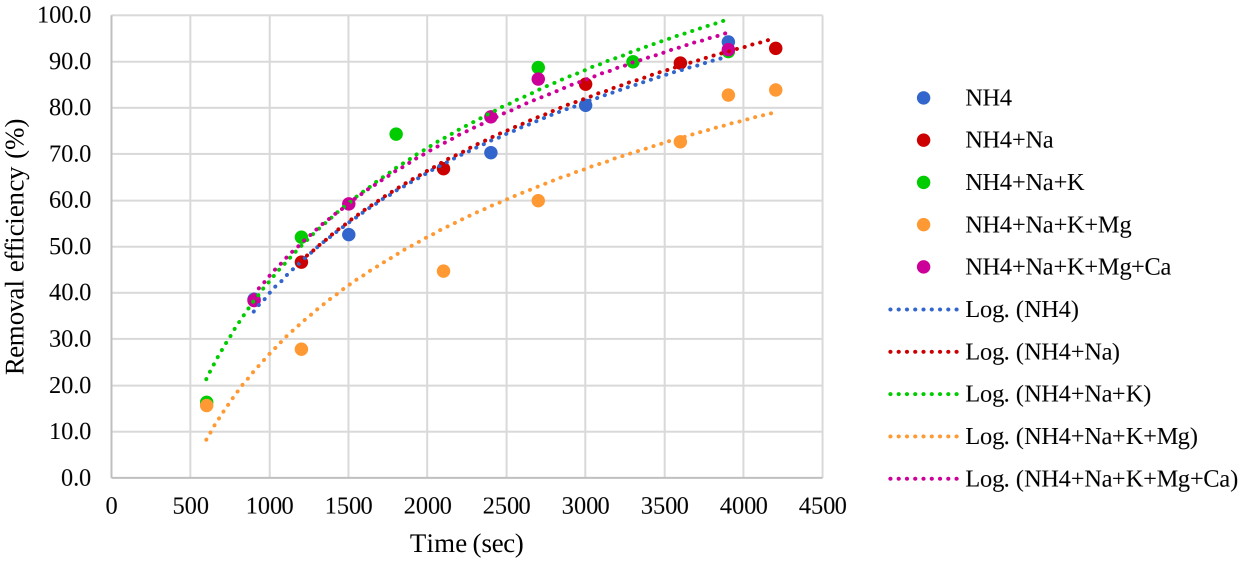

Figure 4.6. NH_4^+ removal efficiency on time for BPC. The points were calculated from obtained data and the fitting curves approximated the overall trend, regarding the best given R^2.

An overall logarithmic trend took place in removal efficiency of NH_4^+ for BPC. Removal efficiency for all experiments appeared to be approximately in the same range, with the exception of the 4th experiment. The difference between them was attributed to the big deviation between the two duplicate experiments. A fitting was applied to estimate the trend on time and the best fitting curve was selected based on the highest R^2. However, a Pearson correlation was also used to estimate whether the linear or non-linear correlation was the more representative. In details, the fitting equations with the corresponding R^2 are presented in Table 4.1.

Table 4.1. Fitting equations and R^2 for removal efficiency on BPC

	Fitting equations	**R^2**
NH_4	Y=37.618ln(X)-219.96	0.9847
NH_4+Na	Y=38.505ln(X)-226.22	0.9886
NH_4+Na+K	Y=41.547ln(X)-244.46	0.9641
NH_4+Na+K+Mg	Y=36.405ln(X)-224.65	0.9438
NH_4+Na+K+Mg+Ca	Y=38.631ln(X)-223.22	0.9833

In addition, the Pearson correlation was used to correlate the removal efficiency with time. Pearson correlation can take a value between -1 to 1, with the first meaning a total negative linear correlation, 0 for no correlation and 1 positive linear correlation. To estimate both the linear and the logarithmic for the best fitting, removal efficiency data was also converted to logarithmic values. The results are indicated in Figure 4.7.

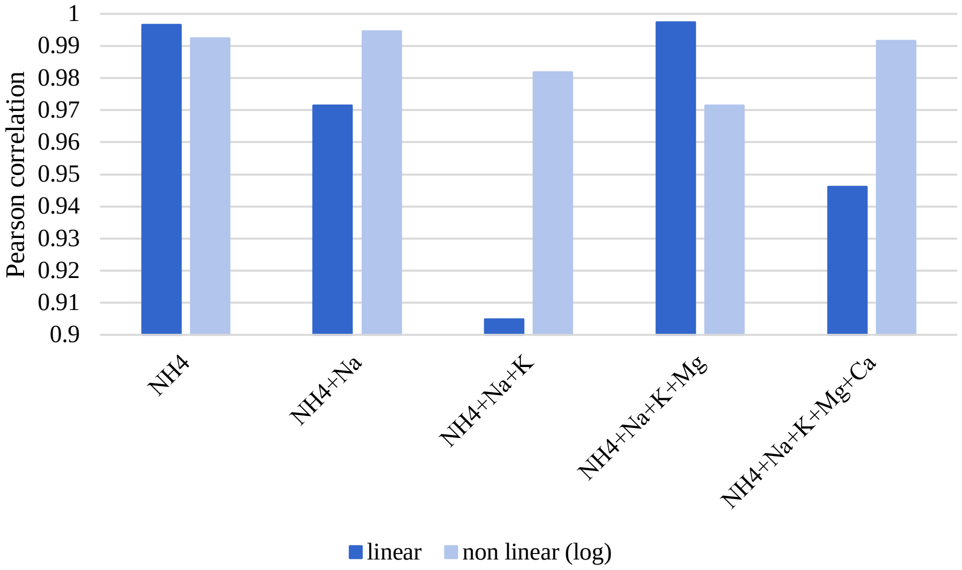

Figure 4.7. Pearson correlation coefficient for removal efficiency in BPC mass ratios experiment.

As shown above a linear correlation was better only for 1st and 4th experiment, while the others showed a remarkable difference between the two tested correlations. For the other three experiments, non-linear and more specifically logarithmic had a better correlation between removal efficiency and time. Linear correlation indicated a non-significance in competition when H^+ were present in the diluate solution, while the latter case expressed a decrease in the removal efficiency rate, as it could be described from the logarithmic curve.

Energy consumption is also a crucial parameter when it comes to electrochemical processes. It was estimated as the MJ consumed to remove 1 kg of N from the feed solution. Given the obtained data the results are presented in Figure 4.8.

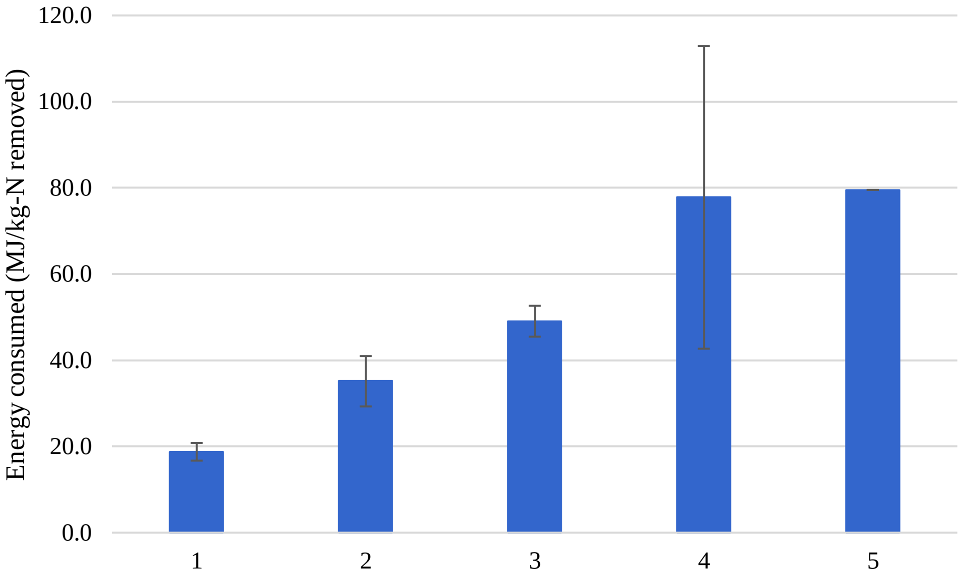

Figure 4.8. Energy consumption of BPC in the five different experiments. Experiment 1: NH_4, Experiment 2: NH_4:Na=1:1, Experiment 3: NH_4:Na:K=1:1:1, Experiment 4: NH_4:Na:K:Mg=1:1:1:0.5, Experiment 5: NH_4:Na:K:Mg:Ca=1:1:1:0.5:0.5.

Energy consumption in BPC presented a gradual increase with respect to the water matrix complexity, indicating that the less the cations included the lower the energy consumed. When only NH_4^+ was included in the feed solution the energy consumed was 18.8±2.1 MJ/kg-N removed, while with the Na^+ addition it reached 35.1±5.8 MJ/kg-N removed respectively. For NH_4^+, Na^+ and K^+ solution the energy consumption in BPC was 49.1±3.6 MJ/kg N removed. Lastly, with the addition of divalent cations the energy consumption increased to 77.8±35.1 MJ/kg-N removed for the 4th experiment and 79.5 MJ/kg-N removed for the 5th experiment. However, the standard deviation for the 4th experiment was relatively higher due to implications occurred during the experimental period for the duplicate experiment.

As mentioned above in bipolar membranes protons were produced and transferred to the diluate solution, leading to an acidic environment. Proton leakage had an important effect to EC in the diluate solution as shown in Figure 4.2. A hypothesis was formed and needed to be proved, that proton leakage and the acidic environment led to slower removal efficiency on time and increasing of energy consumption of the system, without removing an important amount of NH_4^+. Based on that a proposal given by this research was the EC setpoint, which expressed the EC value when proton leakage started affecting removal efficiency and delayed it, as result the higher energy consumption. The EC setpoint could be estimated as the ratio of the EC in the time that proton leakage was highly evident and it reached the minimum value before it stabilized over the initial EC of feed. For that reason, energy consumption was estimated until the time when EC reached the turning point, before high concentration of protons occurred in the diluate. The results are presented in Figure 4.9, compared with the original energy consumption.

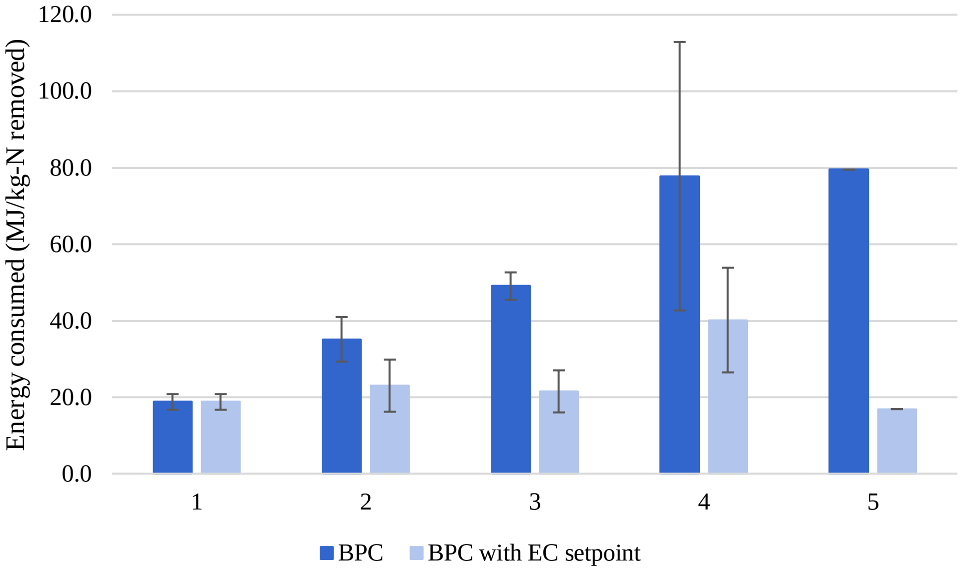

Figure 4.9. Energy consumption of BPC with the application of EC control. Experiment 1: NH_4, Experiment 2: NH_4:Na=1:1, Experiment 3: NH_4:Na:K=1:1:1, Experiment 4: NH_4:Na:K:Mg=1:1:1:0.5, Experiment 5: NH_4:Na:K:Mg:Ca=1:1:1:0.5:0.5.

In the first batch experiment, where NH_4^+ was added in form of NH_4HCO_3, bicarbonate acted like a buffer leading to low proton effect on the diluate and thus zero effect in the energy consumed. For the other cases, as seen in Figure 4.2 the EC was stabilized in time before the end of experiment, indicating an increase in proton production and simultaneous increase in EC and finally stabilization of it. Hypothetically, if the system stopped operating in the time that EC started increasing the energy consumption in any case will be lower. More specifically, for feed solution NH_4^+ and Na^+ the energy consumption with control of EC was 23±6.8 MJ/kg-N removed and 34.5% decrease compared to the actual value, whereas, when K^+ was added it dropped to 21.5±5.5 MJ/kg-N removed and 56.1% decrease. Finally, the addition of Mg^{2+} had a drop of 48.4% from the actual value with the latter one to be 40.2±13.7 MJ/kg-N removed. The more complex water matrix which included NH_4^+, Na^+, K^+, Mg^{2+} and Ca^{2+} had the biggest drop to be 78.7% of the initial value. However, it should be noted that

EC after reaching the first turning point, indicated a small increase and again decrease. Therefore, in this case the equilibrium had not yet reached in the operation and the results could not be representative.

Finally, the applied voltage was measured and indicated in Figure 4.10 and the findings were analyzed further below.

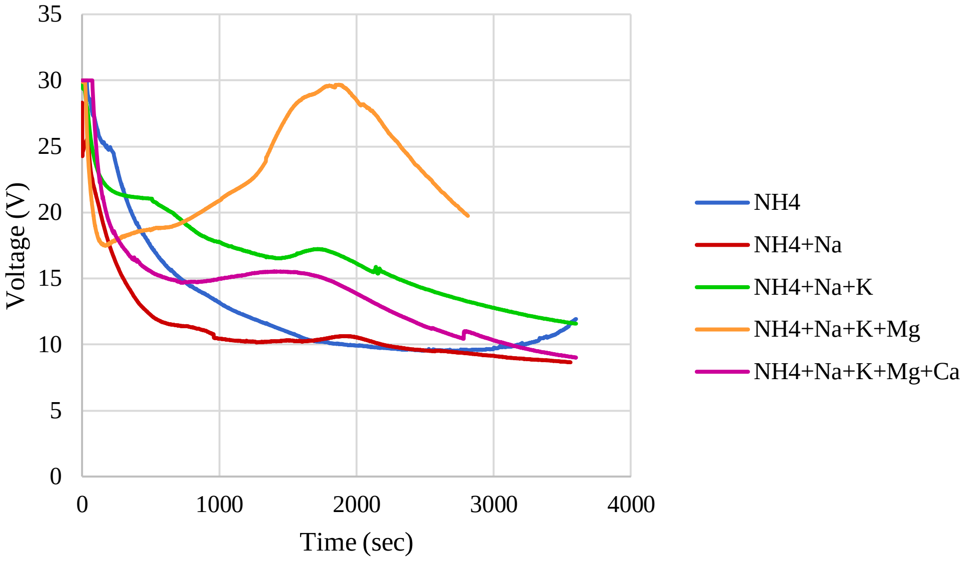

Figure 4.10. Voltage applied in BPC for the five cases.

In Experiment 1, with just NH_4^+, voltage curve had a constant decline on time until it reached a minimum point on 9.5 V at 2500 seconds of operation. Then, it increased again until the end of the batch up to 12 V. When additional salts were present in the feed, voltage curve had a different shape than the initial. The additions of salts led to a more "bell" shaped curve, where in Experiment 2 the curve started from 30 V and fell to 10 V, where it remained mostly stable between 9 and 10.5 V. When K^+ was added, voltage was higher than before and it ranged between 11.6 and 30 V with a constant decrease. However, there was a small peak on 1700 seconds operation. Moreover, when both Mg^{2+} and Ca^{2+} were added in the feed solution, the curve had similar shape with the minimum price at the end of operation to be approximately 9.5 V. Finally, when the only divalent cation in the feed was Mg^{2+} voltage dropped to 17.6 V on 170 seconds and it had an instant increase to 29.5 V on 1800 seconds when it dropped to 20 V on 2800 seconds.

4.2 Mass ratios in ED

In the operation of ED, the same parameters were also measured as in case of BPC. On contrary to BPC, pH and EC were also measured but they are presented in the Appendix, as they were not considered as high importance parameters.

Starting with transport number of cations, in Figure 4.11, it could be observed that transport efficiency decreased with the complexity of water matrix. In the first experiment, NH_4^+ had the highest current efficiency and equal to 0.66 and in the second experiment it decreased by 24% to 0.50. For the third case NH_4^+ transport efficiency reduced almost 50% from the non-competition experiment, included the value for Na^+, with 0.30 the first and 0.13 the lattest one. With the addition of divalent ions the transport number remained approximately the same for both cases, including also the values for the rest of cations.

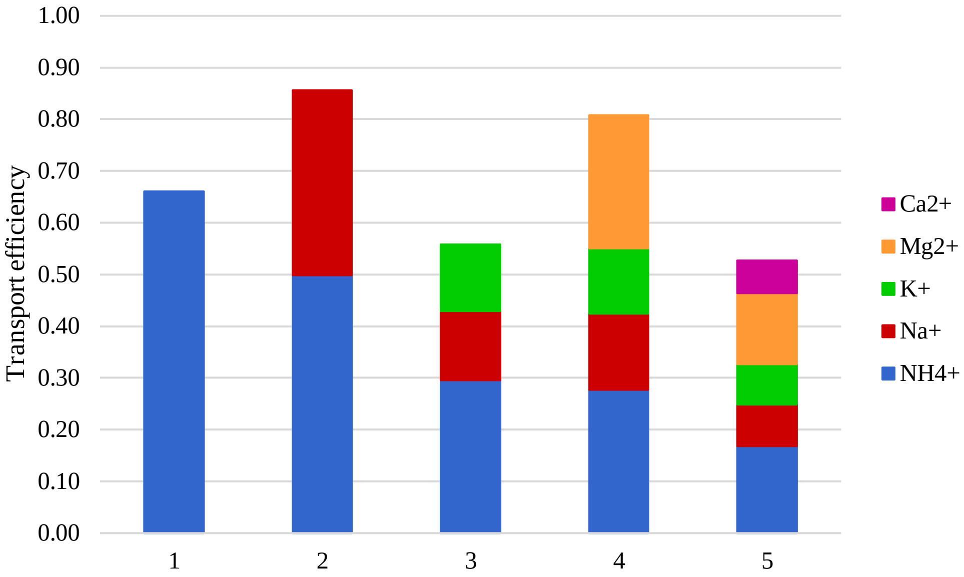

Figure 4.11. Transport number of cations in ED with application of mass ratios. Experiment 1: NH_4, Experiment 2: NH_4:Na=1:1, Experiment 3: NH_4:Na:K=1:1:1, Experiment 4: NH_4:Na:K:Mg=1:1:1:0.5, Experiment 5: NH_4:Na:K:Mg:Ca=1:1:1:0.5:0.5.

Furthermore, removal efficiency was also calculated to evaluate the overall performance of ED with the different compositions. As shown in Figure 4.12, removal efficiency was approximately the same for all experiments. More specifically, the range of overall removal efficiency was between 93.3% to 96.8% and the first experiment presented the highest value. The standard deviations were notably low for all experiments between their corresponding duplicates.

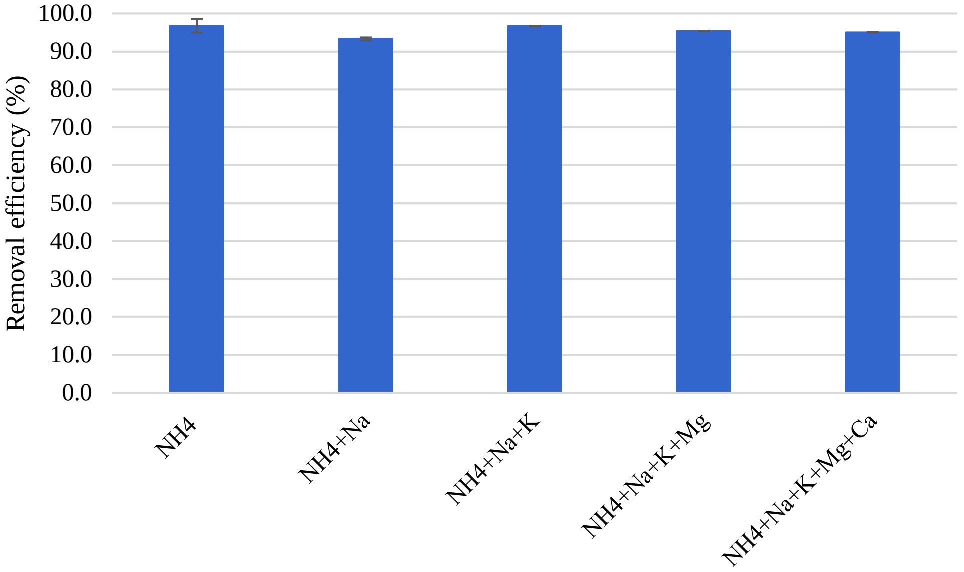

Figure 4.12. Overall removal efficiency in ED

As in the case of BPC, removal efficiency was also estimated on time of operational period. The best approximate fitting curve, based on the best R^2, was the linear. However, as indicated in Figure 4.12, the last two experiments had only two values due to the small operational time and therefore their results cannot be considered accurate. However, in this research we made the assumption that also these experiments could be represented by a linear regression as the rest of the ED batches.

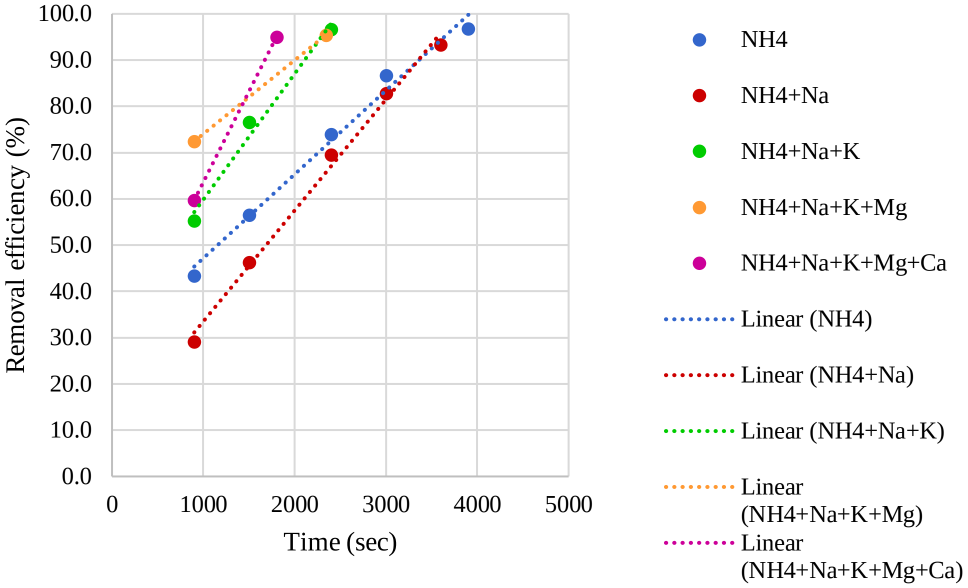

Figure 4.13. Removal efficiency on time in ED for 5 experiments.

Table 4.2. Equations for fitting curves for removal efficiency in ED with mass ratios

	Linear equation	**R^2**
NH_4	Y=0.0181X+29.047	0.9867
NH_4+Na	Y=0.024X+9.5352	0.9929
NH_4+Na+K	Y=0.0272X+32.666	0.9831
NH_4+Na+K+Mg	Y=0.0154X+58.115	
NH_4+Na+K+Mg+Ca	Y=0.0392X+24.404	

To evaluate whether linear regression was the most suitable choice, a Pearson correlation was also applied with linear and non-linear tests, as in case of BPC. The correlation factors were the same for both cases, implying the same correlation independently with the shape of curve. the results from Pearson correlation are presented in Table 4.1. It should be noted that for the last two experiments there could not be any specific conclusion for correlation due to the amount of available data points.

Table 4.3. Pearson correlation for removal efficiency on time with linear and non-linear correlation

Experiment	**Linear**	**Non-linear (logarithmic)**
NH_4	0.99330	0.99646
NH_4+Na	0.99171	0.99388
NH_4+Na+K	0.99152	0.99996
NH_4+Na+K+Mg		
NH_4+Na+K+Mg+Ca		

An additional parameter was the energy consumption for NH_4^+ removal and the results are shown in Figure 4.14. It was observed that the bigger the water complexity the higher the energy consumption. For the first experiment, energy consumption was 15.3±2.1 MJ/kg-N removed and when Na^+ was added it slightly increased to 24.1±2.5 MJ/kg-N removed. In the same scale, the addition of K^+ did not present any difference with 25.2±0.8 MJ/kg-N removed energy consumption. Finally, when the divalent cations were added, energy consumption was almost double with 54.2±3.9 and 65.9±6.2 MJ/kg-N removed for the fourth and fifth experiment respectively.

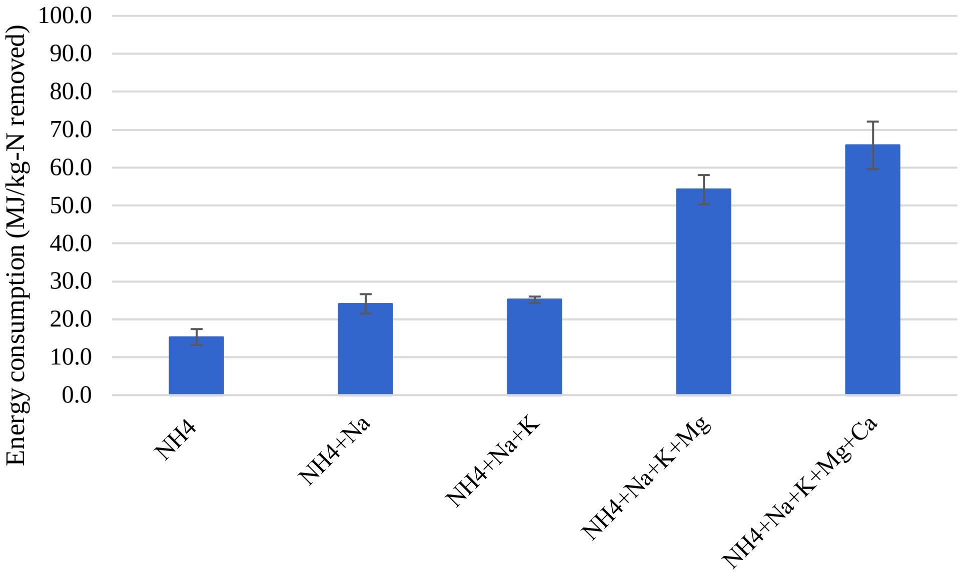

Figure 4.14. Energy consumption of ED in mass ratios

Finally, the last observed value was the applied voltage in the ED. ED voltage curves, regardless of the composition of feed, presented the same shape, with difference on their time extension which was attributed to the EC drop. More specifically, for Experiment 1 and 2, voltage curves had similar trend starting from stable value of 30 V and gradually decreased to their minimum point of 5.5 V and 6.4 V respectively between 1600 and 3000 seconds. For the addition of K^+, the initial voltage was 14.5 V and it dropped to 6.5 V where it reached a plateau from 800 seconds to 1500 seconds. Then, it increased again until it hit the 30 V. In addition, the same pattern occurred for the addition of Mg^{2+}, where the minimum point was on 10.5 V on the same period as the case of Experiment 3, and it reached the maximum voltage on 2300 seconds. Finally, when all studied cations were present the operational period was the smallest (1900 seconds), the initial applied voltage was 19.9 V and the minimum was 8.3 V.

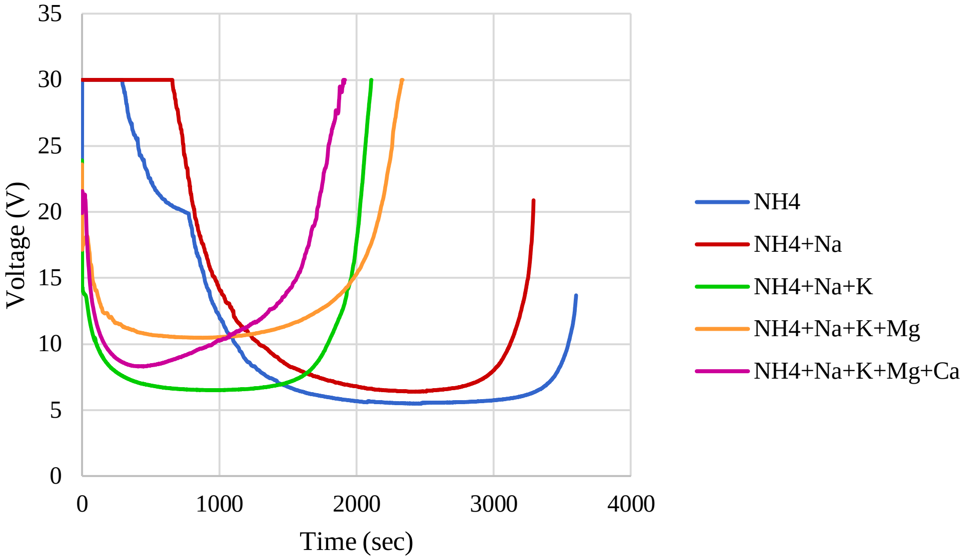

Figure 4.15. Voltage applied in ED for the five cases.

4.3 ED with application of molar ratios

In a conventional ED, molar ratios between 0.30 and 0.90 were tested, including NH_4^+, Na^+, K^+, Mg^{2+} and Ca^{2+} to estimate the effect of the amount of cations in the overall efficiency of the system. The results of this series of experiments are presented in this section.

From the molar ratios applied in the feed solution, the removal efficiency of NH_4^+ was calculated and the results are presented in Figure 4.15.

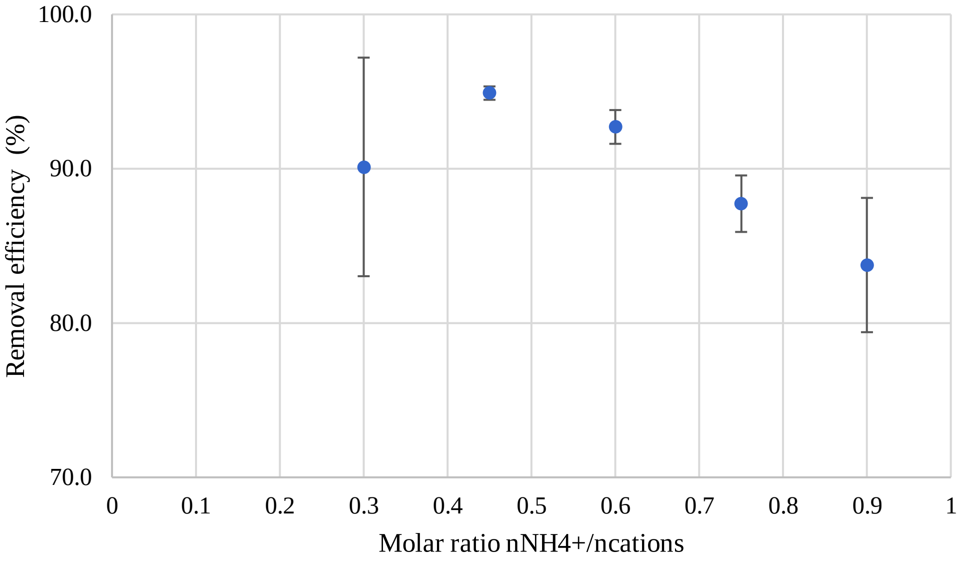

Figure 4.16. Removal efficiency of NH_4^+ regarding the molar ratio of cations in the feed

The results obtained by the batch experiments presented approximately a normal distribution of the values with the change of molar ratio. The highest removal efficiency was indicated for molar ratio of 0.45 which was 94.9%±0.4%. When the concentration of cations was the highest, for molar ratio 0.30, removal efficiency of

NH_4^+ was 90.1%±7.1%. For molar ratio of 0.60 removal efficiency achieved was 92.7%±1.1% and for higher ratios this value decreased. In molar ratio 0.75 and 0.90 the corresponding value was 87.7%±1.8% and 83.8%±4.3% respectively.

Removal efficiency was also estimated on time and how it evolved during the experiment, taking into consideration the mass of NH_4^+ at the beginning of batch and in each time step.

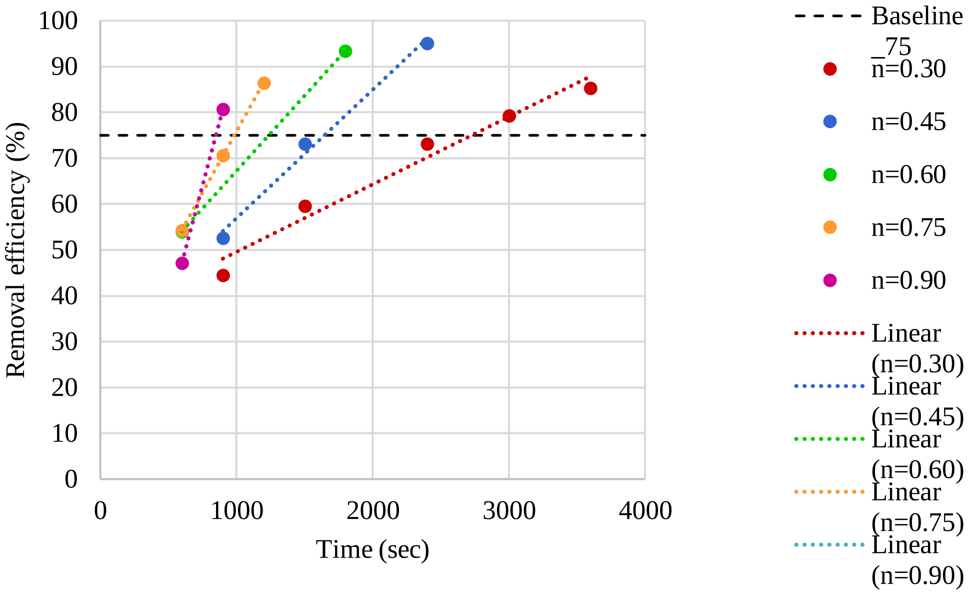

Figure 4.17. Removal efficiency of NH_4^+ on time based on molar ratios

It was indicated that removal efficiency had a linear trend and all experiments had several operational times. That was attributed to the salt concentration of the initial feed solution and the finalization of the batch when the EC in diluate reached approximately 600 μs/cm. Therefore, for the smaller molar ratio, the operational time was higher. A regression was applied for the best fitting curve, as in the previous batches and based on the R^2 occurred linear was more representative. However, to evaluate the results, Pearson correlation was also used for linear and non-linear. In practice, for linear the values were considered as they are while for non-linear, where logarithmic was tested, removal efficiency was considered as the logarithm of the initial value. The results from correlation are presented in Figure 4.17, where linear regression showed the highest correlation and therefore it was taken for all ED batches.

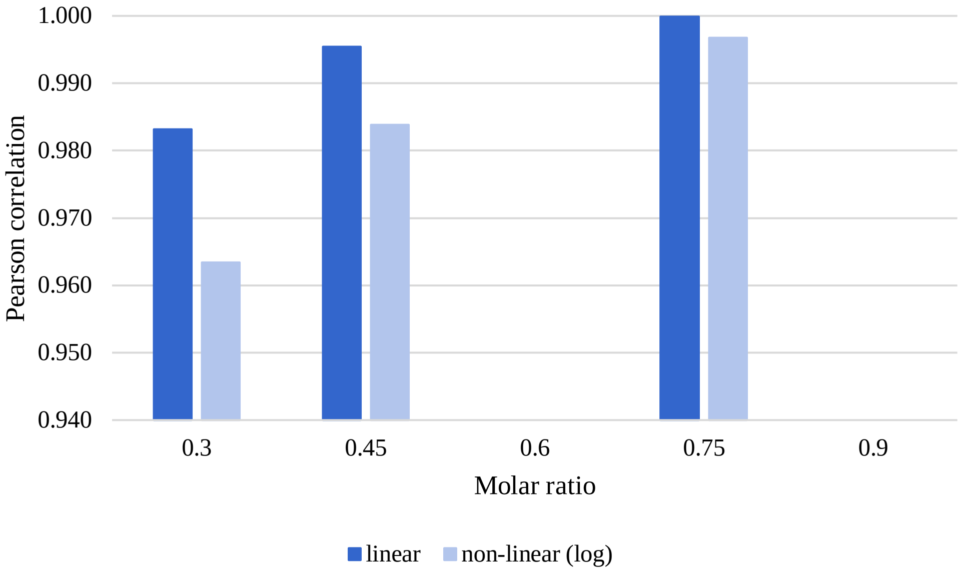

Figure 4.18. Pearson correlation between removal efficiency and time for ED in molar ratios

It was indicated that for lower molar ratios, the removal efficiency rate was lower and with the decrease of the first one it became higher. As removal efficiency rate it was defined as the slope of the fitting line, where it was the removal efficiency achieved in a specific time frame. The linear equations are presented in Table 4.3.

Table 4.4. Removal efficiency fitting curves for several molar ratios

Molar ratio n	**Equation**	**R^2**
0.30	Y=0.0147X+34.837	0.9666
0.45	Y=0.028X+28.896	0.9909
0.60	Y=0.0328X+34.410	
0.75	Y=0.0536X+22.225	0.9998
0.90	Y=0.1114X-19.555	

It can be resulted that for n=0.45 removal efficiency rate is almost double compared to n=0.30 which expresses that the same removal efficiency could be achieved in half of the operational time. The same also appeared between n=0.90 and n=0.75. Thus, it could be resulted that, for the same concentration of NH_4^+, in different molar ratios, removal efficiency rate grew with higher molar ratio. As shown in Figure 4.18, the increase could be described with an exponential curve, for concentration of NH_4^+ 22.2 mmol/L, in ionic competition with Na^+, K^+, Mg^{2+} and Ca^{2+}.

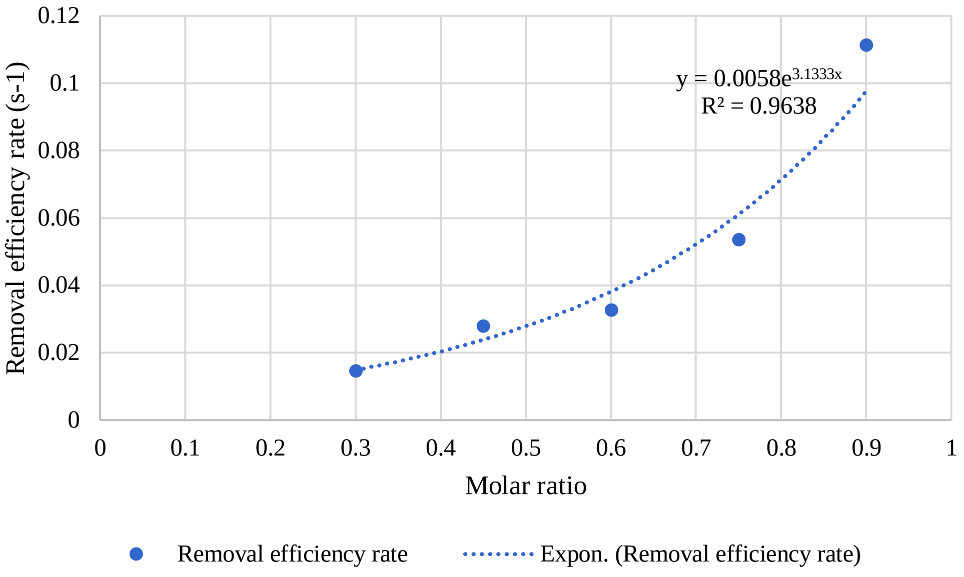

Figure 4.19. Removal efficiency rate

Energy consumption was also estimated based on the amount of N removed from the feed solution for all tested molar ratios and the results are indicated in Figure 4.19.

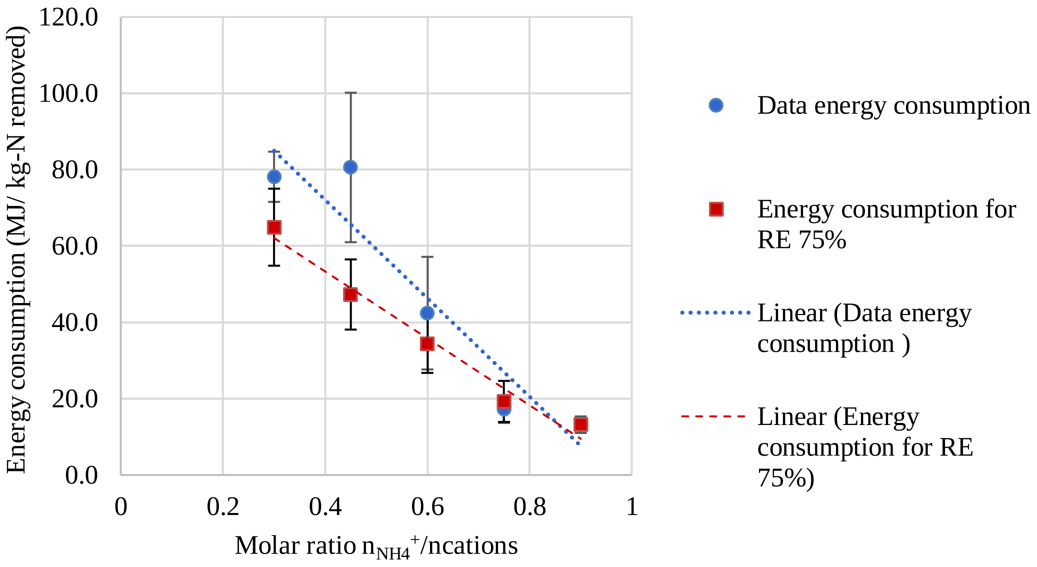

Figure 4.20. Energy consumption based on molar ratio of cations in feed for the overall removal efficiency and for removal efficiency of 75%.

Energy consumption presented a decrease with increase of the feed solution molar ratio. In molar ratio 0.30 the energy consumption was 78.1±6.6 MJ/kg-N removed and in 0.45 the value was slightly higher to 80.6±19.6 MJ/kg-N removed. In addition, energy consumed dropped dramatically to 42.4±14.7 MJ/kg-N removed for n=0.60, while for the last two values the prices did not differ much, with 0.75 to have 17.1±3.5 MJ/kg N removed and 0.90 to reach 13.2±2.2 MJ/kg-N removed.

In the same figure it was also indicated the energy consumption when removal efficiency of NH_4^+ is 75%. For the same molar ratios energy consumption was lower with the highest difference presented for n=0.30, with energy consumption 64.9±5.4 MJ/kg-N removed. The trend was similar to the initial value, with a linear relationship.

When molar ratios were applied in a conventional ED system, the transport efficiency was also estimated for all the cations included (NH_4^+, Na^+, K^+, Mg^{2+}, Ca^{2+}) and the results are presented in Figure 4.20.

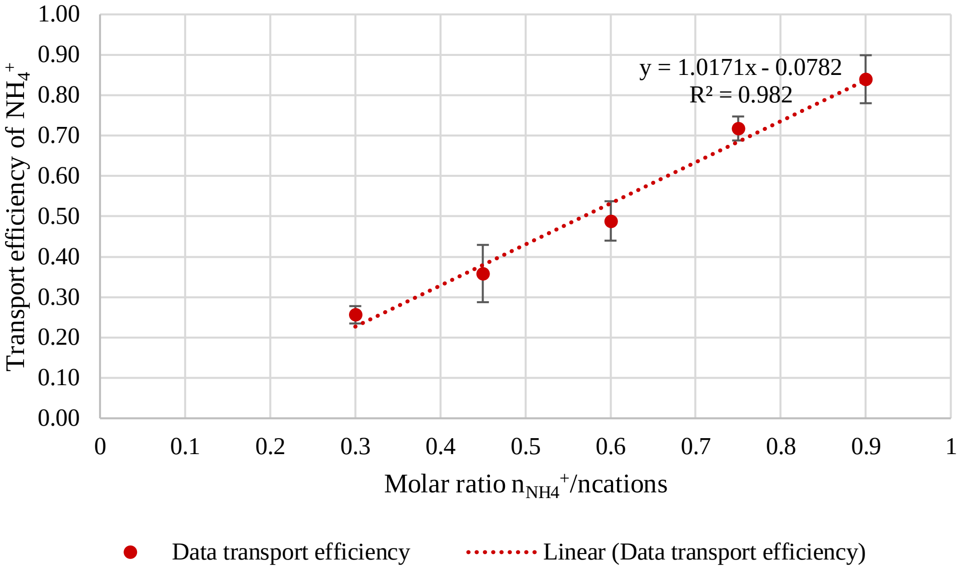

Figure 4.21. Transport efficiency of NH_4^+ based on molar ratio of cations in feed

Transport efficiency of NH_4^+ for the tested range of molar ratios presented a slightly linear trend. In molar ratio 0.30 transport number was 0.26±0.02 and for 0.45 was 0.36±0.07. For 0.60, 0.75 and 0.90 the same value was 0.49±0.05, 0.72±0.03 and 0.84±0.06 respectively. The values were taken as the average values from the duplicate experiments, which gave the standard deviation of the points. Therefore, after fitting the data, the best approximation was a linear regression with equation: $y = 1.0171x-0.0782$ and $R^2=0.982$.

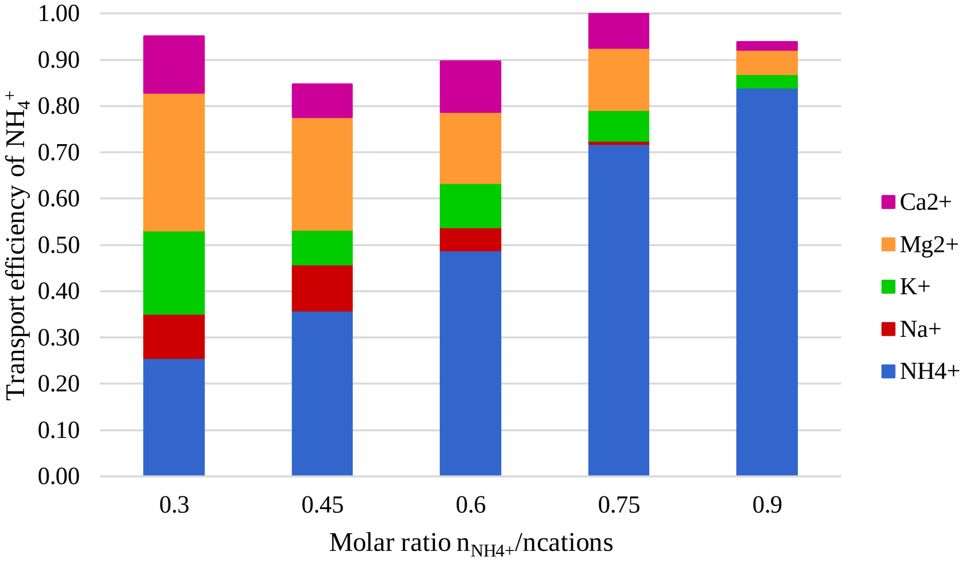

Figure 4.22. Transport efficiency of all cations based on the molar ratio in the feed solution.

In addition, transport efficiency was calculated for all cations and presented in Figure 4.21. It was shown that for the smallest molar ratio all the cations presented the highest transport number, which could be justified by the amount of salts added in the batch. As mentioned in Chapter 3 the amount of NH_4^+ added was the same in all batches, whereas the amount of other salts differed. Therefore, in molar ratio of 0.30 the amount of other cations was higher compared to the other experiments.

Finally, in the tested range, the electrical conductivity was measured during the entire experimental period in order to calculate the percent demineralization. Based on the obtained data, percent demineralization was calculated for removal efficiency of NH_4^+ between 60% to 80% with step of 5%.

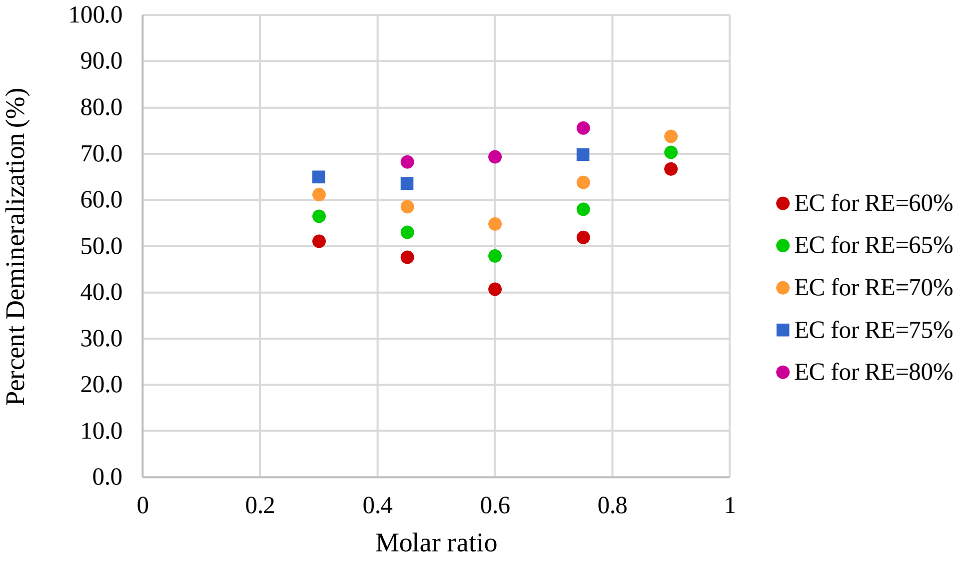

Figure 4.23. Percent demineralization based on the molar ratio of cations in feed.

Percent demineralization was calculated based on the selected removal efficiency. For RE of 75% PD was calculated based on the obtained experimental measurements. However, for molar ratio of 0.60 and 0.90 there was not any accurate point and thus the results were not taken into account for those. PD presented a minor decrease with the increase of molar ratio from 0.30 to 0.45 but the further increase led to increase also in DR to 69.9%. In this research, it was considered that 75% removal was the baseline.

Moreover, the percent demineralization for several RE was estimated, based on the given RE equations (Appendix). All PD presented a similar trend to the actual baseline, with the minimum PD to occur for molar ratio of 0.60 when RE was below 75%.

4.4 Sequence batch experiments with ED and BPC

To estimate if specific conditions were applicable in a sequence batch experiment, that represent more realistic conditions than batch experiments, they were applied for 3 different molar ratios, for 0.30, 0.45 and 0.60. Those values were chosen based on literature and laboratory measurements from already existing reject water, as mentioned in Chapter 3.4.4.

Taking into account the baseline of 75% removal efficiency from batch experiments, the sequence batches were conducted by applying constant current of 0.5 A, while keeping the percent demineralization of each individual batch stable. More specifically, in case of feed molar ratio of 0.30, based on the occurrent results of the batch, the percent demineralization should have been approximately 70%. On the same pattern, for molar ratio of 0.45 and 0.60 the same value should have been around 70%. Therefore, by controlling the EC of the feed, percent demineralization was kept as constant as possible. The results are presented in Figure 4.23.

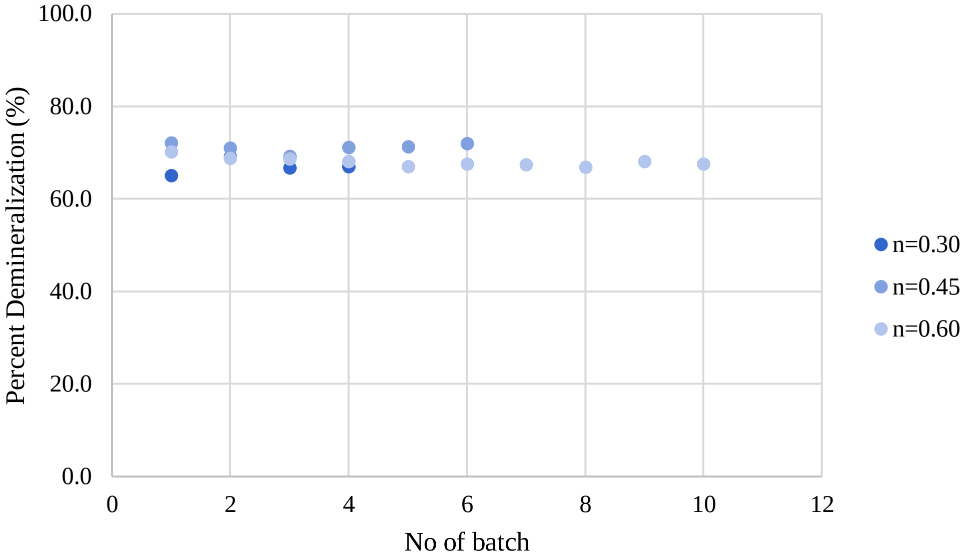

Figure 4.24. Percent demineralization of each batch experiment for the three cases of molar ratios in a sequence batch.

For molar ratio of 0.30 percent demineralization ranged between 65.2% to 69.2%. In case of 0.45, the operational range was from 69.4 to 72.2% and finally, for molar ratio 0.60, it was between 67.1% to 70.3%. Removal efficiency was also estimated from the mass of NH_4^+ in the feed solution.

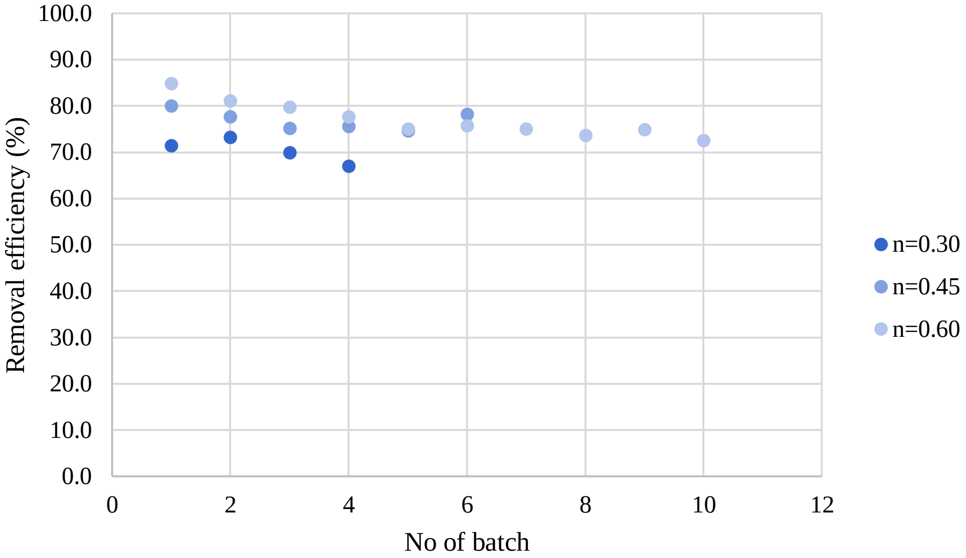

Figure 4.25. Removal efficiency of NH_4^+ of each batch experiment for the three cases of molar ratios in a sequence batch

Removal efficiency, for the smallest applied molar ratio, was between 67.1% to 73.2%. As for the 0.45 and 0.60 molar ratios, the highest removal efficiencies were presented in the first batches, as shown in Figure 4.24.

Transport number of NH_4^+ was estimated for all molar ratios applied and the results are presented in Figure 4.25.

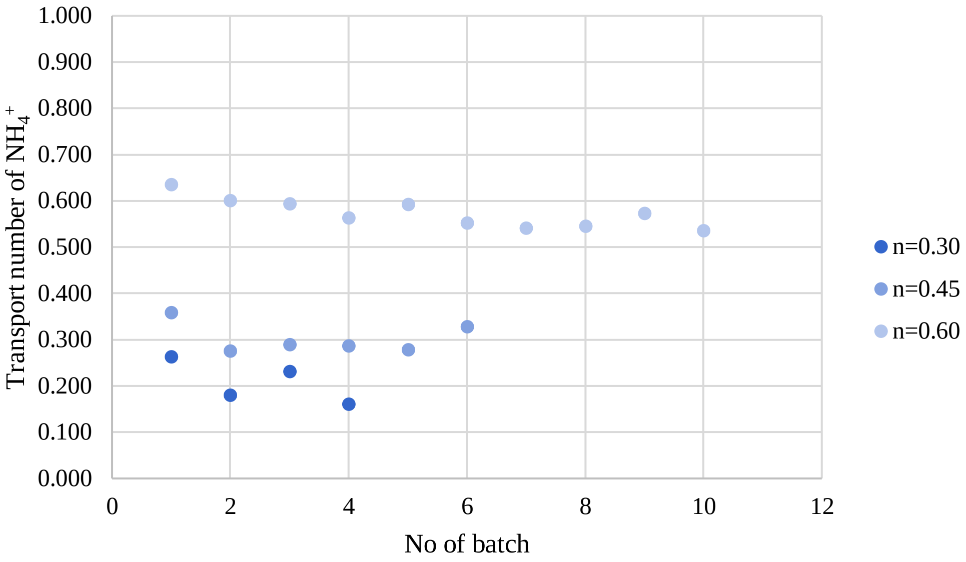

Figure 4.26. Transport number of NH_4^+ of each batch experiment for the three cases of molar ratios in a sequence batch

For molar ratio of 0.30 NH_4^+ transport number presented the lowest values compared to 0.45 and 0.60. In the first batch, NH_4^+ transport number was the highest at 0.263, while on time it became lower and reached 0.161. In case of 0.45, NH_4^+ transport efficiency was higher and between 0.276 and 0.356. The difference between the two molar ratios was the amount of added salts, since in 0.30 the competition for the current applied was higher due to the more Na^+, K^+, Mg^{2+} and Ca^{2+} in the solution. The same trend appeared also in molar ratio of 0.60, where the competitive cations were less, and the transport number of NH_4^+ was higher. In the first batch, current efficiency reached the maximum price of 0.636, while it dropped slightly on the next batches. However, it reached an equilibrium after the sixth batch.

In addition, energy consumption was estimated for every sequence experiment and the results are indicated in Figure 4.26.

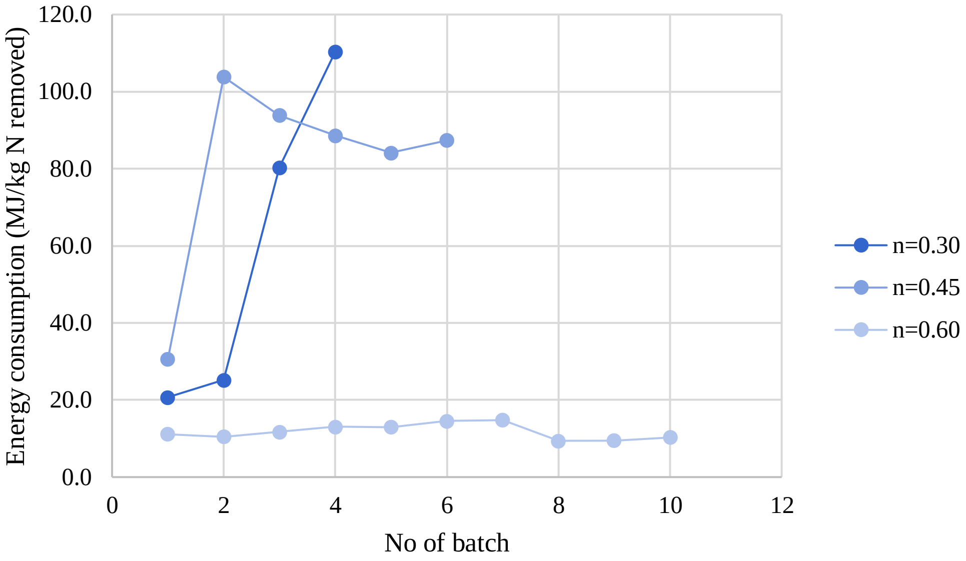

Figure 4.27. Energy consumption of each batch experiment for the three cases of molar ratios in a sequence batch.

The energy consumed for molar ratio 0.30 in the first batch presented an overall increase, starting from 20.7 MJ/kg-N removed and reaching a peak at the end of experiment at 110.3 MJ/kg-N removed. The reverse trend appeared in the 0.45 molar ratio, where the maximum energy consumed, was in the second batch and was 103.8 MJ/kg-N removed and then reached an equilibrium between 80 and 95 MJ/kg-N removed. The lowest value, 30.6 MJ/kg-N removed occurred in the first batch experiment. Finally, for molar ratio 0.60 the system presented an equilibrium in energy consumption and ranged between 9.5 to 15 MJ/kg-N removed in the entire sequence. The high energy consumption when n=0.30 could be attributed to the high salinity content of the feed, while as the n became lower the amount of salts was reduced.

However, the results of energy consumption are related to the voltage applied to the system. Current was kept constant to 0.5 A and thus the current density was also stable to 50 A/m^2. When the resistance of the stack increased, due to fouling or scaling of the membranes, the voltage was reaching its maximum value, at the setpoint of 30V, leading to current decrease. As shown in Figure 4.27 the voltage for n=0.30 and n=0.45 was mainly constant to 30V which increased the final energy consumed. On the contrary, for n=0.60 there was no serious resistance and the voltage applied ranged between 4.5 to 10 V, with constant current density of 50 A/m^2.

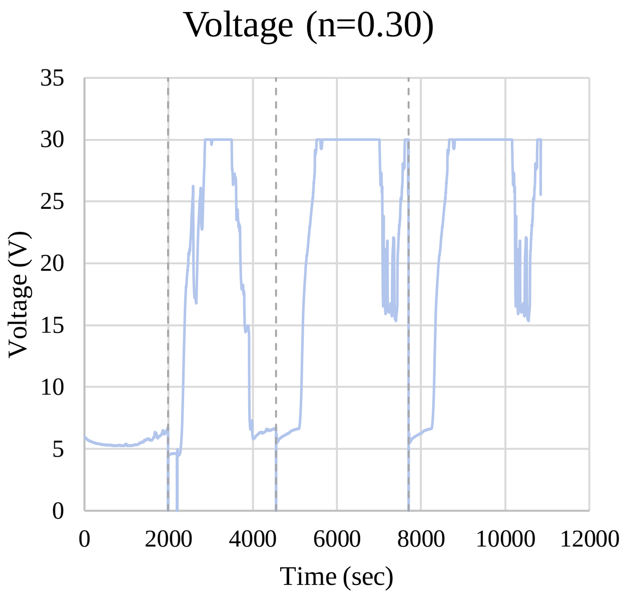

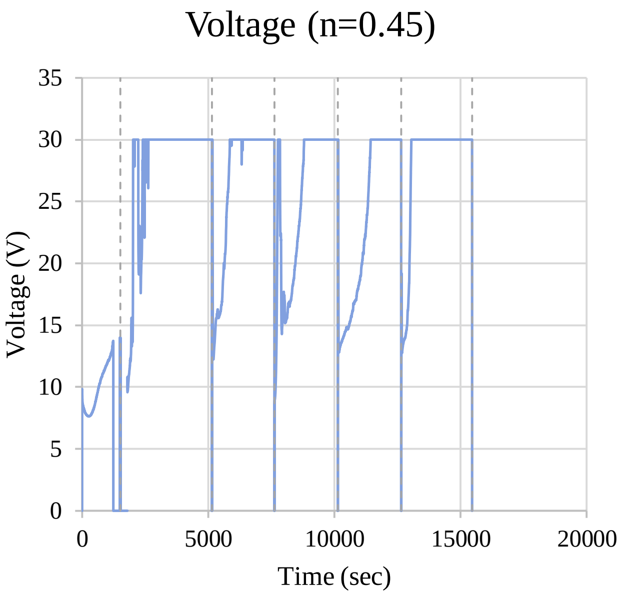

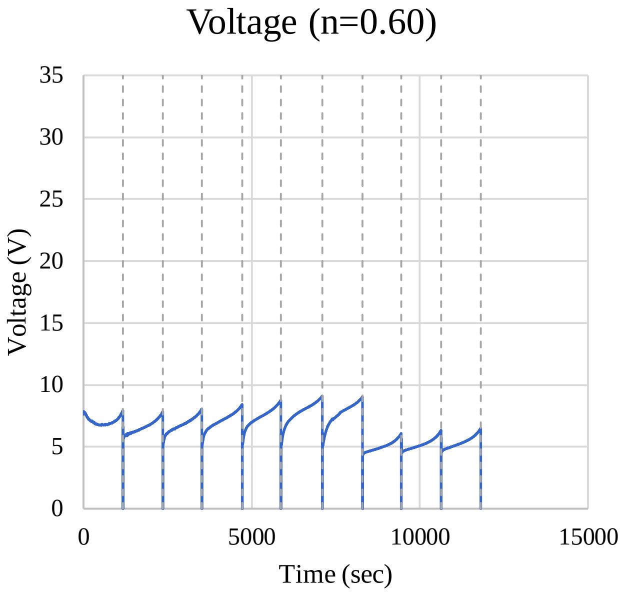

Figure 4.28. Voltage of ED in sequence batch experiments. The vertical dashed lines represent the end time of each batch.

When the EC of the concentrate reached approximately 20 mS/cm it was placed as a feed in BPC. The duration of operation was until the EC reached a minimum point or became stable and the proton leakage became dominant. The removal efficiency of BPC did not present any specific trend with the highest removal to be for n=0.45 at 84.6%, while for n=0.30 and n=0.60 was 12.2% and 42% respectively. Finally, energy consumption presented a decrease with the increase of molar ratio. The results are indicated in Figure 4.28.

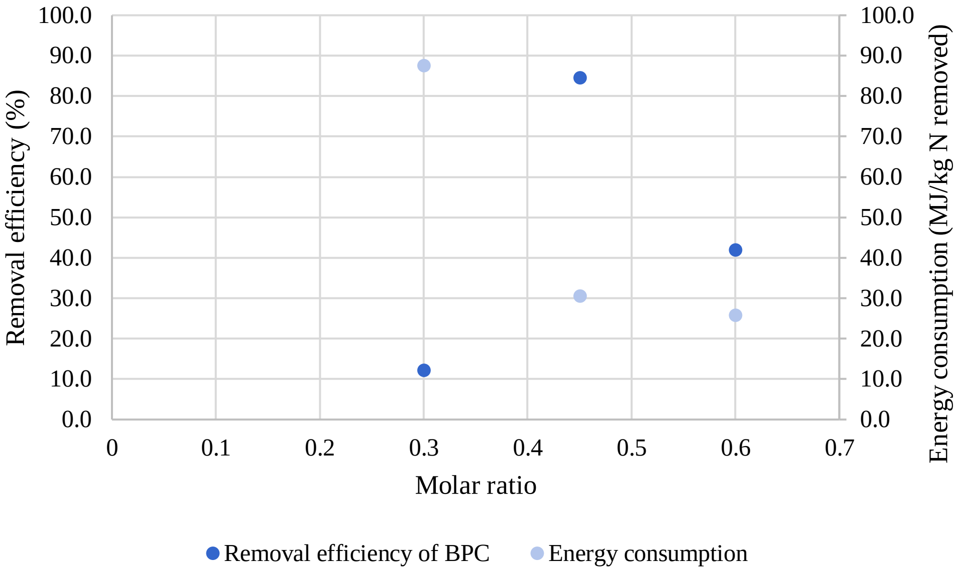

Figure 4.29. Removal efficiency and energy consumption for sequence batch experiments in BPC

4.5 Scaling effect

During the operation of high salinity feed solutions, the scaling potential became higher, especially when the concentration of Ca^{2+} and Mg^{2+} increased. In case of mass ratios experiments, the concentrations of salts was low, without presenting any precipitates. For the molar ratio experiments, when molar ratio took lower values, such as 0.45 and 0.30 the feed solution was highly concentrated, leading to higher scaling potential. In the case of n=0.45, there was no effect that needs to be highlighted, while when n=0.30 the resistance of the system highly increased. However, after the end of cycle the membranes did not present many precipitates on their surface.

Figure 4.30. Feed solution for molar ratio experiment of 0.30 in batch.

As for the sequence batch experiments, scaling on the membranes and spacers was more evident due to the long operational time. For feed solutions of molar ratio 0.45 and 0.30, scaling presented after the ED operation. This phenomenon could also explain the high potential difference developed after the second batch in both cases. Thus, the energy consumption was also increased compared to when molar ratio is 0.60.

Figure 4.31. Scaling on spacer in sequence batch experiment of n=0.45.

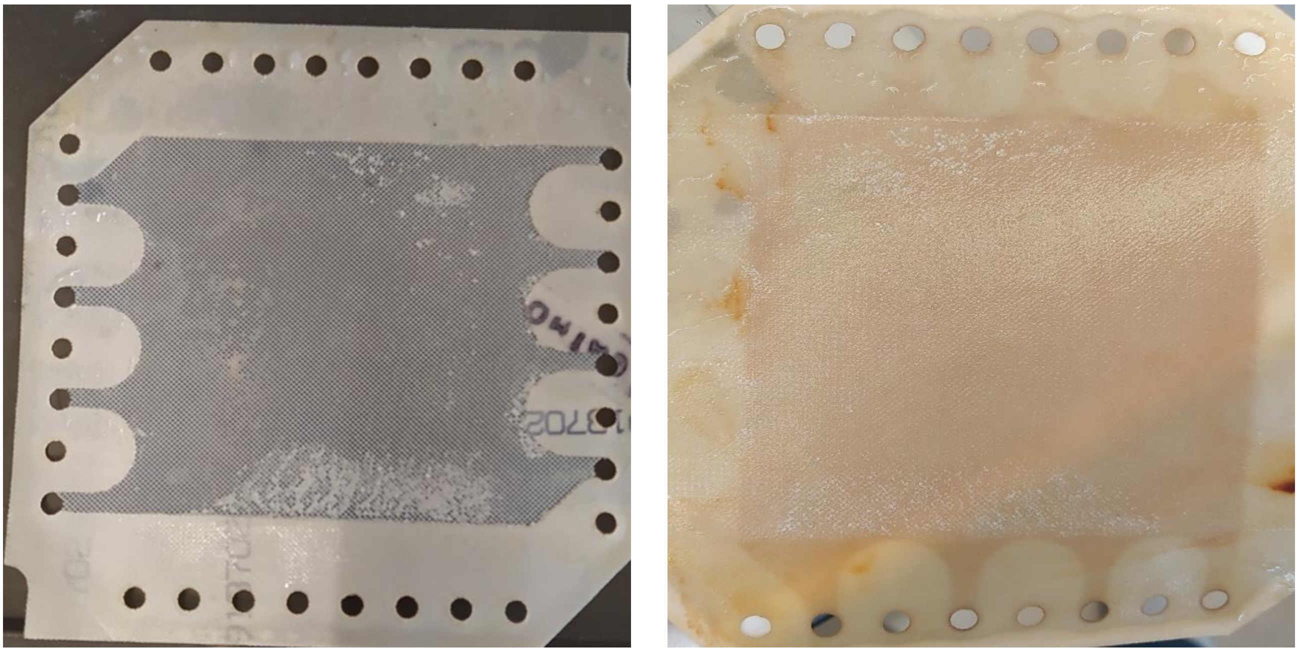

Figure 4.32. Scaling in (a) spacer and (b) anion exchange membrane for sequence batch experiment of n=0.30.

5 Discussion

5.1 Batch experiments

5.1.1 Mass ratios in BPC

BPC with two compartments consists of the feed and the base, with the latest occuring due to water dissociation. At the same time, the feed solution becomes acidic due to recirculation, which influences the overall conditions. When only NH_4HCO_3 was included, no evident competition with protons was presented from the pH of diluate. HCO_3^- worked as a buffer in order to maintain the pH in slightly acidic conditions, instead of acidic conditions in all other cases. EC had a constant decrease, proving that ions were being removed from the feed and the presence of protons was minor and did not affect the overall performance of the system. Removal efficiency indicated a trend on time, which could be also proved from the Pearson correlation coefficient. Linear and logarithmic trend were both equally suitable, which showed a non-important proton effect on this batch experiment.

On the other hand, proton production and competition was higher in all the other batch experiments, which could be shown initially from the instant drop of the pH in the diluate solution. In every case, when other cations were included, proton concentration presented a sudden spike in the diluate solution, whereas the EC concentration had a constant decrease on time until it reached a minimum point. After that, EC increased, which was attributed to the protons overtake in diluate. Based on that, a hypothesis was formed, that at its first stages of operation, energy consumption would be less when proton leakage has not taken place yet while the removal efficiency would be faster on time. Starting from that, removal efficiency on time presented an evident logarithmic trend, proven by Pearson correlation and the R^2 of the tested fitting curve, which meant that, on time, removal efficiency rate had been decreasing and reached an equilibrium. However, in the conducted experiments we could see that the equilibrium state did not reach in the approximately one hour of operation. An important note to make from Figure 4.6 was that the batch experiment No 4, with the presence of NH_4^+, Na^+, K^+ and Mg^{2+} presented a different trend, with lower removal efficiencies for the same timeline, instead of all other cases. This was due to the big deviation of results between the duplicate batches and thus these results could not be considered highly representative of the overall trend.

Energy consumption presented an evident increase with the complexity of built-up compositions. This occured because of the initial EC value. Based on Gao et al. (2021), by increasing the feed salt concentration, the resistance of the stack will decrease, leading to an additional decrease in energy consumption in a BPMED system. Another research, showed that the same could happen in case of an ED which explains the gradual decrease in energy consumption in the batch experiments (Nguyen et al, 2019). As shown in Figure 4.2, the EC was decreasing starting from the first experiment with non-competition to competition with Na^+, K^+, Mg^{2+} and Ca^{2+}. In addition, as mentioned before, removal efficiency on time decreased because of the proton transport in diluate, which increased the overall energy needed for removal. Therefore, the main hypothesis was that, if an operational setpoint could be defined for a parameter, when this setpoint is reached the cycle has finished and further operation will lead to minor improvement of the result. From the results, a setpoint that seemed as the most preferable choice was the EC, meaning that when EC has reached a minimum point during operation and starts increasing then this is defined as an EC setpoint. For the case of batch experiments, for several compositions, a ratio of $EC/EC_{initial}$ was found to define the EC setpoint where it is expected to reach this minimum point. For example, for initial EC of 5800 μS/cm if the ratio resulted from the BPC batch experiments was 0.43 then the EC setpoint will be approximately 2500 μS/cm. Thus, in the case of application of the same composition with $EC_{initial}$ of 6500 μS/cm the ratio will remain the same and the EC setpoint will be 2800 μS/cm. However, this is an assumption that has been further investigated in the sequence batch experiments. Thus, from Figure 4.9 the overall energy consumption will be considerably less than the initial value, when proton production took place.

Finally, voltage presented a similar distribution based on the phenomena appeared. For the non-competitive batch experiment, voltage had a constant decrease, without any minimum or peak points, showing that the proton effect was not present. Contrariwise, where the proton overtake to diluate took place, voltage distribution presented peak points in the time, where proton production initialized and the pH was becoming more acidic. These peak points were related to the depletion of cations and dominance of protons, which could be also shown from the EC distribution and H^+ concentration in Figure 4.2. A BPMED configuration provided higher voltage per unit cell due to the large pH gradient across bipolar membranes (Pretz et al., 2010). This could also be observed as a steep rise in the resistance of the BPM when water dissociated on it (Ortega et al., 2022)

5.1.2 Mass ratios in ED

In case of ED operation, the results occurred were evidently different, for the same built-up compositions as in BPC. Initially, transport number of NH_4^+ was higher with zero competition and decreased with the higher complexity of composition. In addition, removal efficiency was approximately the same for any case and it was not influenced by the complexity of water matrix. Karimi and Ghassemi (2016), by using a pilot scale reported that voltage had a positive effect on the ion removal, since a very low voltage combined with high feed flow rates and low temperatures, prevented the removal of different ions, regardless of their characteristics and initial concentrations. Some of the factors that affected an EDR process, a variation of a conventional ED process, were the applied voltage, the flow rate, the temperature, the membrane properties and the pH (Sedighi et al., 2023). Thus, in the already existing literature it was not recorded that the cations included in an ED process affect the overall ED removal efficiency.

Removal efficiency was also estimated on time to express the overall trend in case of ED operation. To find the best fitting curve two parameters were used as in case of BPC, R^2 of the fitting curves and Pearson correlation coefficient. Pearson correlation was tested for two cases, for linear and non-linear (logarithmic) correlation and the results were approximately the same for both cases. Alternatively, R^2 gave the best approximation for linear correlation and thus it was chosen. As shown in Figure 4.12, the latter two experiments, where divalent cations were included, had only two values for the fitting curve, which were not enough and thus the fitting curve equations were not representative. However, the fitting curve was taken as a linear equation due to the similarity with the tested configurations before. It was also observed that NH_4^+ removal efficiency rate was higher with increasing the complexity of water matrix, which is due to the amount of NH_4^+ available in feed solution. More specifically, in the first batch experiment NH_4^+ concentration was 1.5 g/L while in the second it was 0.75 g/L, in the third it was 0.5 g/L and so on. However, no previous research has been conducted for the factors that affect the removal efficiency of cations in ED and thus it was not possible to evaluate the results and create definite conclusions. Therefore, the phenomena taking place were hypothesized.

As for energy consumption, it increased with matrix complexity, leading to the conclusion that on an ED system, for the same overall cation concentration, the composition of cations was an important factor. The addition of divalent cations led to over 100% increase in energy consumption. Based on Rijnaarts et al. (2018), the presence of divalent cations in feedwater could cause important decreases in efficiencies for membrane processes. The resistance of the stack also increased, while the voltage decreased when divalent cations were present in the solution. In parallel, voltage curve had a different curve compared to BPC curves. There were no peaks, as before due to proton production, and the voltage constantly decreased on time until it reached a depletion phase and increased again. Finally, it was also important to note that the operational time varied based on the overall ion concentration and initial EC. For mass ratio batch experiments in ED the cycle was completed when the EC in diluate reached 600 μS/cm.

5.1.3 Molar ratio in ED

Removal efficiency was an important parameter estimated in all molar ratio experiments. It was calculated based on its evolution on time and the composition of the feed. As shown in Figure 4.16 the lower the molar ratio the longer the experimental period, which was attributed to the concentration of ions in the feed solution, since the amount of NH_4^+ remained constant and the amount of added Na^+, K^+, Mg^{2+} and Ca^{2+} was bigger. Indicatively, the mass of NH_4HCO_3 in the feed solution, was always 22.2 mmol per liter solution. When molar ratio was 0.30, the moles of cations in the solution was 73.9 mmol/L, while in case of molar ratio of 0.90 the same value was 24.6 mmol/L. In the lattest case, the dominant cation was NH_4^+, while in the other cases the dominant cation was dependent on the ratio needed with NH_4HCO_3.

The removal efficiency rate (removal efficiency/time) in case of ED was stable and dependent on the molar ratio. More specifically, for n=0.90 removal efficiency rate was 0.0863 %/sec^{-1} while for n=0.45 it was almost half and equal to 0.0437 %/sec^{-1}. This phenomenon could be attributed to the available NH_4^+ cations and the increased competition with other cations, especially K^+ and Na^+, which are monovalent. In research conducted from Ward et al. (2018), centrare water was pre-treated with struvite crystallization to initially remove PO_4^{3-} and the effluent, composed mainly by Na^+, K^+, Cl^- and NH_4^+ and small amount of Mg^{2+}, was treated by an ED. The chemical analysis of the concentrate showed that Na^+ and NH_4^+ had similar transport rate, especially at the first 10 hours of the experiment, indicating that the competition between those two cations was higher related to others. In addition, electrodialysis was tested with ammonium nitrate and potassium nitrate solutions to investigate the ion transport (Kozaderova et al., 2017). The latter one was chosen based on the similarities of ions in the aqueous solution. The results indicated a decrease in the NH_4^+ flux at the limiting current density due to the competitive transfer of solution ions, the effect of hydrolysis reaction involving NH_4^+ and the barrier effect, which consists of the formation of weak NH_3H_2O. Moreover, the current density that was offered was the same in every case, however when it must be distributed among more ions less energy was available for NH_4^+, leading to smaller removal efficiency. In addition, membrane pores that block the anions to pass through them were becoming blocked quicker due to the increment of the ions pass.

For the several molar ratios applied in an ED, energy consumption at the end of operational cycle and when removal efficiency was 75% was recorded. In that point, it is also important to say that 75% removal efficiency of NH_4^+ was considered in this research as a baseline and minimum requirement. Both cases presented a linear trend based on the molar ratios, with the latter to have a smaller slope, meaning a less drastic change with the alternation of molar ratio. On the other hand, the overall energy consumption presented similar trend to the one of the overall removal efficiency, with the lowest molar ratios to be the more challenging wastewaters. The initial concentration of feed solution played a dominant role in the salt transport number and membrane resistance (Sun et al., 2022). This means that the extremely high concentration of salts increased also the membrane resistance while transport number reduced in the same case. This could also be explained by Donnan equilibrium theory, where the ion transport number decreased with the external salt concentration due to Donnan exclusion effect.

Moreover, transport efficiency for cations was estimated and showed an obvious increase with the increase in molar ratio for NH_4^+. For all cases the amount of NH_4^+ added was the same and thus comparable between different molar ratios. It also presented a linear increase, as it was expected. NH_4^+ when it had higher competition, less current would be applied to it and be distributed to the other cations as well. For molar ratios below 0.60, less than half of the current was used for NH_4^+ transport, leading to the assumption that those types of reject water were more challenging to be treated by ED. For all the other cations, it could be seen that there was an important variation that could be attributed to the corresponding variation in the solution's concentration.

At last, an important parameter that was estimated was the percent demineralization of the feed solution and it was calculated as shown in equation 2.5. Percent demineralization was estimated for 5 different removal efficiencies of NH_4^+. Taking into consideration the removal efficiency curves for each molar ratio the percent demineralization was estimated. However, removal efficiency of 75% was used as a reference point and the percent demineralization was calculated based on actual data, meaning that the concentrations measured were used for the analysis. For the several removal efficiencies, the applied fitting curves were used. Therefore, for removal efficiency of 60, 65,70 and 80% a modeled equation was used to estimate the EC on the time of this removal efficiency and finally the percent demineralization.

For the results occurred in percent demineralization, the minimum DR appeared for molar ratio of 0.60, when RE is below 75%. However, it appeared an increment for RE over the reference line. For the case of reference line, no specific result could be formed since there was no measurement for n=0.60.

5.2 Sequence batch experiments (SBE)

In case of sequence batch experiments three different molar ratios were tested, which were the more realistic based on the literature on the existing reject water compositions. Removal efficiency and percent demineralization were kept as stable as possible during the operational period. The ratio of final and initial EC was estimated from molar ratio experiments in batch mode to reach minimally 75% removal efficiency of NH_4^+ from feed and this value was used to stabilize the percent demineralization. For n=0.30, PD ranged below 70% in which the corresponding removal efficiency was approximately 70%. The lowest value of RE occurred due to the high ionic density of the solution and the difficulty to be treated. In addition, the competition with the other cations was more intense when the concentration of them became higher, leading to less NH_4^+ transport to the concentrate. In case of n=0.45, RE ranged between 75% to 80%, presenting also a constant PD of 71%. For the higher molar ratio, RE in each batch could be described as a quicker process due to the lower salt concentration of feed solution. This also led to more batches required to reach the final EC target for the concentrate of 20mS/cm.

In addition, current efficiency was also estimated and presented a specific pattern in the sequence batch experiments. The lower the molar ratio of cations the lower the transport number of NH_4^+ was. This phenomenon occurred from the concentration of NH_4^+ compared to other cations, indicating the selectivity of membranes for other cations over NH_4^+. Less current was available for NH_4^+ when molar ratio was 0.30, while for the highest molar ratio the same parameter was 3 times higher. As mentioned above, the added moles of NH_4^+ remained the same for all experiments while the other cations varied based on the required molar ratio (detailed cation composition is presented in the Appendix).

Finally, the energy consumption for the sequence batches, for molar ratio n=0.60 was stable on time with deviations while for the two other cases the initial phase presented notably lower energy consumption than in the following batches due to the high concentration of cations and more specifically Mg^{2+} and Ca^{2+}. Calcium and magnesium ions in an ED system would lead more easily to the formation of scaling, since the main components of scale are calcite ($CaCO_3$) and amorphous $Mg(OH)_2$ (Zhang et al., 2020). Scaling is leading to higher energy consumption due to higher resistance of the stack, which could be promoted for that range of molar ratios. It was also indicated in Figure 4.30 and 4.31, that the system, especially for n=0.30, was prone to scaling, even for short-term operation. Moreover, the voltage development shown in Figure 4.27 explained the high energy consumption and the scaling potential in both experiments. Thus, energy consumption in the abovementioned cases could be explained by these phenomena.

6 Conclusion

Overall, for BPC application, the proton leakage through water dissociation influenced the overall removal efficiency and how it was being developed on time. At the beginning of operation, removal efficiency increased with linear correlation with time, while as proton competition became more dominant in diluate, removal efficiency rate decreased, indicating the negative influence proton competition to NH_4^+ removal. In addition, energy consumption, without considering proton production led to higher values which could be controlled by establishing an EC set point. As the EC is dropping and then increasing again by the H^+ presence, it could be assumed that the operational cycle has ended in that specific time. Moreover, for the same feed solution, conventional ED presented a linear correlation of removal efficiency on time without any disturbance in the overall operation. Energy consumption was lower compared to BPC, which was attributed to the higher resistance developed by the bipolar membrane. Finally, for non-competition in both configurations led to approximately the same removal efficiency and energy consumption since the buffer capacity of HCO_3^- added with NH_4^+ prevented proton competition and acidic environment in diluate solution.

Moreover, several molar ratios were applied in a conventional ED configuration with removal efficiency to follow a similar pattern with the previous case, as a linear curve on time. Energy consumption was also investigated for the case that removal efficiency of NH_4^+ is 75%, when it presented a moderate decrease compared to the overall energy consumption. Transport efficiency, on the other hand, increased with the increment of molar ratio due to the bigger amount of NH_4^+ compared to other cations when the current provided was the same in all cases. Furthermore, percent demineralization was estimated based on the EC for the removal efficiency fitting curves. The results obtained showed that the lowest the chosen removal efficiency the lowest will be the percent demineralization for all molar ratios with lowest point to be for molar ratio $n = 0.60$. However, for removal efficiencies higher than the baseline of 75%, percent demineralization takes a slightly exponential shape.

Finally, sequence batch experiments were used in order to apply the findings from batch and investigate the effect of municipal reject water molar ratios in a more applicable configurations. Percent demineralization and removal efficiency remained constant in each case, with the application of the corresponding EC set point in each molar ratio. Transport number of NH_4^+ increased with the increase of molar ratio due to the lower competition with other cations. In addition, energy consumption presented an increase for the lowest molar ratios due to high voltage and resistance. This is also explained by the formation of scaling in the membranes and spacers that was observed. As for the BPC, proton leakage took place even in high salinity feed, without achieving a highly concentrated base solution at the end of the operational cycle.

7 Recommendations

The results obtained in ion competition for both ED and BPC configurations could be considered as a first step to understand the phenomena taking place and the limitations in applications. However, further research needs to be conducted to gain more detailed knowledge and cover a bigger spectrum of this topic. Thus, it is recommended to investigate the following:

- Application of selective cation exchange membranes with combination of bipolar membranes for synthetic reject water. During this research, a small insight was gained regarding the real case of reject water in several electrodialysis configurations. As presented in the Appendix, reject water from Horstermeer was tested in three different cases: in ED, in BPC and in BPSC, with the latest one to be a combination of bipolar membranes and selective cation exchange membranes that retain the divalent cations in the diluate compartment and allows monovalent to pass to the basic compartment leading to lower scaling potential. Also, it was observed that the amount of divalent cations retained in the feed compartment in BPC was bigger than BPSC, indicating potentially better performance in their removal. However, more research needs to be done, especially as far as the composition is concerned, to investigate the effect of several molar ratios for the feed solution.
- Application of a bigger range of molar ratios in BPC to understand the phenomenon of proton production when all cations are included in different amounts. In this research the molar ratio effect was mainly investigated in the conventional ED configuration
- Applications of sequence batch configuration, in collaboration with BPC, with real reject waters, with different molar ratios. Real reject water can contain humic acids and COD that could affect the overall performance due to organic fouling of membranes. Sequence batch experiments resemble the real case scenarios and thus the results could be more representative.

8 References

Al-Amshawee, S., Yunus, M. Y. B. M., Azoddein, A. A. M., Hassell, D. G., Dakhil, I. H., & Hasan, H. A. (2020). Electrodialysis desalination for water and wastewater: A review. In Chemical Engineering Journal (Vol. 380). Elsevier B.V. https://doi.org/10.1016/j.cej.2019.122231

Andreeva, M. A., Gil, V. v., Pismenskaya, N. D., Dammak, L., Kononenko, N. A., Larchet, C., Grande, D., & Nikonenko, V. v. (2018). Mitigation of membrane scaling in electrodialysis by electroconvection enhancement, pH adjustment and pulsed electric field application. Journal of Membrane Science, 549, 129–140. https://doi.org/10.1016/j.memsci.2017.12.005

Andreeva, M. A., Gil, V. v., Pismenskaya, N. D., Dammak, L., Kononenko, N. A., Larchet, C., Grande, D., & Nikonenko, V. v. (2018). Mitigation of membrane scaling in electrodialysis by electroconvection enhancement, pH adjustment and pulsed electric field application. Journal of Membrane Science, 549, 129–140. https://doi.org/10.1016/j.memsci.2017.12.005

Asraf-Snir, M., Gilron, J., & Oren, Y. (2016). Gypsum scaling of anion exchange membranes in electrodialysis. Journal of Membrane Science, 520, 176–186. https://doi.org/10.1016/j.memsci.2016.07.013

Borges, F. J., Roux-de Balmann, H., & Guardani, R. (2008). Investigation of the mass transfer processes during the desalination of water containing phenol and sodium chloride by electrodialysis. Journal of Membrane Science, 325(1), 130–138. https://doi.org/10.1016/j.memsci.2008.07.017

Breunig, H. M., Amirebrahimi, J., Smith, S., & Scown, C. D. (2019). Role of Digestate and Biochar in Carbon-Negative Bioenergy. Environmental Science and Technology. https://doi.org/10.1021/acs.est.9b03763

Bukhovets, A., Eliseeva, T., & Oren, Y. (2010). Fouling of anion-exchange membranes in electrodialysis of aromatic amino acid solution. Journal of Membrane Science, 364(1–2), 339–343. https://doi.org/10.1016/j.memsci.2010.08.030

Chen, Q. B., Ji, Z. Y., Liu, J., Zhao, Y. Y., Wang, S. Z., & Yuan, J. S. (2018). Development of recovering lithium from brines by selective-electrodialysis: Effect of coexisting cations on the migration of lithium. Journal of Membrane Science, 548, 408–420. https://doi.org/10.1016/j.memsci.2017.11.040

Chojnacka, K., Skrzypczak, D., Szopa, D., Izydorczyk, G., Moustakas, K., & Witek-Krowiak, A. (2023). Management of biological sewage sludge: Fertilizer nitrogen recovery as the solution to fertilizer crisis. In Journal of Environmental Management (Vol. 326). Academic Press. https://doi.org/10.1016/j.jenvman.2022.116602

Cohen, B., Lazarovitch, N., & Gilron, J. (2018). Upgrading groundwater for irrigation using monovalent selective electrodialysis. Desalination, 431, 126–139. https://doi.org/10.1016/j.desal.2017.10.030

Dufton, G., Mikhaylin, S., Gaaloul, S., & Bazinet, L. (2018). How electrodialysis configuration influences acid whey deacidification and membrane scaling. Journal of Dairy Science, 101(9), 7833–7850. https://doi.org/10.3168/jds.2018-14639

Frilette, V., The Preparation of Bipolar Ion-exchange Membranes. (1956). https://pubs.acs.org/sharingguidelines

Galama, A. H., Saakes, M., Bruning, H., Rijnaarts, H. H. M., & Post, J. W. (2014). Seawater predesalination with electrodialysis. Desalination, 342, 61–69. https://doi.org/10.1016/j.desal.2013.07.012

Gao, W., Fang, Q., Yan, H., Wei, X., & Wu, K. (2021). Recovery of acid and base from sodium sulfate containing lithium carbonate using bipolar membrane electrodialysis. Membranes, 11(2), 1–15. https://doi.org/10.3390/membranes11020152

Gjelstad, A., Rasmussen, K. E., & Pedersen-Bjergaard, S. (2007). Simulation of flux during electro-membrane extraction based on the Nernst-Planck equation. Journal of Chromatography A, 1174(1–2), 104–111. https://doi.org/10.1016/j.chroma.2007.08.057

Guo, X., Chen, J., Wang, X., Li, Y., Liu, Y., & Jiang, B. (2023). Sustainable ammonia recovery from low strength wastewater by the integrated ion exchange and bipolar membrane electrodialysis with membrane contactor system. Separation and Purification Technology, 305. https://doi.org/10.1016/j.seppur.2022.122429

H. Strathmann, Ion-Exchange Membrane Separation Processes, Elsevier Science,Stuttgart, 2004
Han, L., Galier, S., & Roux-de Balmann, H. (2015). Ion hydration number and electro-osmosis during electrodialysis of mixed salt solution. Desalination, 373, 38–46. https://doi.org/10.1016/j.desal.2015.06.023

Hoek, E. M. V., Bhattacharjee, S., & Elimelech, M. (2003). Effect of membrane surface roughness on colloid-membrane DLVO interactions. Langmuir, 19(11), 4836–4847. https://doi.org/10.1021/la027083c

Ippersiel, D., Mondor, M., Lamarche, F., Tremblay, F., Dubreuil, J., & Masse, L. (2012). Nitrogen potential recovery and concentration of ammonia from swine manure using electrodialysis coupled with air stripping. Journal of Environmental Management, 95(SUPPL.). https://doi.org/10.1016/j.jenvman.2011.05.026

J. Pretz, E. Staude, Reverse electrodialysis (RED) with bipolar membranes, an energy storage system, Berichte Der Bunsengesellschaft Für Phys. Chemie. 102 (2010) 676–685, https://doi.org/10.1002/bbpc.19981020412

Kedwell, K. C., Jørgensen, M. K., Quist-Jensen, C. A., Pham, T. D., van der Bruggen, B., & Christensen, M. L. (2021). Selective electrodialysis for simultaneous but separate phosphate and ammonium recovery. Environmental Technology (United Kingdom), 42(14), 2177–2186. https://doi.org/10.1080/09593330.2019.1696410

Kim, I. T., Lee, Y. E., Jeong, Y., & Yoo, Y. S. (2020). A novel method to remove nitrogen from reject water in wastewater treatment plants using a methane- and methanol-dependent bacterial consortium. Water Research, 172. https://doi.org/10.1016/j.watres.2020.115512

Kozaderova, O. A., Niftaliev, S. I., & Kim, K. B. (2018). Ionic Transport in Electrodialysis of Ammonium Nitrate. Russian Journal of Electrochemistry, 54(4), 363–367. https://doi.org/10.1134/S1023193518040043

L. Karimi, A. Ghassemi, Effects of operating conditions on ion removal from brackish water using a pilot-scale electrodialysis reversal system, Desalin. Water Treat. 57 (2016) 8657–8669, https://doi.org/10.1080/19443994.2015.1024748

Larchet, C., Auclair, B., & Nikonenko, V. (2004). Approximate evaluation of water transport number in ion-exchange membranes. Electrochimica Acta, 49(11), 1711–1717. https://doi.org/10.1016/j.electacta.2003.11.030

Lee, H.-J., Hong, M.-K., Han, S.-D., Cho, S.-H., & Moon, S.-H. (2009). Fouling of an anion exchange membrane in the electrodialysis desalination process in the presence of organic foulants. Desalination, 238, 60–69. https://doi.org/10.1016/j.desal.200

Li, Y., Wang, R., Shi, S., Cao, H., Yip, N. Y., & Lin, S. (2021). Bipolar Membrane Electrodialysis for Ammonia Recovery from Synthetic Urine: Experiments, Modeling, and Performance Analysis. Environmental Science and Technology, 55(21), 14886–14896. https://doi.org/10.1021/acs.est.1c05316

Luo, T., Abdu, S., & Wessling, M. (2018). Selectivity of ion exchange membranes: A review. In Journal of Membrane Science (Vol. 555, pp. 429–454). Elsevier B.V. https://doi.org/10.1016/j.memsci.2018.03.051

Mani, K. N. (1991.). Electrodialysis water splitting technology.

Mehta, C. M., Khunjar, W. O., Nguyen, V., Tait, S., & Batstone, D. J. (2015). Technologies to recover nutrients from waste streams: A critical review. In Critical Reviews in Environmental Science and Technology (Vol. 45, Issue 4, pp. 385–427). Taylor and Francis Inc. https://doi.org/10.1080/10643389.2013.866621

Mondor, M., Masse, L., Ippersiel, D., Lamarche, F., & Massé, D. I. (2008). Use of electrodialysis and reverse osmosis for the recovery and concentration of ammonia from swine manure. Bioresource Technology, 99(15), 7363–7368. https://doi.org/10.1016/j.biortech.2006.12.039

Nakayama, A., Sano, Y., Bai, X., & Tado, K. (2017). A boundary layer analysis for determination of the limiting current density in an electrodialysis desalination. Desalination, 404, 41–49. https://doi.org/10.1016/j.desal.2016.10.013

Nguyen, L. D., Gassara, S., Bui, M. Q., Zaviska, F., Sistat, P., & Deratani, A. (2019). Desalination and removal of pesticides from surface water in Mekong Delta by coupling electrodialysis and nanofiltration. Environmental Science and Pollution Research, 26(32), 32687–32697. https://doi.org/10.1007/s11356-018-3918-6

Öner, M. R., Kanca, A., Ata, O. N., Yapici, S., & Yaylali, N. A. (2021). Bipolar membrane electrodialysis for mixed salt water treatment: Evaluation of parameters on process performance. Journal of Environmental Chemical Engineering, 9(4). https://doi.org/10.1016/j.jece.2021.105750

Ortega, A., Arenas, L. F., Pijpers, J. J. H., Vicencio, D. L., Martínez, J. C., Rodríguez, F. A., & Rivero, E. P. (2022). Modelling water dissociation, acid-base neutralization and ion transport in bipolar membranes for acid-base flow batteries. Journal of Membrane Science, 641. https://doi.org/10.1016/j.memsci.2021.119899

Ozkul, S., van Daal, J. J., Kuipers, N. J. M., Bisselink, R. J. M., Bruning, H., Dykstra, J. E., & Rijnaarts, H. H. M. (2023). Transport mechanisms in electrodialysis: The effect on selective ion transport in multi-ionic solutions. Journal of Membrane Science, 665. https://doi.org/10.1016/j.memsci.2022.121114

Reig, M., Farrokhzad, H., van der Bruggen, B., Gibert, O., & Cortina, J. L. (2015). Synthesis of a monovalent selective cation exchange membrane to concentrate reverse osmosis brines by electrodialysis. Desalination, 375, 1–9. https://doi.org/10.1016/j.desal.2015.07.023

Reig, M., Valderrama, C., Gibert, O., & Cortina, J. L. (2016). Selectrodialysis and bipolar membrane electrodialysis combination for industrial process brines treatment: Monovalent-divalent ions separation and acid and base production. Desalination, 399, 88–95. https://doi.org/10.1016/j.desal.2016.08.010

Rijnaarts, T., Shenkute, N. T., Wood, J. A., de Vos, W. M., & Nijmeijer, K. (2018). Divalent Cation Removal by Donnan Dialysis for Improved Reverse Electrodialysis. ACS Sustainable Chemistry and Engineering, 6(5), 7035–7041. https://doi.org/10.1021/acssuschemeng.8b00879

Rosca, V., Duca, M., DeGroot, M. T., & Koper, M. T. M. (2009). Nitrogen Cycle Electrocatalysis. Chemical Reviews, 109(6), 2209–2244. https://doi.org/10.1021/cr8003696

Rottiers, T., Ghyselbrecht, K., Meesschaert, B., van der Bruggen, B., & Pinoy, L. (2014). Influence of the type of anion membrane on solvent flux and back diffusion in electrodialysis of concentrated NaCl solutions. Chemical Engineering Science, 113, 95–100. https://doi.org/10.1016/j.ces.2014.04.008

Saabas, D., & Lee, J. (2022). Recovery of ammonia from simulated membrane contactor effluent using bipolar membrane electrodialysis. Journal of Membrane Science, 644. https://doi.org/10.1016/j.memsci.2021.120081

Sadrzadeh, M., & Mohammadi, T. (2009). Treatment of sea water using electrodialysis: Current efficiency evaluation. Desalination, 249(1), 279–285. https://doi.org/10.1016/j.desal.2008.10.029

Sedighi, M., Behvand Usefi, M. M., Ismail, A. F., & Ghasemi, M. (2023). Environmental sustainability and ions removal through electrodialysis desalination: Operating conditions and process parameters. In Desalination (Vol. 549). Elsevier B.V. https://doi.org/10.1016/j.desal.2022.116319

Sun, B., Zhang, M., Huang, S., Cao, Z., Lu, L., & Zhang, X. (2022). Study on mass transfer performance and membrane resistance in concentration of high salinity solutions by electrodialysis. Separation and Purification Technology, 281. https://doi.org/10.1016/j.seppur.2021.119907

Sutton, M. A., Erisman, J. W., Dentener, F., & Möller, D. (2008). Ammonia in the environment: From ancient times to the present. In Environmental Pollution (Vol. 156, Issue 3, pp. 583–604). https://doi.org/10.1016/j.envpol.2008.03.013

Tanaka, Y. (2007). Chapter 3 Bipolar Membrane Electrodialysis. In Membrane Science and Technology (Vol. 12, pp. 405–436). https://doi.org/10.1016/S0927-5193(07)12017-9

Tansel, B., Lunn, G., & Monje, O. (2018). Struvite formation and decomposition characteristics for ammonia and phosphorus recovery: A review of magnesium-ammonia-phosphate interactions. In Chemosphere (Vol. 194, pp. 504–514). Elsevier Ltd. https://doi.org/10.1016/j.chemosphere.2017.12.004

Tedesco, M., Hamelers, H. V. M., & Biesheuvel, P. M. (2017). Nernst-Planck transport theory for (reverse) electrodialysis: II. Effect of water transport through ion-exchange membranes. Journal of Membrane Science, 531, 172–182. https://doi.org/10.1016/j.memsci.2017.02.031

Valera-Medina, A., Xiao, H., Owen-Jones, M., David, W. I. F., & Bowen, P. J. (2018). Ammonia for power. In Progress in Energy and Combustion Science (Vol. 69, pp. 63–102). Elsevier Ltd. https://doi.org/10.1016/j.pecs.2018.07.001

van Linden, N., Bandinu, G. L., Vermaas, D. A., Spanjers, H., & van Lier, J. B. (2020). Bipolar membrane electrodialysis for energetically competitive ammonium removal and dissolved ammonia production. Journal of Cleaner Production, 259. https://doi.org/10.1016/j.jclepro.2020.120788

van Linden, N., Spanjers, H., & van Lier, J. B. (2019). Application of dynamic current density for increased concentration factors and reduced energy consumption for concentrating ammonium by electrodialysis. Water Research, 163. https://doi.org/10.1016/j.watres.2019.114856

Wang, Z., Anand, D., & He, Z. (2023). Phosphorus Recovery from Whole Digestate through Electrochemical Leaching and Precipitation. Environmental Science & Technology. https://doi.org/10.1021/acs.est.3c02843

Wang, Z., He, P., Zhang, H., Zhang, N., & Lü, F. (2022). Desalination, nutrients recovery, or products extraction: Is electrodialysis an effective way to achieve high-value utilization of liquid digestate? Chemical Engineering Journal, 446. https://doi.org/10.1016/j.cej.2022.136996

Ward, A. J., Arola, K., Thompson Brewster, E., Mehta, C. M., & Batstone, D. J. (2018). Nutrient recovery from wastewater through pilot scale electrodialysis. Water Research, 135, 57–65. https://doi.org/10.1016/j.watres.2018.02.021

Wu, X., & Modin, O. (2013). Ammonium recovery from reject water combined with hydrogen production in a bioelectrochemical reactor. Bioresource Technology, 146, 530–536. https://doi.org/10.1016/j.biortech.2013.07.130

Yang, D., Liu, H., & She, Q. (2023). Mixed cation transport behaviours in electrodialysis during simultaneous ammonium enrichment and wastewater desalination. Desalination, 545. https://doi.org/10.1016/j.desal.2022.116155

Ye, Z. L., Ghyselbrecht, K., Monballiu, A., Pinoy, L., & Meesschaert, B. (2019). Fractionating various nutrient ions for resource recovery from swine wastewater using simultaneous anionic and cationic selective-electrodialysis. Water Research, 160, 424–434. https://doi.org/10.1016/j.watres.2019.05.085

Zamfirescu, C., & Dincer, I. (2009). Ammonia as a green fuel and hydrogen source for vehicular applications. Fuel Processing Technology, 90(5), 729–737. https://doi.org/10.1016/j.fuproc.2009.02.004

Zhang, C., Ding, W., Zeng, X., & Xu, X. (2020). Recovery of ammonia nitrogen from landfill leachate using a biopolar membrane equipped electrodialysis system. Water Science and Technology, 82(9), 1758–1770. https://doi.org/10.2166/wst.2020.438

Zhang, Y., Ghyselbrecht, K., Meesschaert, B., Pinoy, L., & van der Bruggen, B. (2011). Electrodialysis on RO concentrate to improve water recovery in wastewater reclamation. Journal of Membrane Science, 378(1–2), 101–110. https://doi.org/10.1016/j.memsci.2010.10.036

Appendix

Organic fouling in IEX

Membrane fouling is one of the most frequent drawbacks in all membranes' properties. They decrease membrane's life span and membranes require usual cleaning to obtain the initial overall efficiency. One of the reasons of this phenomenon is the presence of organic matter in reject water. Even though the concentration of organic material is not high, since a big amount has already been removed from the previous wastewater treatment steps, it can still be a threat for a long-term operation in an ED system.

Organic matter is mostly negatively charged, which means that in an electrodialysis set-up it could be removed through the anion exchange membrane. In ED membrane fouling results in the increase of membrane resistivity which also turn causes a decrease of ions flux through a membrane and an increase in energy consumption. Ion-exchange membranes can be fouled by ionic components of medium molecular weight such as ionic surface-active agents or proteins having charges opposite to the ones of the membrane (Bukhovets et al., 2010). In addition, suspended solids and colloids, polyelectrolytes, organic anions can cause severe problems in membranes of ED system due to precipitation at their surface or partial penetration into them. As for the cleaning and treatment, acids and bases could be used to restore the original properties.

Bukhovets et al. (2010) investigated the fouling of heterogenous anion exchange membranes during electrodialysis of solutions containing aromatic amino acid and mineral salt. The results showed that anion exchange membrane MA-41 indicated fouling and there was no big difference between the membrane potential during ED of NaCl solution and Phe-NaCl solution at the same current density value. Voltage values on the other side presented a difference on the fresh and the fouled membranes. In addition, because of water splitting in the interphase boundary anion-exchange membrane-diluate solution the pH decreases at the surface facilitate the organic fouling.

Moreover, Lee et al. (2009) investigated the fouling of anion exchange membranes in desalination processes with organic foulants presence, and more specifically humate, bovine serum albumin (BVA) and sodium dodecylbenzenesulfonate (SDBS). All the foulants were highly negatively charged according to zeta potential measurements, with SDBS showing the higher adsorption capacity on the AEM. The hypothesis was evaluated with SDBS having the largest increase in the energy consumption and decrease in the current efficiency after fouling, implying that the foulant with the highest adsorption capacity affecting the ED desalination process performance.

Finally, the organic fouling mechanism of anion exchange membranes was studied based on electrostatic interaction, affinity interaction and geometrical factors were measured (Tanaka et al., 2012). Commercially available anion exchange membranes and NaCl solution containing organic substances with different chemical structures were used. The results obtained indicated that aromatic organic substances caused more sever fouling due to affinity interaction between them and the membrane matrix. Anion-exchange membranes with an aromatic polymer matrix and low water content was fouled more severely by aromatic compounds with high molecular weight.

Batch experiments – Mass ratio in BPC

In BPC configuration, due to water dissociation, there is proton leakage to the diluate solution and hydroxide transport to base solution, thus the basic environment that creates.

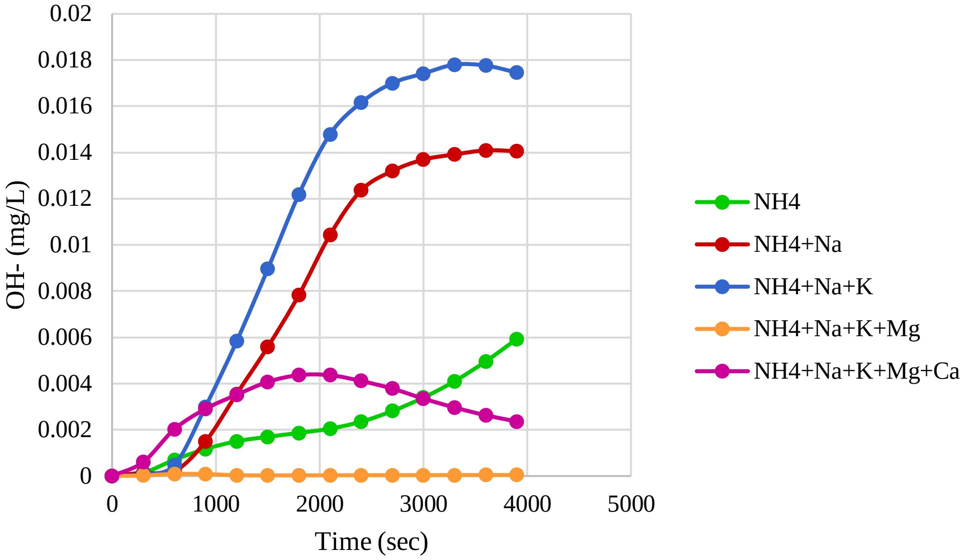

Figure 1. OH^- concentration in base solution in BPC.

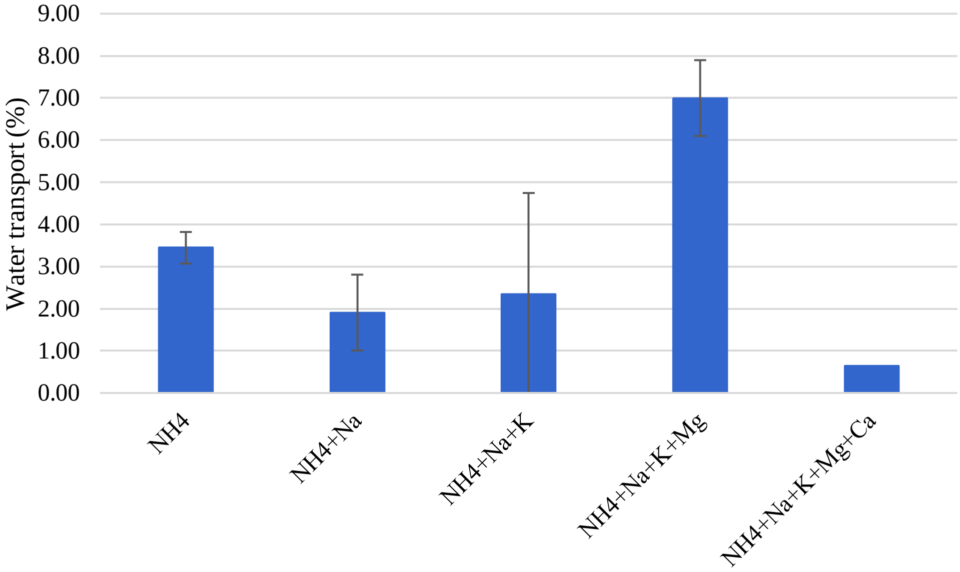

Figure 2. Water transport in BPC mass ratios.

In addition, water transport for diluate was calculated for BPC configuration as shown in literature review.

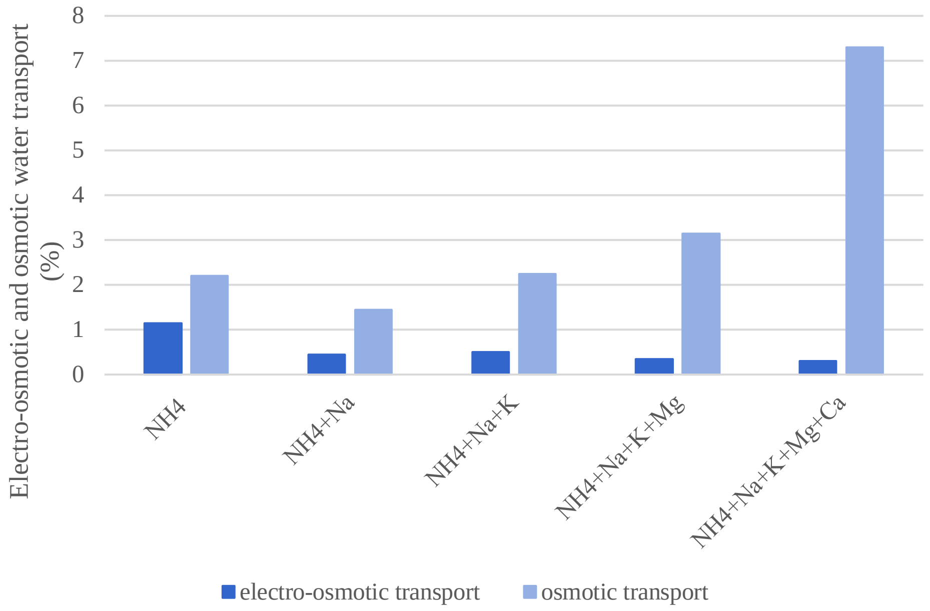

Figure 3. Electro-osmotic and osmotic water transport

Batch experiments – Mass ratio in ED

Water transport was also calculated for ED system where the values were higher than the corresponding BPC.

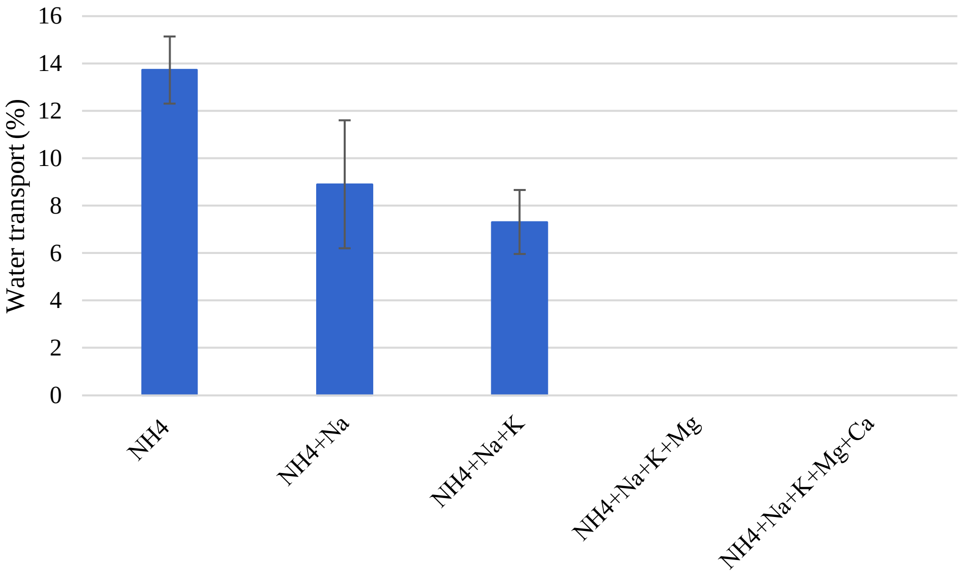

Figure 4. Water transport for ED in mass ratio experiments

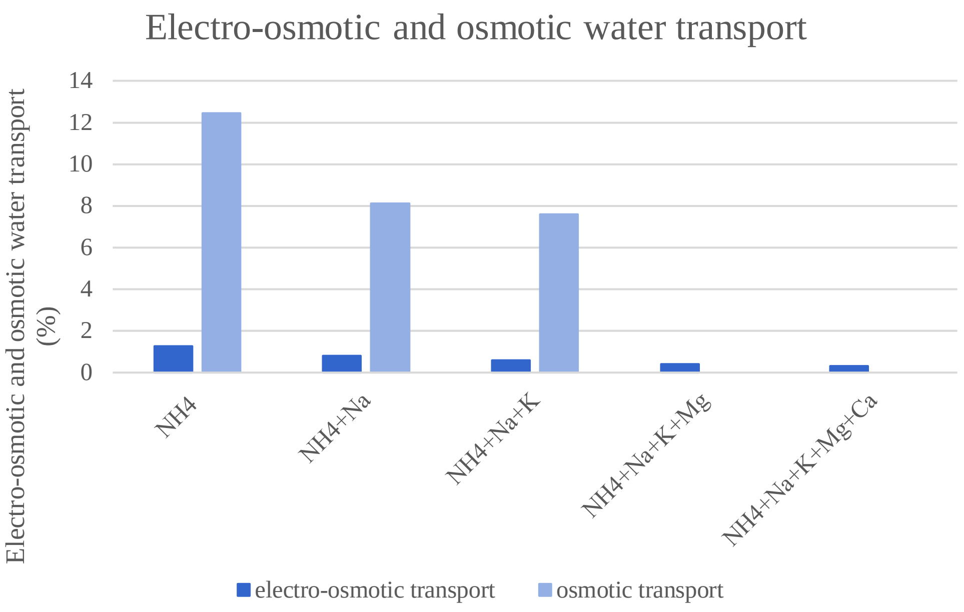

Figure 5. Electro-osmotic and osmotic water transport

Batch experiments – Molar ratio in ED

In the batch experiments 5 different molar ratios were applied, where the NH_4^+ mass remained constant for every case and the rest of salts' masses changed. The detailed concentrations are presented in Table 1.

Table 1. Concentration of salts in molar ratios experiments in ED.

Molar ratio	NH_4HCO_3 (g/L)	Na_2SO_4 (g/L)	K_2HPO_4 (g/L)	$MgCl_2$ (g/L)	$CaCl_2$ (g/L)
0.30	1.7529	0.9186	0.9642	1.2311	1.4354
0.45	1.7529	0.4812	0.5051	0.6449	0.7519
0.60	1.7529	0.2625	0.2755	0.3517	0.4101
0.75	1.7529	0.1312	0.1378	0.1759	0.2051
0.90	1.7529	0.0437	0.0459	0.0586	0.0684

For molar ratios experiments in batch conditions the percent demineralization was calculated as mentioned in the methodology and shown in Figure 4.23.

Table 2. Percent demineralization

Molar ratio	EC for RE=60%	EC for RE=65%	EC for RE=70%	EC for RE=75%	EC for RE=80%
0.3	51.2	56.5	61.2	65.0	
0.45	47.7	53.1	58.7	63.6	68.3
0.6	40.8	48.0	54.9		69.4
0.75	52.0	58.0	63.9	69.9	75.7
0.9	66.8	70.3	73.8		

Table 3. EC for molar ratios for different removal efficiencies based on the fitting curves for all removal efficiencies, excluded the RE of 75%.

molar ratio	EC for RE=60%	EC for RE=65%	EC for RE=70%	EC for RE=75%	EC for RE=80%	EC initial
0.3	3740	3330	2970	2680		7660
0.45	2800	2510	2210	1947	1696	5350
0.6	2190	1924	1668		1133	3700
0.75	1661	1452	1250	1042	841	3460
0.9	901	804	709			2710

In addition, removal efficiency rate was calculated based on the removal efficiency fitting curves and the results are presented in Table 4.

Table 4. Removal efficiency rate for ED molar ratio batch experiments.

molar ratio	Removal efficiency rate
0.3	0.015
0.45	0.028
0.6	0.033
0.75	0.054
0.9	0.111

Finally, the current applied and the voltage are presented below, for both duplicates.

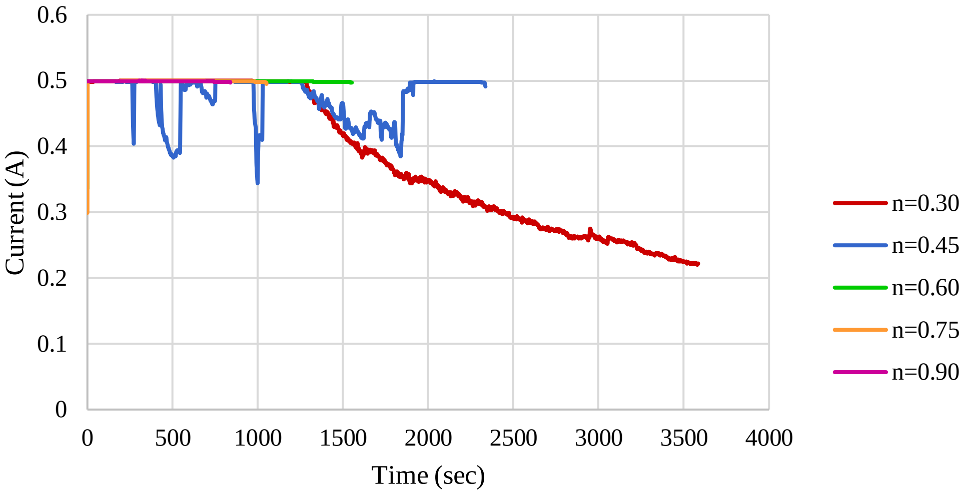

(a)

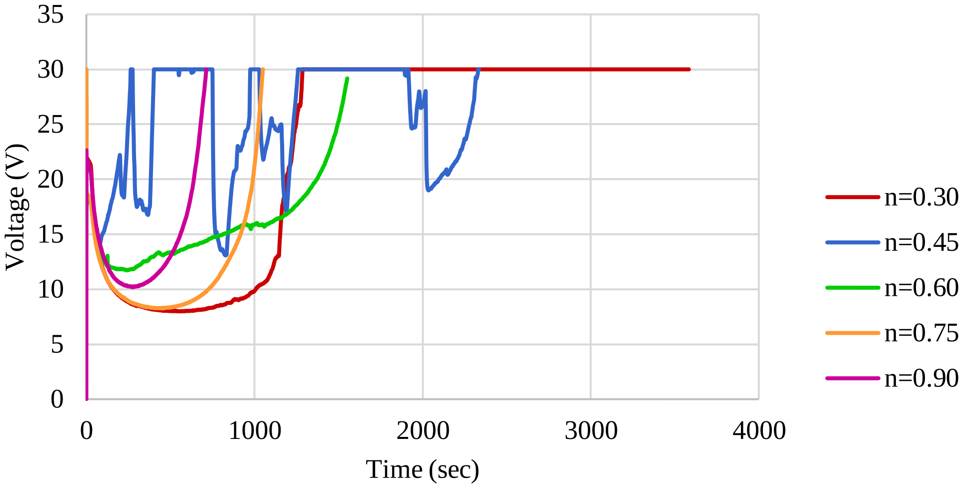

(b)

Figure 5. Power supply data for molar ratio (a) Current (b) Voltage.

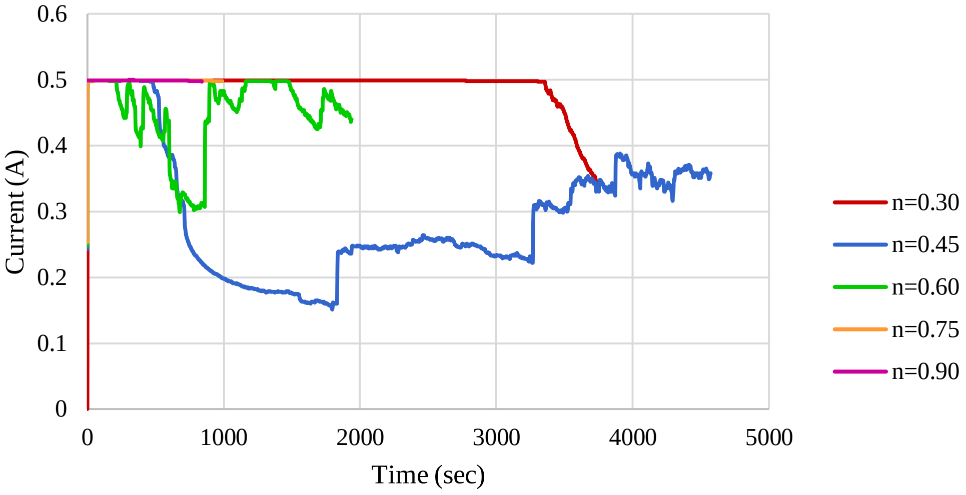

(a)

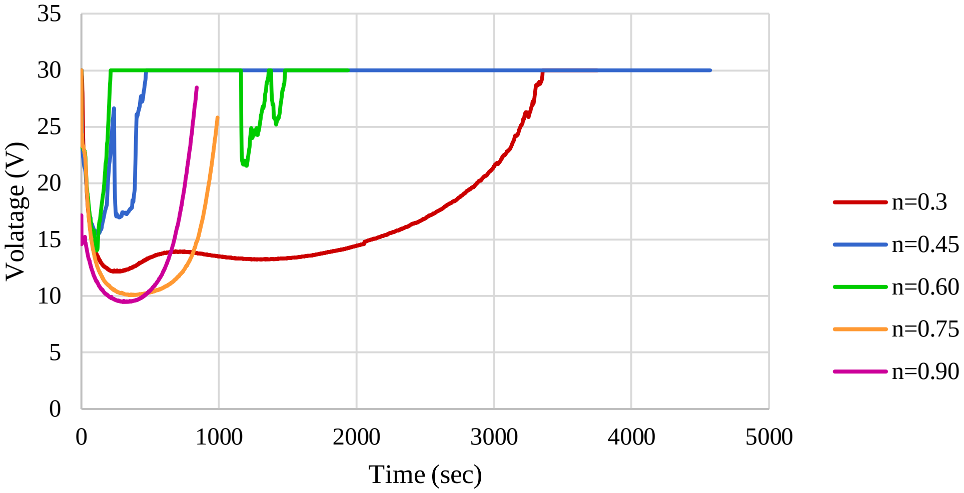

(b)

Figure 6. Power supply data for molar ratios in ED in duplicates (a) Current (b) Voltage

Sequence batch experiment

In the sequence batch experiment the molar ratio kept constant regarding the corresponding molar ratio. Thus. the added concentrations are presented in Table 1.

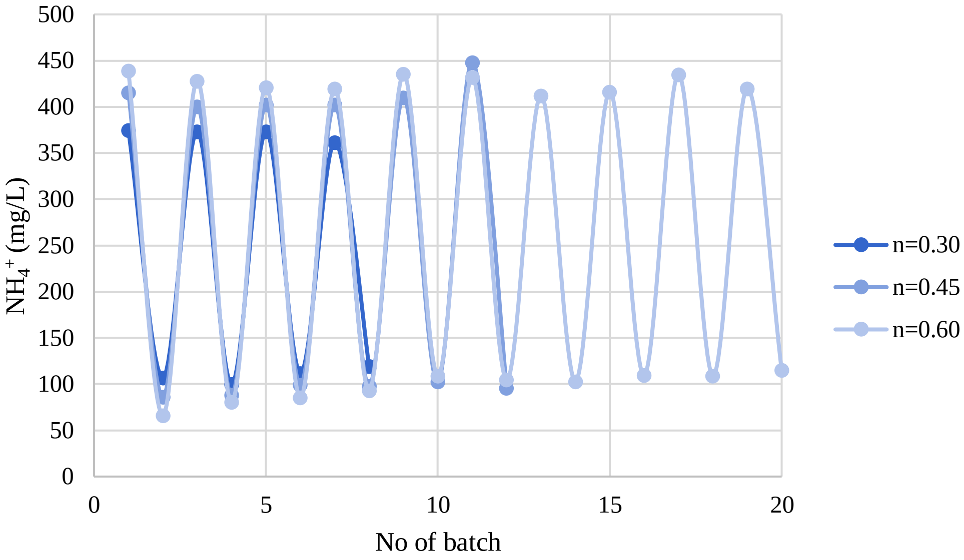

Figure 7. NH_4^+ concentration in diluate for sequence batch experiments in ED.

As for the concentrate, the concentration of NH_4^+ increased with time. It could be seen that the overall removal efficiency of the operation was higher for the bigger molar ratios.

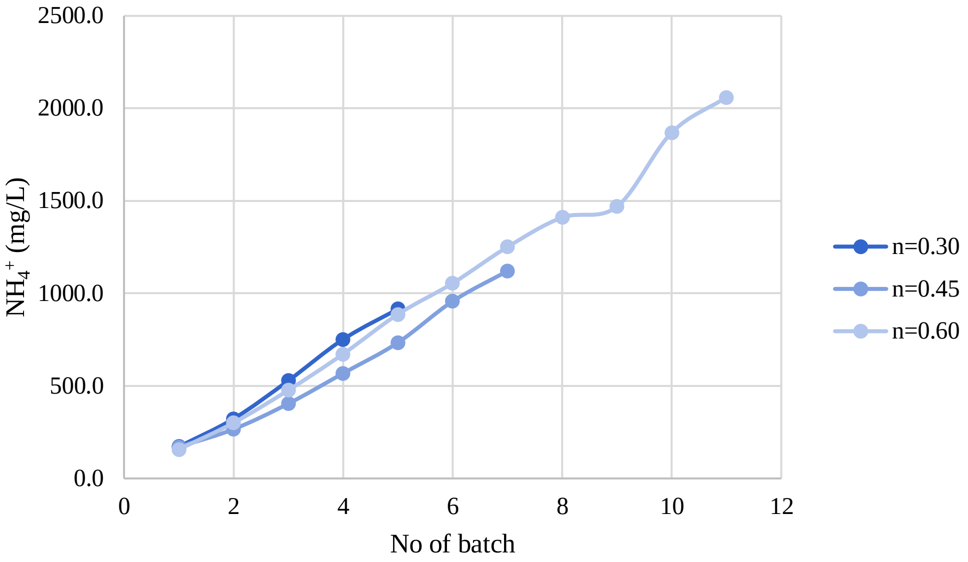

Figure.8. NH_4^+ concentration in concentrate for sequence batch experiments in ED.

In case of the second phase of the sequence batch experiment, a single batch was operated in a BPC where the EC values for the diluate are presented in Figure 10.

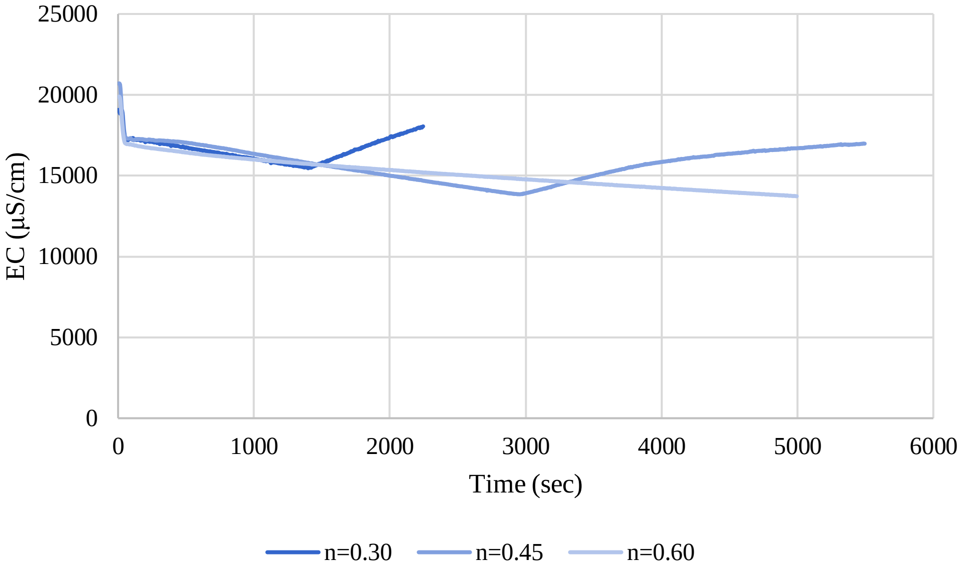

Figure 9. EC in diluate for sequence batch experiments in BPC

The pH in this case for the lower molar ratios presented an instant decrease, as explained also in the batch operation of BPC. However, for molar ratio of 0.60 pH remained constant in the entire operational period. This possibly could be attributed to a system malfunction.

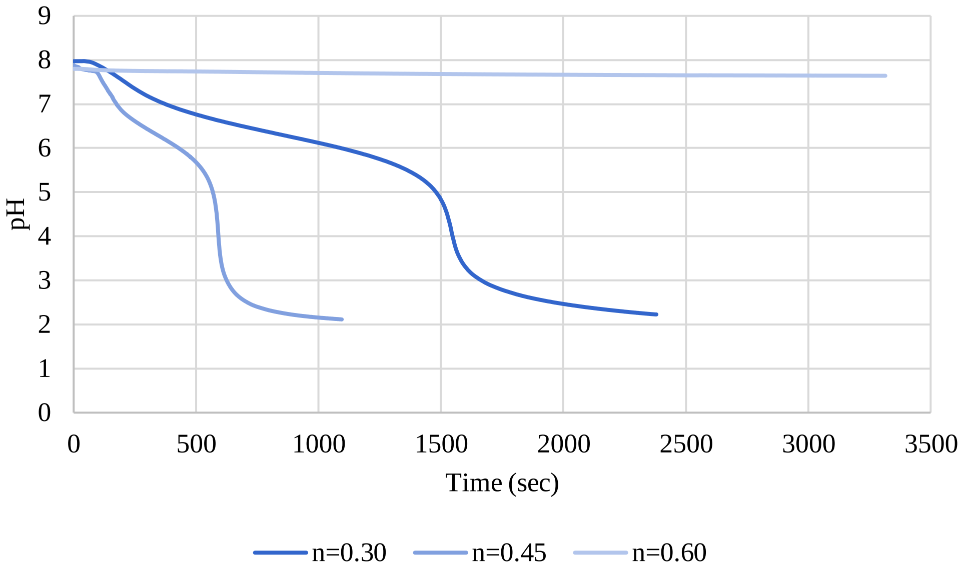

Figure 10. pH in diluate for sequence batch experiments in BPC

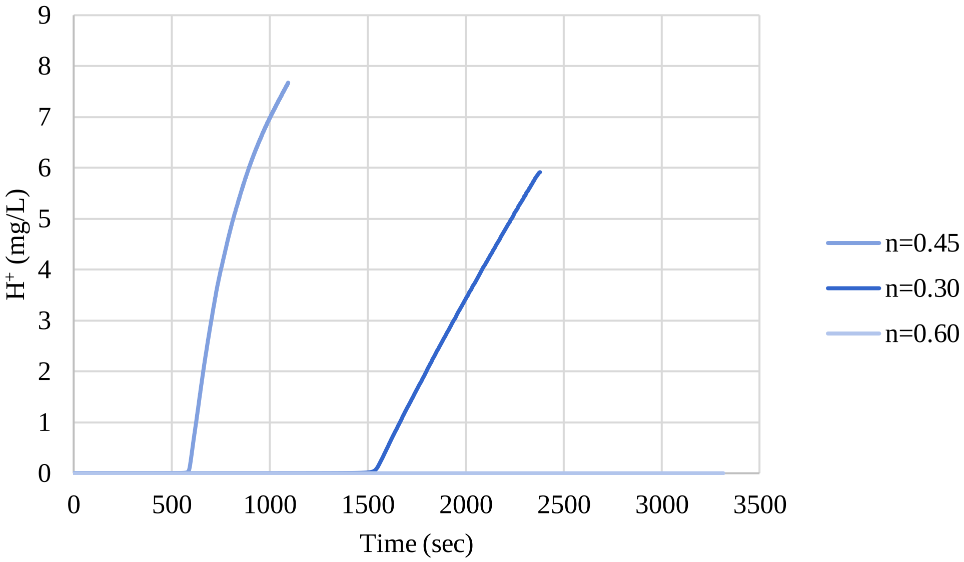

Figure 11. H^+ concentration in diluate for sequence batch experiments.

Real reject water

Transport efficiency

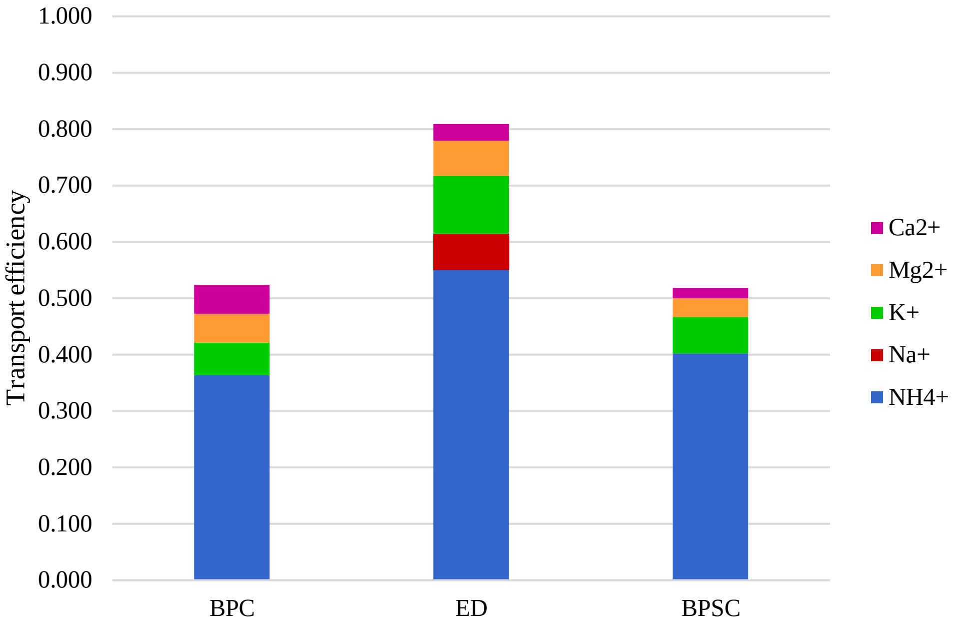

Figure 12. Transport efficiency of cations in reject water of Horstermeer in the operated configurations

Removal efficiency

In reject water, three different configurations were tested independently. Removal efficiency was estimated on time for all of them and presented in Figure 14.

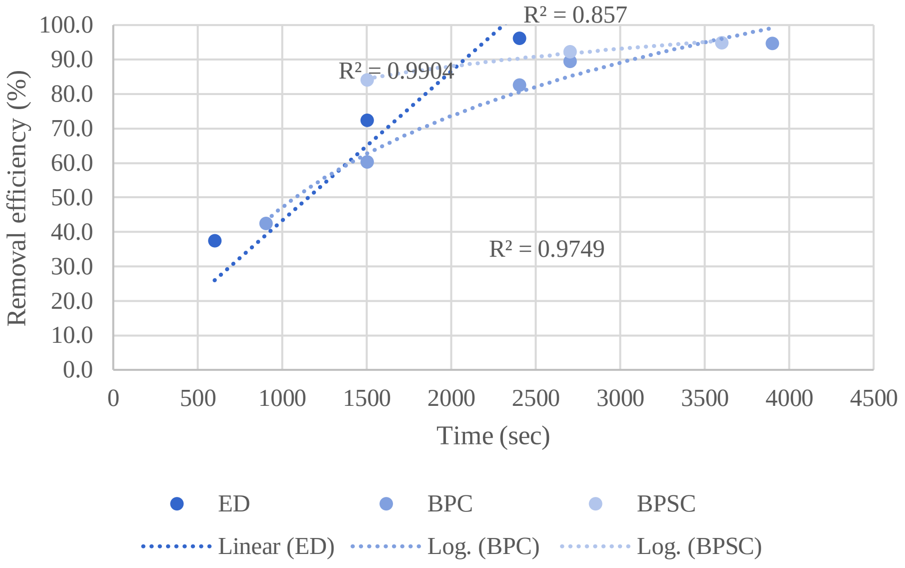

Figure 13.Removal efficiency of NH_4^+ on time in reject water of Horstermeer in the operated configurations.

Based on the data analysis, a fitting of the values was conducted to reach an approximation of the trend in each configuration. Removal efficiency, in a system including bipolar membranes, presented a logarithmic trend on time of the experiment conducted. More specifically, BPSC indicated a steeper curve and reached high values in early time of the experiment, while in case of BPC the same values were reached later on time. However, the BPSC had an equilibrium in lower maximum removal efficiency over the BPC. Moreover, conventional ED had a linear trend in removal efficiency over time. For the bipolar configuration, the R^2 was 0.97 for BPC and 0.99 for BPSC, while for ED was 0.98.

In addition, it was observed that the retained percentage of divalent cations (Mg^{2+}, Ca^{2+}) in the diluate compartment was higher in case of BPSC compared to BPC. For the first case, for Mg^{2+} 71.3% of the total was retained and 24.7% of Ca^{2+}, while for BPC the same percentages were 12.8% for Mg^{2+} and almost all the amount of Ca^{2+} was removed from diluate.

Energy consumption in digestate treatment

Energy consumption for all configurations is presented in Figure 15.

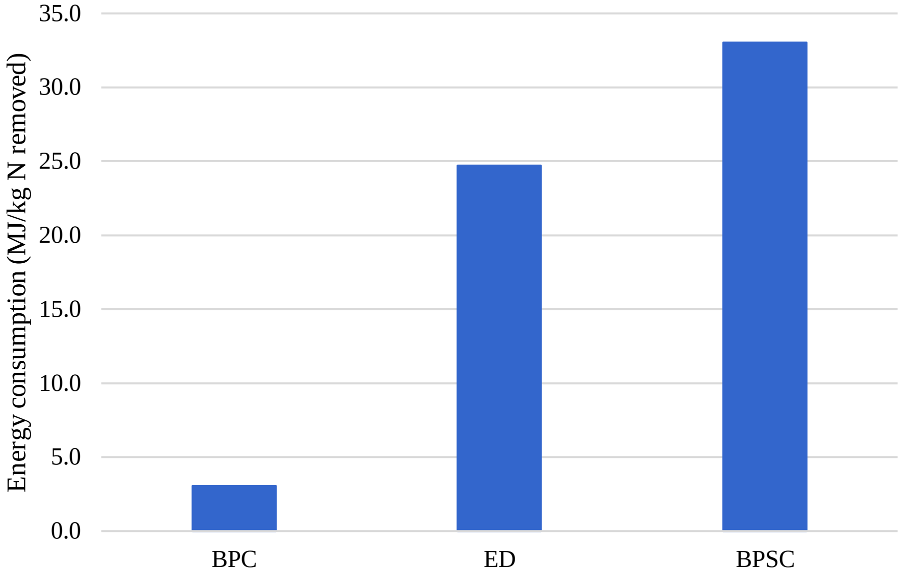

Figure 14. Energy consumption in reject water of Horstermeer in the operated configurations

BPC presented the lowest energy consumption and it was 3.1 MJ/kg N removed, while the highest was for the bipolar membrane with combination of selective cation membrane. The latter one was 10 times higher than the first one, at 33.0 MJ/kg N removed. For conventional ED this value was 24.7 MJ/kg N removed.

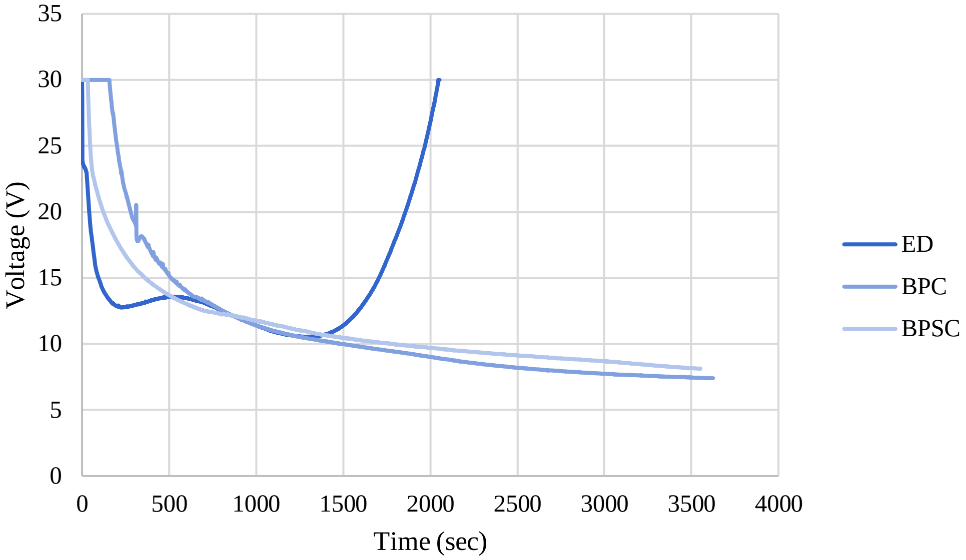

Figure 15. Voltage applied in reject water of Horstermeer in the operated configurations.

As shown in Figure 8.14, ED had the shortest operational time, approximately 2000 seconds, since it was stopped when it reached 30 V. For the other cases, the initial voltage was 30 V, due to high resistance, while it dropped after approximately 5 minutes of operation. The voltage showed a constant drop, for both BPC and BPSC, until it reached approximately 7.5 V.